Jorge Manuel Marques Silva

Licenciado em Ciências da
Engenharia Eletrotécnica e de Computadores

Application of Superconducting Bulks and Stacks of Tapes in Electrical Machines

Dissertação para obtenção do Grau de Mestre em
Engenharia Eletrotécnica e de Computadores

Orientador: João Miguel Murta Pina, Professor Auxiliar, FCT-UNL

Co-orientador: Xavier Granados García, Cientista Titular, ICMAB

Júri:

Presidente: João Almeida das Rosas, Professor Auxiliar, FCT-UNL

Arguente: Anabela Monteiro Gonçalves Pronto, Professora Auxiliar, FCT-UNL

Vogal: João Miguel Murta Pina, Professor Auxiliar, FCT-UNL

FACULDADE DE CIÊNCIAS E TECNOLOGIA
UNIVERSIDADE NOVA DE LISBOA

Março, 2015

Application of Superconducting Bulks and Stacks of Tapes in Electrical Machines

À minha Mãe e ao meu Pai.

À memória do meu avó António e à presença da minha avó Rita.

Acknowledgements

At this moment, when presenting this thesis for evaluation by the distinct members of the jury, it is my duty to express my gratitude to Faculdade de Ciências e Tecnologia of Universidade Nova de Lisboa (FCT-UNL) and to the teachers who, have provided me with knowledge over the last five years, therefore contributing to my development as a young man in training and a student in the Integrated Master in Electrical and Computer Engineering (MIEEC).

Throughout this academic journey, I had the opportunity to enjoy two intermediate stays during the Master: the first under the Erasmus Study Programme in Technische Universiteit Delft (TU Delft) in the Netherlands, for five months during 2013; and the second under the Erasmus Traineeship Programme, a six month stay, during the first semester of the academic year 2014/2015, at Institut de Ciència de Materials de Barcelona (ICMAB) in Spain, where this dissertation was developed. If during the first stay in Delft, the support in the application and preparation by the Master coordinator, Professora Maria Helena Fino, and Lodging and Mobility Office employees, Gracinda Caetano and Ana Dallot, were precious and fundamental, in Barcelona I could count on the monitoring of my co-supervisor Dr. Xavier Granados as well, to whom I express my acknowledgment.

Apart from these two enriching experiences, I would like to register my participation as a monitor in the course of Electrical Circuits Theory, a very rewarding experience for me and, I hope, useful for my younger colleagues, whose recognition together with the confidence placed by the course coordinator, Professora Maria Helena Fino, have very positively marked me.

To Professor João Murta Pina, whom I express my gratitude for providing me the opportunity to experience this internship in Barcelona, where I got the chance to have a close contact with the laboratory environment, and also for monitoring my work, especially in this final phase.

Now, on a personal level I must also emphasize the companion of my fellow friends with whom I could share (non)academic life experiences, contributing further to my growth. Among them, I highlight: Edgar, Inês, Catarina, Cláudia, Ari, Miguel, Mariana, António, Halyna, Celso as well as friends I made

in Delft, including Giulio and Pablo, and more recently in Barcelona: Thomas, Joanna, Filip, Pien, Kyra, Tomás, Ana, Joana, Alexa and other members of Hakuna Party Matata group ☺.

Last but not least, I owe to my parents my deep-felt appreciation for the fundamental and constant support, both in affective and financial terms, and, by word and example, have always encouraged me to continue with relative autonomy in my way as a student and as a person.

Abstract

The present dissertation focuses on the research of the recent approach of innovative high-temperature superconducting stacked tapes in electrical machines applications, taking into account their potential benefits as an alternative for the massive superconducting bulks, mainly related with geometric and mechanical flexibility.

This work was developed in collaboration with Institut de Ciència de Materials de Barcelona (ICMAB), and is related with evaluation of electrical and magnetic properties of the mentioned superconducting materials, namely: analysis of magnetization of a bulk sample through simulations carried out in the finite elements COMSOL software; measurement of superconducting tape resistivity at liquid nitrogen and room temperatures; and, finally, development and testing of a frequency controlled superconducting motor with rotor built by superconducting tapes.

In the superconducting state, results showed a critical current density of 140.3 MA/m^2 (or current of 51.15 A) on the tape and a 1 N·m developed motor torque, independent from the rotor position angle, typical in hysteresis motors.

Keywords: Superconductivity; Tapes; Bulks; Superconducting motor.

Resumo

A presente dissertação foca-se na pesquisa da recente abordagem das inovadoras fitas supercondutoras de alta temperatura (dispostas em pilha) em aplicações de máquinas elétricas, tendo em conta os seus potenciais benefícios como uma alternativa aos blocos supercondutores maciços, principalmente relacionados com a flexibilidade geométrica e mecânica.

Este trabalho foi desenvolvido em colaboração com o Institut de Ciència de Materials de Barcelona (ICMAB), e está relacionado com a avaliação de propriedades elétricas e magnéticas dos materiais supercondutores mencionados, a saber: análise da magnetização de um bloco através de simulações realizadas no *software* de elementos finitos COMSOL; medição da resistividade da fita supercondutora às temperaturas ambiente e do azoto líquido; e, finalmente, o desenvolvimento e teste de um motor supercondutor controlado por frequência com rotor construído por fitas supercondutoras.

No estado supercondutor, os resultados mostraram uma densidade de corrente crítica de 140,3 MA/m^2 (ou corrente de 51,15 A) na fita e um binário de 1 N·m no motor, independente do ângulo do rotor, típico em motores de histerese.

Palavras-chave: Supercondutividade; Fitas; Blocos; Motor supercondutor.

Symbology and Notations

a	Half thickness of the superconducting slab [m].
b	Half length region with no magnetic induction [m].
B	Flux density or magnetic induction field [T].
$\boldsymbol{B}$	Flux density spatial vector [T].
$\langle \boldsymbol{B} \rangle$	Average flux density spatial vector [T].
B_{ap}	Applied flux density [T].
B_{max}	Maximum flux density [T].
$B_{max_{tube}}$	Maximum flux density using a steel tube [T].
B_p	Flux density of penetration [T].
B_x, B_y and B_z	Flux density spatial components [T].
d_{wheel}	Wheel diameter [mm].
E	Electrical field [V/m].
E_c	Critical electrical field [V/m].
E_{silver}	Electrical field in the silver conductor [V/m].
$\boldsymbol{E_{silver}}$	Electrical field in the silver conductor spatial vector [V/m].
E_{YBCO}	Electrical field in the YBCO bulk [V/m].
$\boldsymbol{E_{YBCO}}$	Electrical field in the YBCO bulk spatial vector [V/m].

$\boldsymbol{e_x}$	Spatial vector unit along x-axis.
$\boldsymbol{e_y}$	Spatial vector unit along y-axis.
$\boldsymbol{e_z}$	Spatial vector unit along z-axis.
f	Frequency [Hz].
F_{motor}	Motor force applied on the wheel [gf].
f_p	Pinning force density [N/m^3].
$\boldsymbol{f_p}$	Pinning force density spatial vector [N/m^3].
f_{p_y}	Pinning force density spatial y-component [N/m^3].
f_{ref}	Reference frequency [Hz].
f_s	Sample frequency [Hz].
H	Magnetic field [A/m].
$\boldsymbol{H}$	Magnetic field spatial vector [A/m].
H_c	Critical magnetic field [A/m].
H_{c_1}	Lower critical magnetic field [A/m].
H_{c_2}	Upper critical magnetic field [A/m].
H_{irr}	Irreversibility magnetic field [A/m].
H_p	Penetration magnetic field [A/m].
I	Current [A].
I_c	Critical current [A].
i_{phase}	Current on one of the phases [A].
I_{phase}	Current amplitude on one of the phases [A].
J	Current density [A/m^2].
$\boldsymbol{J}$	Current density spatial vector [A/m^2].
$\boldsymbol{J_{ap}}$	Applied current density spatial vector [A/m^2].
J_{ap_z}	Applied current density spatial z-component [A/m^2].
J_c	Critical current density [A/m^2].

J_{max}	Maximum current density [A/m^2].
J_x, J_y and J_z	Current density spatial components [A/m^2].
k	Proportional ratio [H/m].
l	Length of the COMSOL sample or length of the tape fragment [mm].
M	Magnetization [A/m].
$\boldsymbol{M}$	Magnetization spatial vector [A/m].
M_{irr}	Irreversible magnetization [A/m].
M_{rev}	Reversible magnetization [A/m].
n	Exponent parameter in the resistivity expression.
r	Radius [m].
r_{wheel}	Wheel radius [mm].
ΔR	Resistance of the tape fragment [Ω].
S	Cross section of the tape fragment [µm^2].
t_{max}	Instant when the applied current density is at its maximum [ms].
T	Temperature [K].
T_c	Critical temperature [K].
T_{cycle}	Cycle period [s].
tk	Thickness of the tape [µm].
T_{motor}	Motor torque [N·m].
T_s	Sample time [s].
ΔU	Voltage drop on the tape fragment [V].
w	Width of the COMSOL layer or width of the tape fragment [mm].
w_h	Magnetic energy volumetric density [J/m^3].
δ	Penetration depth [m].

δ_{step}	Angle step [°].
μ_o	Magnetic permeability in the vacuum [4π×10^{-7} H/m].
ρ_{silver}	Electrical resistivity in the silver conductor [Ω·m].
σ	Tensile stress [MPa] or electrical conductivity [S/m].
σ_{tube}	Tensile stress caused by the steel tube [MPa].
χ_m	Magnetic susceptibility.
1G	First generation superconducting tape.
2G	Second generation superconducting tape.
BSCCO	Bismuth Strontium Calcium Copper Oxide.
CMOS	Complementary Metal Oxide Semiconductor.
FC	Field Cooling.
HTS	High Temperature Superconductor.
ICMAB	Institut de Ciència de Materials de Barcelona.
LED	Light Emitting Diode.
LTS	Low Temperature Superconductor.
PIT	Process In Tube.
PWM	Pulse Width Modulation.
(RE)BCO	(Rare Element) Barium Copper Oxide.
RPM	Revolutions Per Minute.
SP	Super Power.
UNEX	Universidad de Extremadura.
YBCO	Yttrium Barium Copper Oxide.
ZFC	Zero Field Cooling.

Content

List of Figures

List of Tables

1

1. Introduction

1.1. Motivation

Energy availability is a central issue in contemporary society, together with other as water and environmental sustainability. The near future will be marked by the search of new forms of conversion and use of energy. Just consider, for example, the new alternative energies and comparability with the classic; or the potential conflicts at national and international level on the production, transmission and use of energy for realizing the scientific, technological and social relevance of this matter.

On the one hand, energy and electric power in particular poses problems of sustainability in environmental terms, but includes also the economic components both for the sustainability of companies and for the citizens' quality of life. However, strategies have been developed in order to reduce the collateral damages in terms of environmental externalities through implementation and application of clean coal technologies. This issue involves contentions in economic terms, i.e., the costs are derived not only from research and development processes but also from more qualified labor.

Feasible solutions are related with the application of converters, inductances or current limiters, which, although conceptually simple, pose other problems. Therefore, it is important to characterize and evaluate new ways of converting energy and consider the advantages, disadvantages and shortcomings

of alternative answers around the clean technologies and alternative energy sources.

Facing these challenges, in particular the gains obtained in the production, transmission and conversion of energy, the implementation of superconductivity emerges as relevant solution not only from an environmental point of view as economic, as becoming less dependent on fossil sources and other classical sources of energy production.

Finally, it should be noted the advantages in energy distribution for superconductivity, namely to diversify energy sources and avoid problems caused by short circuits when traditional chains fail to overcome and protect users. In this sense, superconductivity has the possibility to limit the failures arising from short circuits. However, the implementation of superconductivity based technologies is complex and does not have uniform criteria nor universal, so this will certainly be a strong incentive to motivate the advancement in the design of tools able to innovate, create and develop superconducting technologies in energy systems, particularly in the use of High Temperature Superconducting (HTS) materials, also capable of being cooled by abundant and cheap liquid nitrogen.

1.2. Objectives

This work aims to achieve the following objectives:

- Simulate, in the finite elements COMSOL software, a sample of Yttrium Barium Copper Oxide (YBCO) HTS bulk, in an effort to observe the flux and current densities;
- Measure and test the resistivity of a Second Generation (2G) HTS tape in two different states: the normal state (at room temperature) and in superconducting state (temperatures around 77 K);
- And finally, create and develop a superconducting motor, based on an induction motor, although with the innovation of applying stacks of 2G HTS tapes in the rotor. The development of this motor was conducted by my co-supervisor Dr. Xavier Granados.

1.3. Original Contributions

The original contributions in this work fall mainly on the construction of the superconducting motor, where the stacks of 2G HTS tapes were applied in the rotor, constituting an innovation. Also important to point out is the development of the frequency controlled motor part: the computer-motor interface and the development of an Arduino script that controls the field frequency and the resulting mechanical motor speed.

1.4. Dissertation Organization

This dissertation is organized in six chapters:

- Chapter 1: Introduction – the present chapter of Introduction;
- Chapter 2: Literature Review – the literature review on superconductivity and related general concepts. Here there are defined the two types of superconductivity and distinguished HTS from Low Temperature Superconductors (LTS) and from a regular conductor. There is a special focus on HTS bulks and stacks of tapes, as they are the materials to be used during the experimented work;
- Chapter 3: COMSOL Simulation – a description of the simulation of a YBCO HTS bulk, carried out in the finite elements COMSOL software and some considerations regarding flux and currents densities;
- Chapter 4: HTS Tape Resistivity – a report of the experimented measurement of a 2G HTS tape resistivity in two different states: the normal state (at room temperature) and in superconducting state (temperatures around 77 K);
- Chapter 5: HTS Motor – a summary on the development of the superconducting motor, including all the constituent parts needed to the implementation. Analysis of the results;
- Chapter 6: Conclusions and Future Work – a reflection on the developed work and a possible future challenge.

2

2. Literature Review

2.1. General concepts of Superconductivity

2.1.1. Definition

Superconductivity is a phenomenon that occurs in certain materials when cooled below a critical temperature, T_c. Under this condition, the superconductor material starts to conduct with zero resistance and expels the magnetic field.

This property of complete exclusion and expulsion of the magnetic field from the superconductor interior is called the Meissner Effect (Meissner *et al.*, 1933)[1]. This magnetic property of the material is known as perfect diamagnetism. As long as the applied magnetic field $\boldsymbol{H}$ does not exceed a certain critical value, H_c, there is no magnetic induction inside the superconductor, except on the surface. The correspondent flux density vector $\boldsymbol{B}$ (also called magnetic induction) is given by

$$\boldsymbol{B} = \mu_0(\boldsymbol{H} + \boldsymbol{M}) \tag{2.1}$$

where $\boldsymbol{M}$ is the magnetization of the superconductor. When inside the superconductor $\boldsymbol{B} = 0$, Equation (2.1) becomes

$$\boldsymbol{H} = -\boldsymbol{M} \Longrightarrow \boldsymbol{H} = \chi_m \boldsymbol{M} \tag{2.2}$$

where χ_m is called the magnetic susceptibility. In this case, magnetic field and magnetization vectors have equal intensity but opposite senses, so $\chi_m = -1$,

[1] Translated reference in (Forrest, 1983).

confirming the perfect diamagnetism of a superconductor. Magnetization is further described in Section 2.2.

The Meissner Effect proved superconductivity to be a thermodynamic state (Rodríguez, 2013) where there are persistent electric current flows on the surface of the superconductor, acting to exclude the magnetic field of the magnet (Faraday's law of induction). These currents effectively form an electromagnet that repels the magnet, as observed in Figure 2.1.

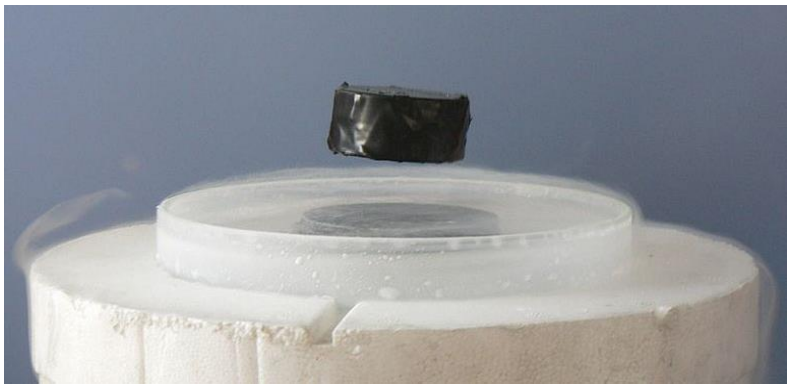

Figure 2.1 – A magnet levitating above a high temperature superconductor (HTS), cooled with liquid nitrogen. Picture source link: http://upload.wikimedia.org/wikipedia/commons/thumb/5/55/Meissner_effect_p1390048.jpg/800px-Meissner_effect_p1390048.jpg.

Even though achieving the critical temperature is fundamental to obtain the superconductivity state, this is not enough. As previously mentioned, experiments have shown that superconductivity is destroyed for a given upper threshold of critical magnetic field, H_c. Later, the critical field and temperature dependence was empirically found (Tinkham, 1996):

$$H_c(T) = H_c(0) \cdot \left[1 - \left(\frac{T}{T_c}\right)^2\right] \tag{2.3}$$

where $H_c(0)$ represents the field value at the absolute zero temperature (0 K).

Considering a current I flowing in a superconducting wire of radius r, the peripheral magnetic field is determined by Ampere's Law (Poole *et al.*, 2007):

$$H = \frac{I}{2\pi r} \tag{2.4}$$

Therefore, a critical current I_c is related with the critical field H_c, being

$$I_c = 2\pi r \cdot H_c \tag{2.5}$$

At the same time, the critical current density in the superconducting wire J_c can be calculated. It is important to keep in mind that the current only flows within a very thin layer at the surface – skin effect – with a penetration depth δ, which is significantly smaller than actual radius r ($\delta \ll r$), as portrayed in Figure 2.2. Consequently, J_c comes (Poole *et al.*, 2007)

$$J_c = \frac{I_c}{\pi r^2 - \pi(r-\delta)^2} \approx \frac{I_c}{2\pi r \cdot \delta} = \frac{H_c}{\delta} \tag{2.6}$$

Thus, it can be concluded there is also a critical current density J_c, which also defines whether the material is in superconducting state or not. In summary, there are three physical quantities that mainly influence the superconductivity, specifically:

- The temperature T;
- The current density J;
- The magnetic field H (or flux density B).

These variables are not independent and they can be represented in three-dimensional axis, called the T-J-H diagram. The critical values of these variables form a surface (cf. Figure 2.3) which encloses the necessary conditions for the material to be supercondutor, i.e. under this surface the material is in the superconducting state (Murta-Pina, 2010).

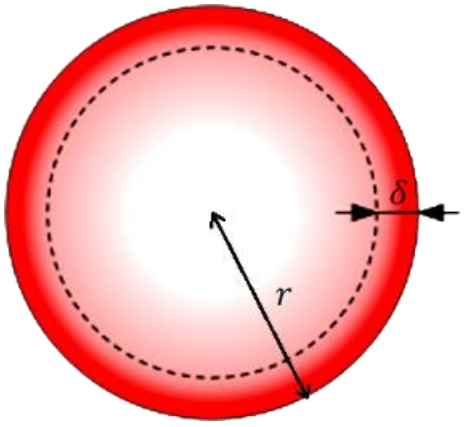

Figure 2.2 – Skin effect representation in the cross section of a wire.

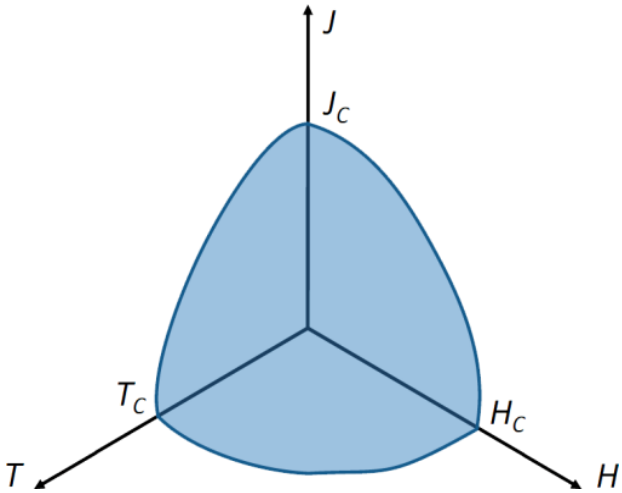

Figure 2.3 – T-J-H diagram (Murta-Pina, 2010).

2.1.2. Superconductor Types I and II

Type-I superconductors are elements, in chemical terms. They totally expel any magnetic field (cf. Figure 2.4), just as stated in Section 2.1.1. As they are not able to withstand significant fields before they lose superconductivity, these superconductors are rarely employed (Tinkham, 1996).

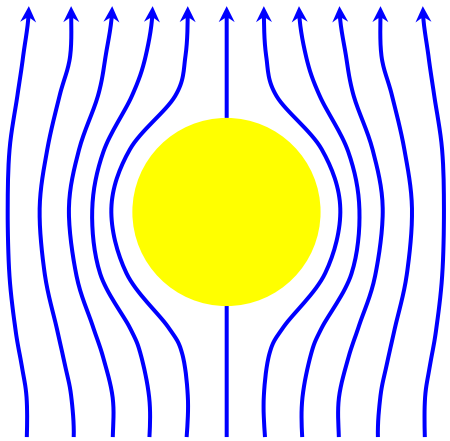

Figure 2.4 – Type-I superconductor. Picture source link: http://en.theva.biz/user/eesy.de/theva.biz/dwn/Superconductivity.pdf.

However, there was discovered a second type of superconductors, which revealed some penetration of the magnetic field in the form of flux lines (cf. Figure 2.5), in contrast with type-I. This penetration is a result of the non-pure sections/zones of these superconductors, for instance, normal conducting defects or degraded superconductivity, where the core of the flux line is pinned, creating a surrounding vortex of supercurrent. This characteristic allows them to sustain much higher fields (Murta-Pina, 2010).

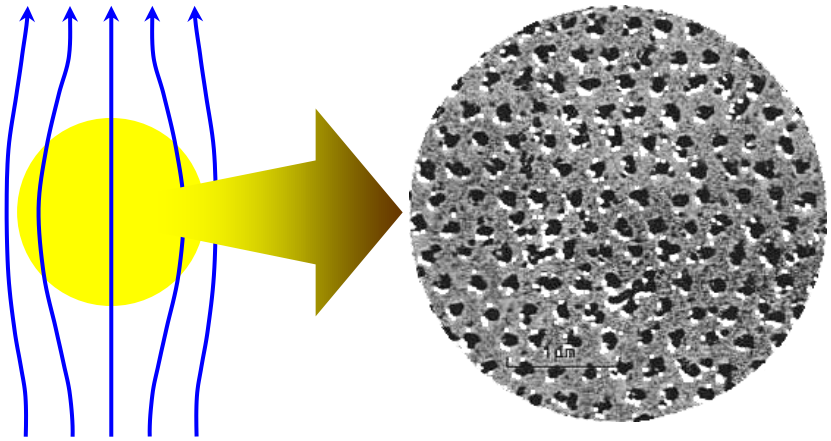

Figure 2.5 – Type-II superconductor. Picture source link: http://en.theva.biz/user/eesy.de/theva.biz/dwn/Superconductivity.pdf.

2.1.3. High Temperature Superconductors (HTS)

High Temperature Superconductors (abbreviated HTS) are materials that behave as superconductors at unusual high temperatures. Whereas "ordinary" or metallic Low Temperature Superconductors (LTS) usually have transition temperatures below 30 K (-243.2 °C), HTS have been observed with transition temperatures as high as 138 K (-135 °C) (Ford *et al.*, 2005).

Most of metal alloys and all HTS are type-II superconductors. In order to better distinguish the differences between these concepts, a representation of the observed resistance of a HTS, a LTS and a regular conductor as a function of temperature is shown in Figure 2.6.

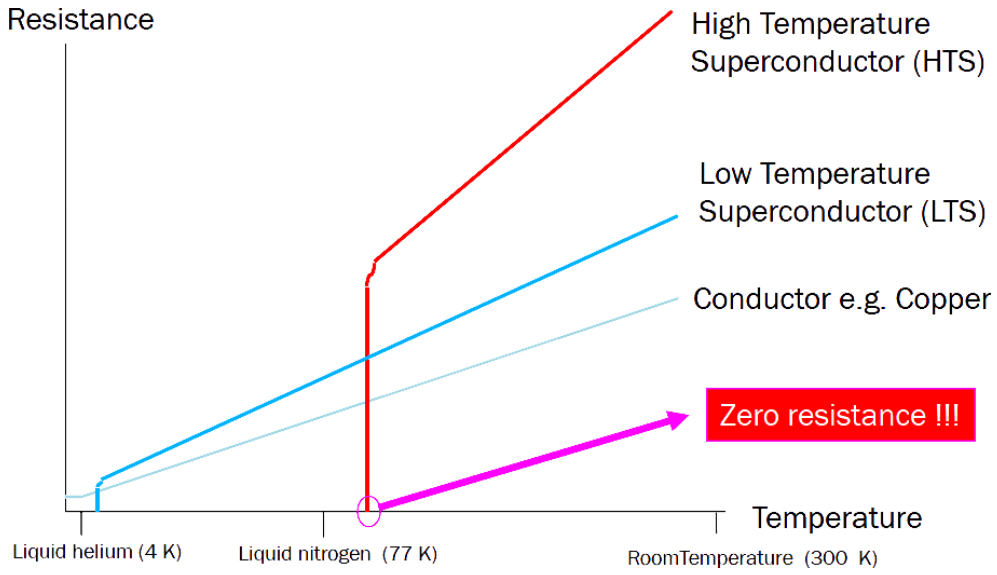

Figure 2.6 – Resistance comparison of a HTS, a LTS and a regular conductor as a function of temperature (Selvamanickam, 2014).

2.2. HTS Magnetization

As previously referred, all HTSs are type-II superconductors. Some of their basic properties can be described by the field-dependent magnetization. From Equation (2.1), the magnetization is characterized by

$$\boldsymbol{M} = \frac{\langle \boldsymbol{B} \rangle}{\mu_0} - \boldsymbol{H} \tag{2.7}$$

with $\boldsymbol{H}$ as the external magnetic field and $\langle \boldsymbol{B} \rangle$ as the average flux density $\boldsymbol{B}$ in the superconductor. The magnetization *versus* field dependence of HTS sample is represented in Figure 2.7.

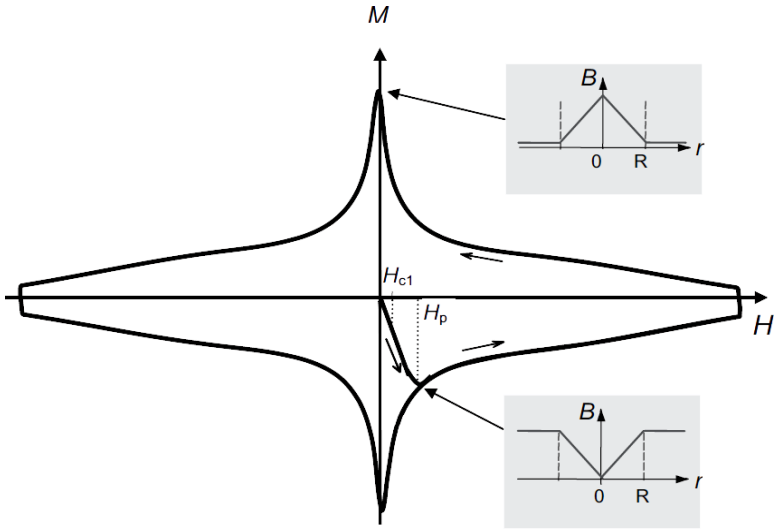

Figure 2.7 – Magnetization curve of a type-II superconductor (Krabbes *et al.*, 2006).

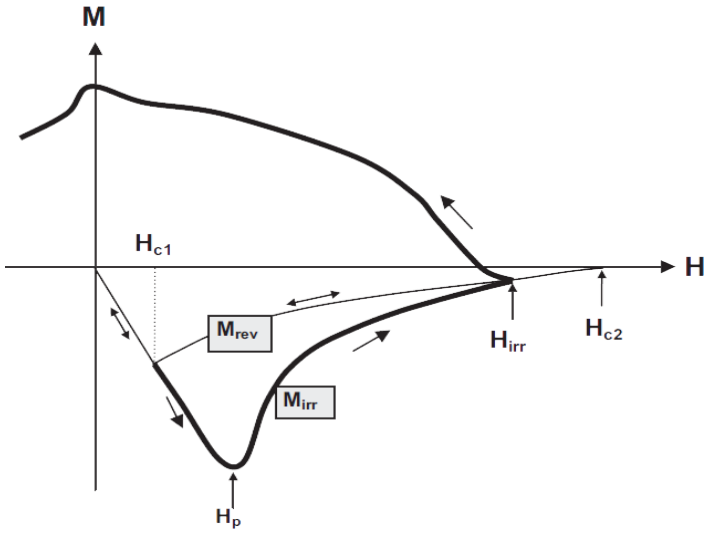

Figure 2.8 – Irreversible and reversible magnetizations of a type-II superconductor (Krabbes *et al.*, 2006).

In a defect-free type-II superconductor with lower field applied, i.e. $H < H_{c_1}$ (H_{c_1} as the lower critical field), there is a surface current which expels the external magnetic field so that the magnetic induction B in the superconductor vanishes. As long as the applied field is increased (following the reversible magnetization line in Figure 2.8), within the range $H_{c_1} < H < H_{c_2}$ (H_{c_2} as the upper critical field), magnetic flux penetrates the superconductor in the form of flux lines. As the external field increases towards H_{c_2}, the region between the flowing flux cores in the superconductor shrinks to zero, and the sample makes a continuous transition to the normal state. This $M(H)$ dependence in the superconductor, M_{rev}, is reversible and after switching off the external field, no magnetic flux is trapped within the superconductor.

The magnetization becomes highly irreversible if the superconductor includes defects like dislocations, precipitates, etc. These defects interact with the flux lines and restrains them to penetrate freely at $H = H_{c_1}$. An applied field higher than the lower critical field, $H > H_{c_1}$, the magnetic field starts to penetrate the superconductor until reaching the center of the superconductor (at the penetration field H_p) where the magnetization has its maximum diamagnetic value. With higher applied fields the magnetization intensity, $|M_{irr}|$, starts to decrease (in absolute value), reflecting the reduction of the critical current density J_c with increasing magnetic field H. The irreversible magnetization, M_{irr}, becomes zero at $H = H_{irr}$ (H_{irr} as the irreversibility field) in contrast to the reversible magnetization which disappears at $H = H_{c_2}$. As the external field is reduced, the gradient of the local field near the edge changes its sign, but has the same absolute value as before. The magnetization now becomes positive because a magnetic field is trapped in the superconductor (Krabbes *et al.*, 2006).

2.2.1. Bean Critical State Model

In the critical state models the distributions of magnetic flux density $\boldsymbol{B}$ and current density $\boldsymbol{J}$, are ruled by the equation

$$\boldsymbol{J} \times \boldsymbol{B} + \boldsymbol{f_p} = 0 \tag{2.8}$$

where $\boldsymbol{f_p}$ is the volumetric density of pinning force in the material.

The Bean Critical State Model (Bean, 1962) (Bean, 1964), assumes that the current density in a superconductor is independent from the flux density. Con-

sidering that the critical current J_c is either a constant value or zero, from Equation (2.8), it can be inferred

$$|J| = J_c \Leftrightarrow f_p \propto B \tag{2.9}$$

With the purpose to demonstrate the Bean Model, a superconducting slab with infinite dimensions along x and z axes and $2a$ of thickness along y-axis, as represented in Figure 2.9, is used as an example. The slab is immersed in an induction field $\boldsymbol{B}$ along z-axis, defined by

$$\boldsymbol{B} = B_z \boldsymbol{e_z} = B_{ap} \boldsymbol{e_z} \tag{2.10}$$

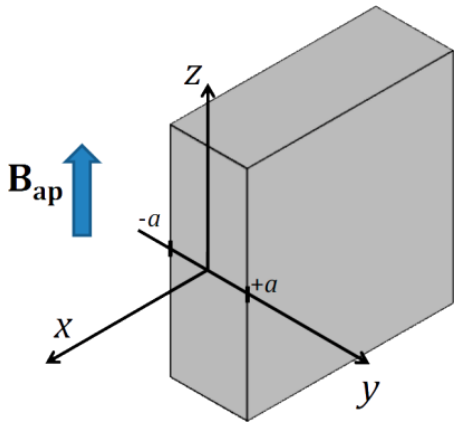

Figure 2.9 – Sketch of a type-II superconducting slab with infinite dimensions along axis x and y. Magnetic induction field applied B_{ap} along z-axis (Murta-Pina, 2010).

Inside the superconducting slab the Ampère's Law can be verified. Writing this law in its differential form,

$$\nabla \times \boldsymbol{H} = \boldsymbol{J} \Leftrightarrow \nabla \times \boldsymbol{B} = \mu_0 \boldsymbol{J} \tag{2.11}$$

where $\nabla \times$ stands for the curl vector operator. Hence,

$$\nabla \times \boldsymbol{B} = \begin{vmatrix} \boldsymbol{e_x} & \boldsymbol{e_y} & \boldsymbol{e_z} \\ \dfrac{\partial}{\partial x} & \dfrac{\partial}{\partial y} & \dfrac{\partial}{\partial z} \\ B_x & B_y & B_z \end{vmatrix} = \left(\frac{\partial B_z}{\partial y} - \frac{\partial B_y}{\partial z}\right)\boldsymbol{e_x} + \left(\frac{\partial B_x}{\partial z} - \frac{\partial B_z}{\partial x}\right)\boldsymbol{e_y} + \left(\frac{\partial B_y}{\partial x} - \frac{\partial B_x}{\partial y}\right)\boldsymbol{e_z} \tag{2.12}$$

Since $\boldsymbol{B}$ only has component along z, $B_x = B_y = 0$, and remembering the slab is considered to be infinitely long in x-axis, B_z is independent from x, so

$$\frac{\partial B_z}{\partial x} = 0 \tag{2.13}$$

and Equations (2.11) and (2.12) turn into

$$\nabla \times \boldsymbol{B} = \frac{\partial B_z}{\partial y}\boldsymbol{e_x} = \mu_0 \boldsymbol{J} \Leftrightarrow \boldsymbol{J} = J_x(y)\boldsymbol{e_x} = \frac{1}{\mu_0}\frac{\partial B_z}{\partial y}\boldsymbol{e_x} \tag{2.14}$$

The current density $\boldsymbol{J}$ only has component along x, given the infinite slab length along x-axis, neglecting J_y. Merging Equations (2.8) and (2.14),

$$\boldsymbol{f_p} = -\boldsymbol{J} \times \boldsymbol{B} = -\begin{vmatrix} \boldsymbol{e_x} & \boldsymbol{e_y} & \boldsymbol{e_z} \\ J_x(y) & 0 & 0 \\ 0 & 0 & B_z(y) \end{vmatrix} = J_x(y)B_z(y)\boldsymbol{e_y} = f_{p_y}(y)\boldsymbol{e_y} \tag{2.15}$$

The way the superconductor is magnetized – Zero Field Cooling (ZFC) or Field Cooling (FC) – is undoubtedly relevant, because it leads to different effects/results. According to (Poole et al., 2007), four different situations may be considered: low applied field (ZFC); high applied field (ZFC); excitation reversal (ZFC); and finally field applied using FC.

2.2.1.1. Zero Field Cooling (ZFC)

When a superconductor is cooled without applying any field, we are observing ZFC. If that is the case, the surface currents prevent the penetration of the applied magnetic field, creating a strong field concentration caused by the existing diamagnetism (Krabbes *et al.*, 2006).

2.2.1.1.1. Low Applied Field

An initially null external field is progressively applied until there is a full penetration of the complete field in the superconductor. This means that there is a central zone totally free of field and current.

Considering the origin of the y-axis referential as the center of the slab along the same axis, as depicted in Figure 2.9, this field-free zone is delimited by $|y| = b$, with $b < a$. The field starts to penetrate from the borders and decreases until becoming zero at $|y| = b$, so both flux density and current density, from Equation (2.14), are

$$B_z(y) = \begin{cases} B_{ap}\dfrac{|y| - b}{a - b} & , \quad b < |y| \leq a \\ 0 & , \quad |y| \leq b \end{cases} \tag{2.16}$$

$$J_x(y) = \begin{cases} J_c \cdot \mathrm{sgn}(y) & , \quad b < |y| < a \\ 0 & , \quad |y| \leq b \end{cases} \tag{2.17}$$

where the function $\mathrm{sgn}(y)$ returns the sign of the variable y (also equivalent to $\mathrm{sgn}(y) = y/|y|$). Additionally, the critical current density is

$$-J_c = \frac{1}{\mu_0}\frac{B_{ap}}{a-b} \Leftrightarrow b = a - \frac{B_{ap}}{\mu_0 J_c} \tag{2.18}$$

When the increasing applied field equals to the penetrating field H_p (cf. Figure 2.8), there is no region free of field nor current, because the flux density B just reached the center from both sides. This corresponds to the situation when $b = 0$. So, from Equation (2.18),

$$b = a - \frac{B_p}{\mu_0 J_c} = 0 \Leftrightarrow B_p = \mu_0 J_c a \tag{2.19}$$

The behavior of both flux density and current density is illustrated in Figure 2.10, according to the Bean Model, and at two different situations: when $b = \frac{a}{2}$ and $b = 0$. The latter is achieving the penetration field H_p (in Figure 2.8), i.e. the penetration induction field B_p.

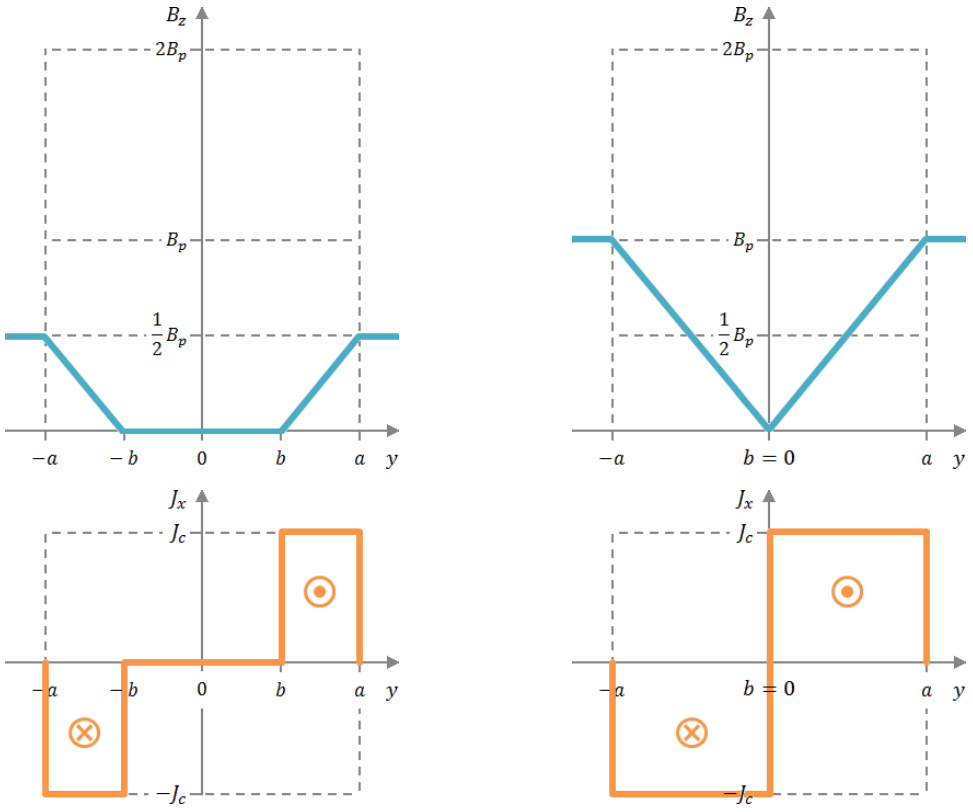

a) $b = \frac{1}{2}a$ and $B_{ap} = \frac{1}{2}B_p$. **b)** $b = 0$ and $B_{ap} = B_p$.

Figure 2.10 – Flux and current densities along *y*-axis of a type-II superconductor slab, at half (a) and at total (b) penetration field B_p, according to the Bean Model (Murta-Pina, 2010).

In a ZFC magnetization the trapped field in the sample center remains zero for applied fields lower than the penetration field, $H < H_p$.

Finally, the pinning force density $f_p(y)$ results

$$f_{p_y}(y) = \begin{cases} J_c B_{ap} \dfrac{|y| - b}{a - b} \cdot \mathrm{sgn}(y) & , \quad b < |y| \leq a \\ 0 & , \quad |y| \leq b \end{cases} \tag{2.20}$$

2.2.1.1.2. High Applied Field

Applying field above penetration field H_p, the flux and current densities and the pinning force density are defined as

$$B_z(y) = B_{ap} + B_p \frac{|y| - a}{a} \quad , \quad |y| \leq a \tag{2.21}$$

$$J_x(y) = J_c \cdot \mathrm{sgn}(y) \quad , \quad |y| \leq a \tag{2.22}$$

$$f_{p_y}(y) = J_c \left(B_{ap} + B_p \frac{|y| - a}{a} \right) \cdot \mathrm{sgn}(y) \quad , \quad |y| \leq a \tag{2.23}$$

And the respective graphic representation in Figure 2.11:

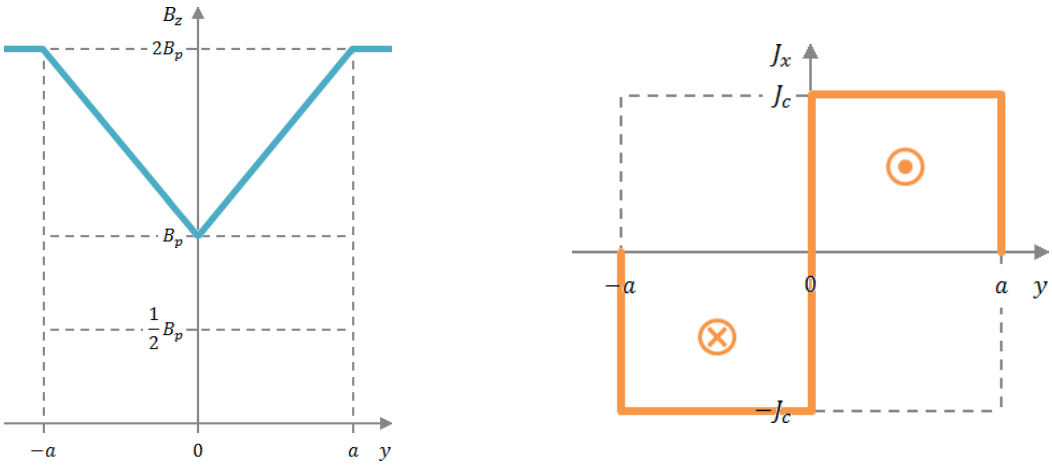

Figure 2.11 – Flux and current densities along y-axis of a type-II superconductor slab, when applying field higher than H_p, according to the Bean Model (Murta-Pina, 2010).

This situation could determine the irreversibility of the magnetization if the upper critical field H_{c_2} or irreversibility field H_{irr} are exceeded (cf. Figure 2.8).

2.2.1.1.3. Excitation Reversal

After applying such high field and since the field has reached the center of the slab, when the excitation is reverted, field and current will vary differently:

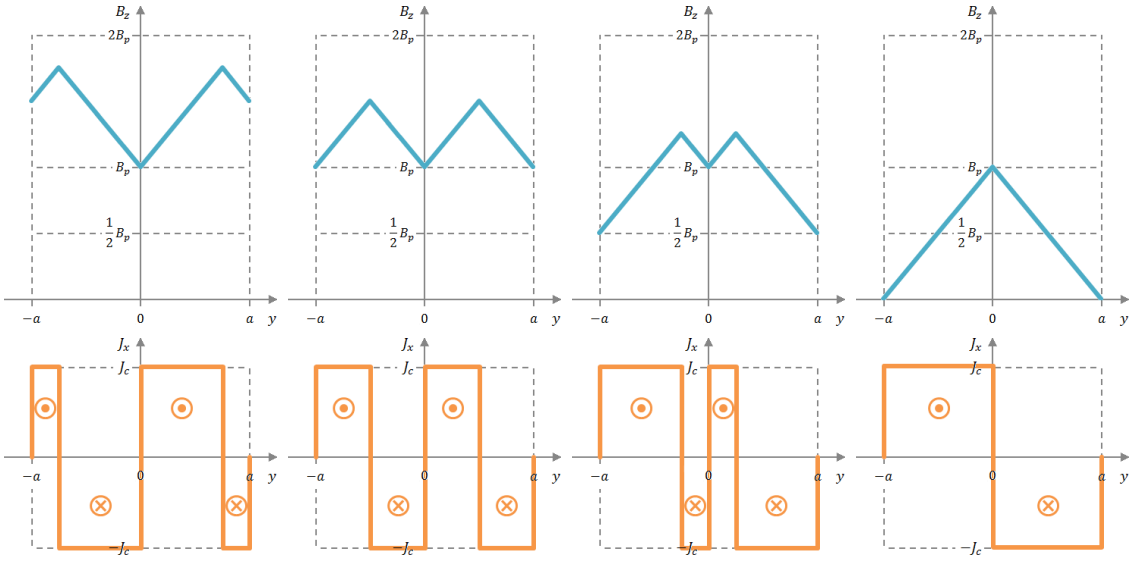

Figure 2.12 – Flux and current densities evolution when a type-II superconductor slab is subjected to a decreasing applied field, according to the Bean Model (Murta-Pina, 2010).

In above Figure 2.12, especially in the last case, further to the right, although there is no field at the slab boarders, there is trapped field exactly in the center, equal to the penetration field B_p. To accomplish this trapped field at the center it was necessary to externally apply a field twice as higher (cf. Figure 2.11).

2.2.1.2. Field Cooling (FC)

Finally, if the superconductor is cooled under the critical temperature T_c in presence of a constant magnetic field, the superconductor suffers a stronger magnetization – larger magnetic susceptibility χ_m. The superconductor will get oriented according to the field (Krabbes *et al.*, 2006).

As a result and from Equation (2.14), there are no currents involved because there is no field variation (cf. Figure 2.13a). When the field is gradually switched off, the field variation is felt and, consequently, currents are emerging (cf. Figure 2.13b) until they penetrate within the entire superconductor, when the applied field is reduced to zero (cf. Figure 2.13c).

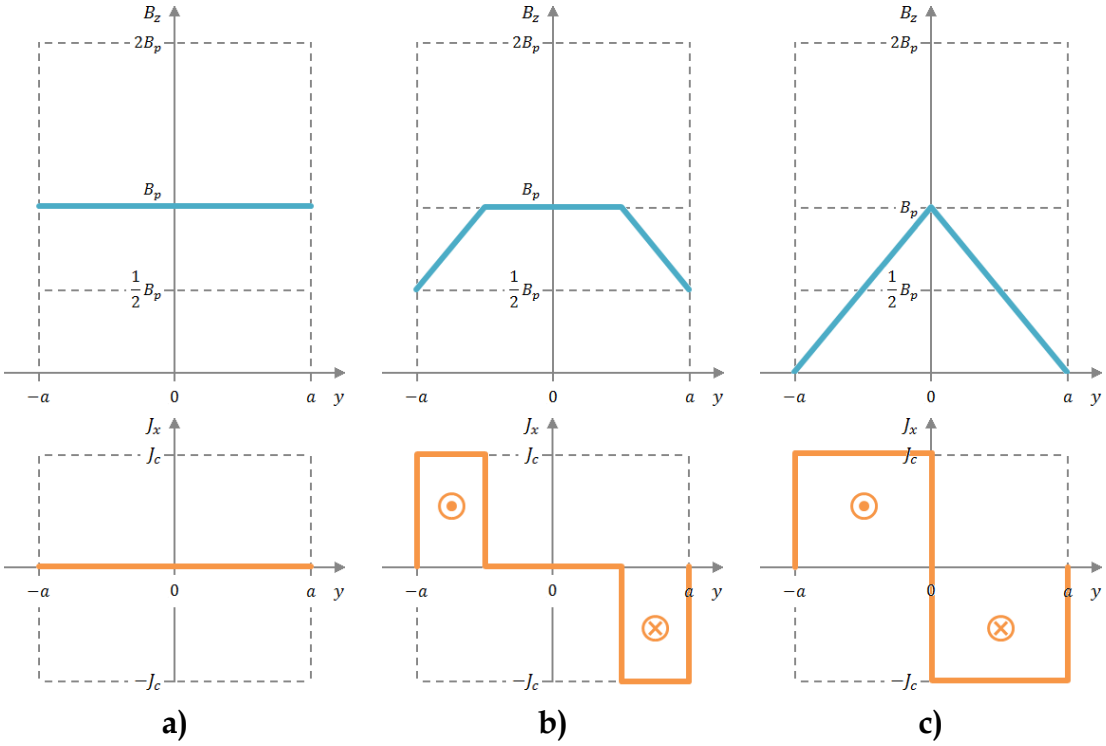

Figure 2.13 – Flux and current densities evolution when a type-II superconductor slab is first cooled in presence of field and after subjected to a its progressively reduction, according to the Bean Model (Murta-Pina, 2010).

All in all, cooling the superconductor in the presence of the field leads to trap field at the center too, yet requiring only half of the field needed in the previous situation, in Figure 2.11, because the superconductor is entering in the superconducting state at the same time it is sensing the external field.

2.3. HTS Bulks

The most used HTS bulks are chemically composed by Yttrium, Barium, Copper and Oxygen (YBCO) (cf. Figure 2.14), which can handle considerably high critical current densities at 77 K, and can be used in several applications, for instance, superconducting magnetic bearings.

Figure 2.14 – Examples of YBCO HTS bulks.

2.3.1. Grain Structure

The orientation of the grains in a HTS bulk is crucial for the current flow. Randomly oriented grains deprive the current to flow freely due to weaken bounds between them. This, in turn, limits the flowing currents, disabling any practical use of the bulk (cf. Figure 2.15a).

These weak bounds can be avoided, granting higher currents, if the HTS bulk is modified in such a way that grains get aligned in the *c*-axis direction (perpendicular direction to the *ab*-plane surface of the sample) as seen in Figure 2.15b, using melt-texturing techniques (Krabbes *et al.*, 2006).

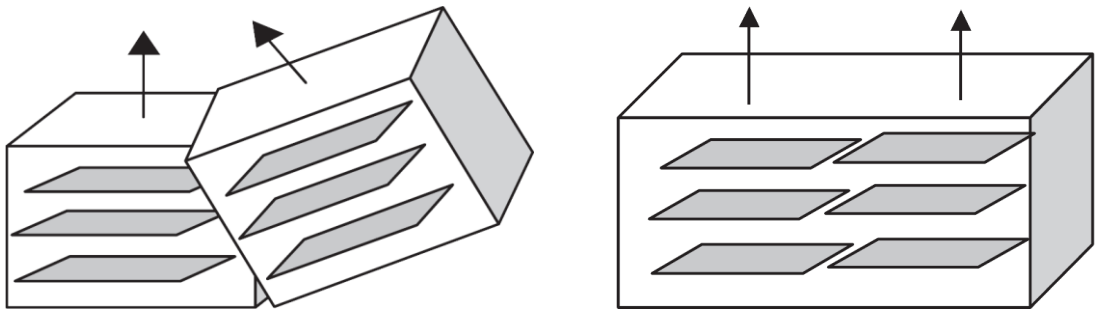

a) **b)**

Figure 2.15 – Grain boundaries in a bulk: a) with granular texture; b) with *c*-axis texture (Krabbes *et al.*, 2006).

The grain structure is easily controlled by applying a magnetic field in *c*-axis and magnetizing by FC. By doing so, the flux lines penetrate effortlessly in the material and supercurrents are induced in the *ab* plane of the HTS bulk sample (Krabbes *et al.*, 2006).

2.3.2. Mechanical Reinforcements

One of the drawbacks brought by the HTS bulks is related with mechanical issues, when a very high field is applied. Given the respective low tensile strength, these materials are not able to withstand such large fields, causing an eventual material cracking and consequent loss of its diamagnetic properties.

Nevertheless, some approaches can be taken to overcome this problems, among them, reinforcing the bulk with steel tubes or impregnating resin in its interior (Krabbes *et al.*, 2006).

2.3.2.1. Using Steel Tubes

In case of using steel tubes, the effect of field enhancement is pictured in Figure 2.16. The cracking tensile stress is 30 MPa. Without the steel tube, the tensile stress σ shows proportionality with the square maximum trapped field ${B_{max}}^2$ (Krabbes *et al.*, 2006),

$$\sigma \propto {B_{max}}^2 \Leftrightarrow \sigma = \frac{1}{2\mu} \cdot {B_{max}}^2 \Leftrightarrow {B_{max}}^2 = 2\mu \cdot \sigma \tag{2.24}$$

where μ [H/m] is the magnetic permeability. In this case, considerable low trapped fields are capable of cracking the YBCO bulk.

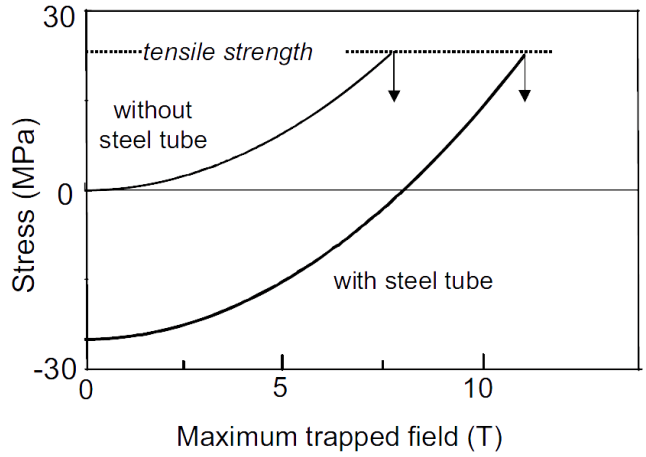

Figure 2.16 – Relation between maximum tensile stress and maximum trapped field in a YBCO HTS bulk sample, with or without reinforcement by a steel tube (Krabbes *et al.*, 2006).

However, if a steel tube is used, a negative, compressive and constant stress σ_{tube} acts on the encapsulated YBCO bulk (Krabbes *et al.*, 2006). With increasing trapped field, the bulk tensile stress is steadily counterbalancing this tube stress until exceeding and finally cracking both bulk and tube. In this other case, we have

$$\sigma = \frac{1}{k} \cdot {B_{max_{tube}}}^2 - |\sigma_{tube}| \Leftrightarrow {B_{max_{tube}}}^2 = k \cdot (\sigma + |\sigma_{tube}|) \tag{2.25}$$

From Equations (2.24) and (2.25), it is evident

$$B_{max_{tube}} > B_{max} \tag{2.26}$$

which is also noticeable in the Figure 2.16. The bulk is now more resistant because it cracks at a much higher trapped field.

2.3.2.2. Using Resin Impregnation

Another solution for the mechanical issue is using impregnating resin in the bulk interior. Molten resin can be added inside a YBCO bulk, through microcracks at the surface. In this way, an enhancement of the tensile strength from 18.4 to 77.4 MPa was achieved (cf. Figure 2.17) (Krabbes *et al.*, 2006).

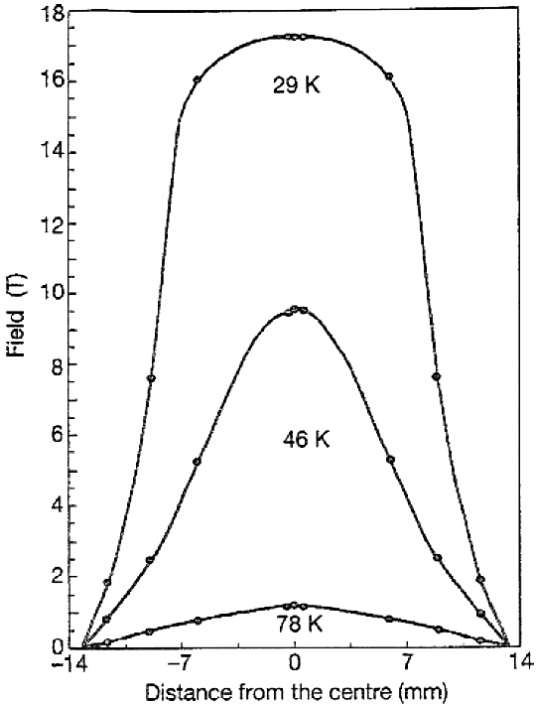

Figure 2.17 – Distribution of the trapped field in a across a resin-impregnated HTS bulk, measured at several temperatures (Krabbes *et al.*, 2006).

2.3.1. Flux Density Measurements

In order to analyze the performance of a YBCO bulk (32 mm × 40 mm × 10 mm), some measurements of trapped flux density were conducted in Universidad de Extremadura (UNEX) in Badajoz, Spain (Murta-Pina, *et al.*, 2014).

The ideal trapped flux density is represented in Figure 2.18, according to the Bean Critical State Model (Section 2.2.1) and Figure 2.19 shows the real measured flux density in the YBCO bulk.

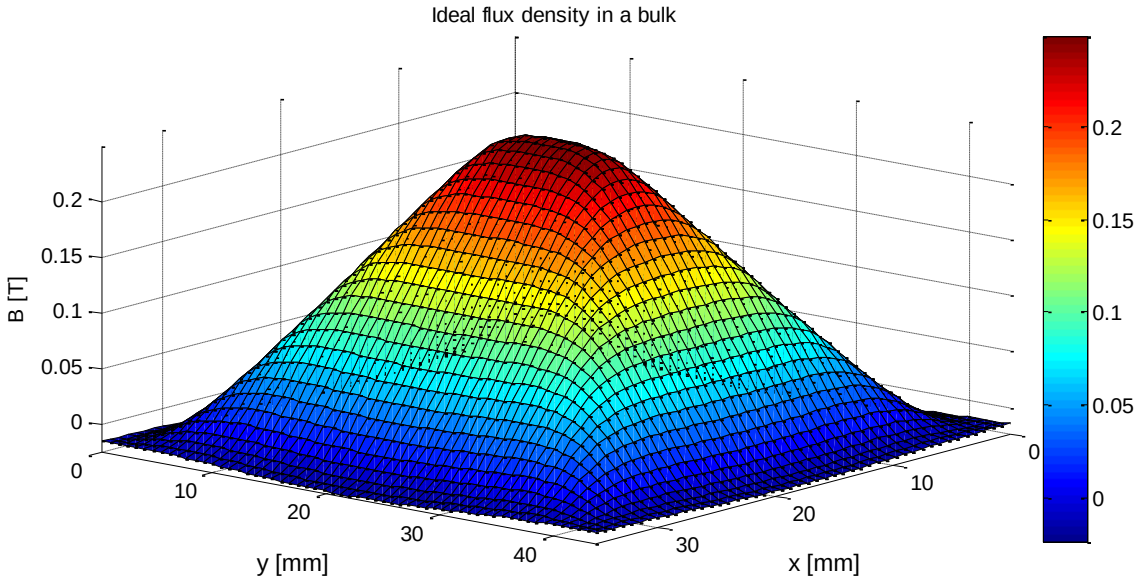

Figure 2.18 – Ideal flux density in a YBCO bulk.

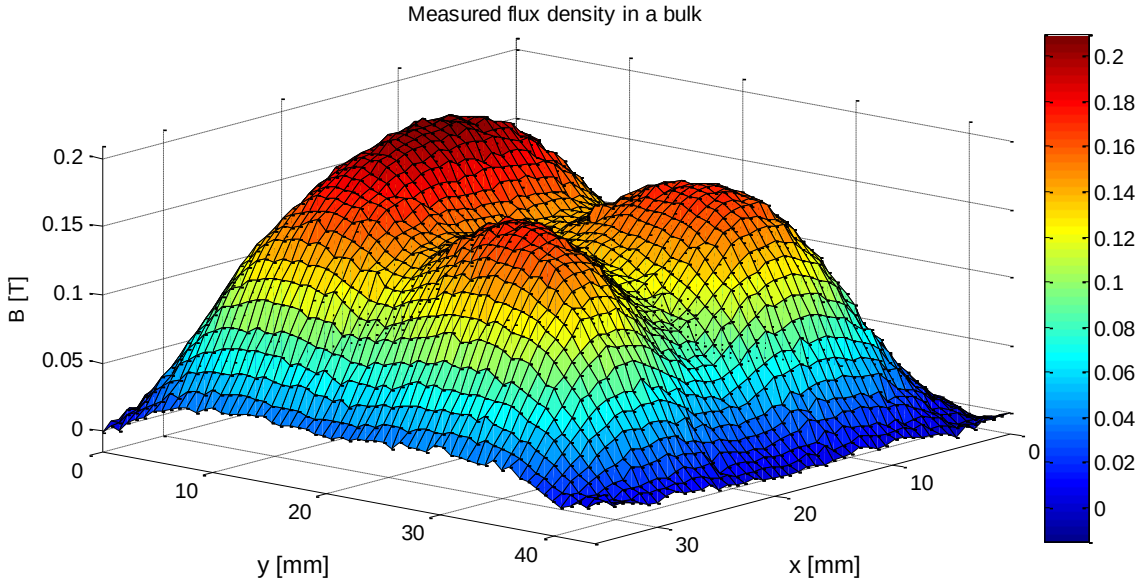

Figure 2.19 – Measured flux density in a YBCO bulk. The measurements were executed at the distance of 1 mm from the sample.

The data related to these graphic representations is detailed in Appendix 1: script_measurements_bulk_tapes.m.

To conclude, three "field hills" can be observed in the measurements, corresponding to three different domains instead of a main one. This happens because the bulks are often subjected to mechanical cracks, given its low tensile strength resulting in the consequent division in subdomains and providing lower trapped fields.

2.4. HTS Tapes

There is no technology which can currently provide as compact a source of high magnetic field as magnetized superconducting bulks. When using the FC method of magnetization, fields over 17 T have been trapped between two YBCO bulks (Tomita *et al.*, 2003).

However, a significant problem with existing bulks is the thermal instability below 30 K (Krabbes *et al.*, 2006) which makes it impossible or impractical to exploit large J_c values which exist at low temperatures. Besides, the previously mentioned reasons are also pertinent: the existing superconducting bulks require external mechanical reinforcement for very high trapped fields, due to the poor mechanical strength.

In an attempt to overcome the limitations identified in the bulks, a recent approach on innovative HTS stacked tapes in electrical machines applications is considered, bringing potential benefits, mainly related with geometric and mechanical flexibility. In this regard, a stack of (RE)BCO coated conductor tapes, (RE stands for a Rare-Earth element) is mechanically stronger due to the metallic substrate supporting the superconducting layer and therefore seems a natural choice for trapping very high fields.

2.4.1. First Generation (1G)

A first generation (1G) tape consists of one or more filaments of superconducting powder encased in cylindrical sheaths (silver or silver alloy) (see Figure 2.20). Commonly, the material used in this superconducting powder is Bismuth Strontium Calcium Copper Oxide (BSCCO). When the material is used as part of electrical systems, the silver coat provides an alternate path for current when the superconductor transits to normal (Ceballos Martínez, 2011).

a) **b)**

Figure 2.20 – Micrographs of two 1G BSCCO tapes: (a) monofilament; (b) multifilament (Ceballos Martínez, 2011).

To produce this tape, it is used the Powder In Tube (PIT) process, described in 3 phases: drawing, rolling and sintering. The drawing process compacts the superconductor powder. Rolling orients the grains with the *ab* planes parallel to the direction of the tape, favoring supercurrents along it. Finally, sintering provides the superconducting character with continuity (Ceballos Martínez, 2011). This whole process is illustrated in Figure 2.21.

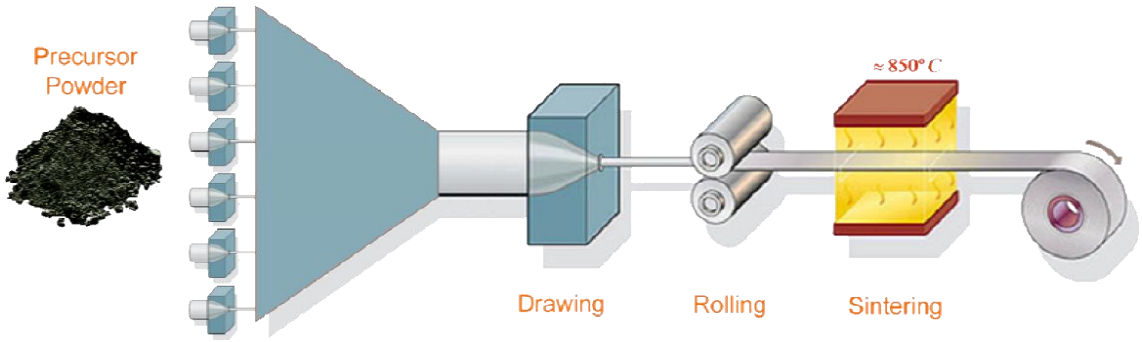

Figure 2.21 – Powder In Tube (PIT) process (Ceballos Martínez, 2011).

Overall, 1G tapes are not always the best choice because it is made of expensive materials, requiring an intensive manufacturing labor and reveals performance limitations, especially in high magnetic fields.

2.4.2. Second Generation (2G)

In fact, 2G tapes appeared as an alternative to 1G tapes so that they could work in environments with magnetic fields stronger than those that the latter can support, as mentioned above. Therefore 2G tapes are better suited to electrical applications.

In contrast to 1G, the structure of 2G tape consists of a series of layers, arranged one above the other in a certain order. The manufacturing process starts from a substrate in tape form, where several intermediate layers are stacked – alumina, yttrium, among others, for the Super Power (SP) tape. These layers are deposited in order to facilitate the adhesion of the superconducting layer and to protect the superconductor from possible contamination by atoms of the substrate. This is followed by the deposition of a thin layer of superconducting material (usually YBCO) to generate a crystal structure sufficiently aligned in the direction of current flow. Finally, to protect the superconducting layer and allow electrical connections, a layer of silver is added by electroplating. This last

layer provides mechanical stability, by keeping the superconducting layer away from the surface and increases electrical stability, improving current flow once the superconducting layer is saturated (Ceballos Martínez, 2011). In brief, the tape is produced in a continuous reel-to-reel process, only 1% of wire is the superconductor and approximately 97% is inexpensive nickel alloy and copper. The internal design of a 2G superconducting tape is portrayed in Figure 2.22.

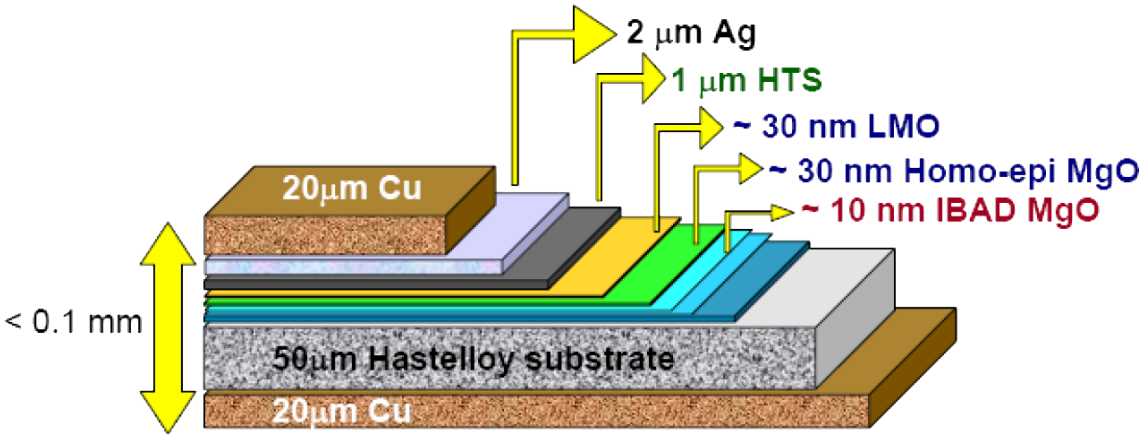

Figure 2.22 – Internal layers of a 2G superconducting tape (Xiong *et al.*, 2007).

By virtue of all the advantages and efficiency brought by the 2G HTS tapes, they have been used in the respective laboratory experiments for the present work. In order to achieve higher trapped fields, several tapes stacked on top of each other were used, assembling the so-called stack of HTS tapes.

2.4.3. Potential for Applications

The potential of a stack of HTS tapes to be used as trapped field magnets in different energy applications is very significant. Such samples have relatively uniform J_c when compared to bulks, resulting in predictable performance. Some significant benefits of HTS tapes in energy applications are, among others (Selvamanickam, 2014):

- The liquid nitrogen used as coolant is a dielectric medium. Using this material, the possibility of oil fires and related environmental hazards is eliminated;
- Superconducting generators, motors & transformers made of HTS tapes can be less than 50% the size and weight of conventional equipment;
- More efficient electrical equipment, leading to less energy lost.

Some examples of possible applications using the superconductor wire (i.e. stack of tapes) are labeled in the organization chart below, in Figure 2.23.

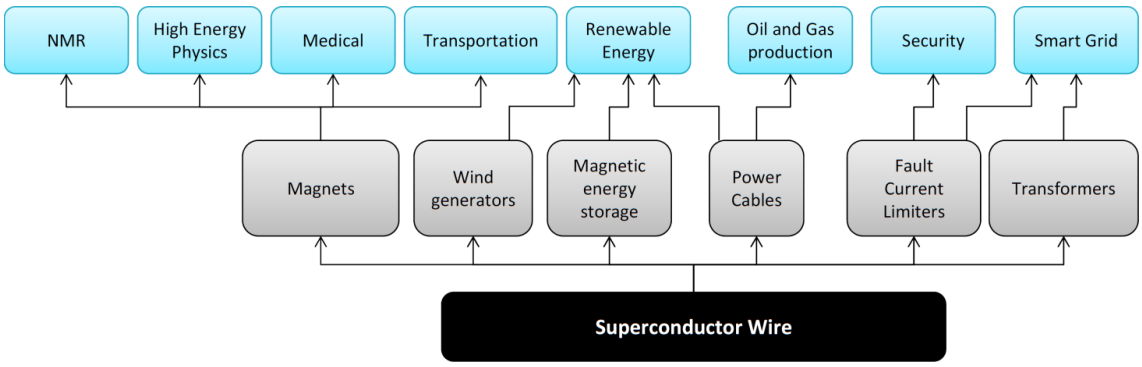

Figure 2.23 – Applications for superconducting wire (stack of HTS tapes in this case) (Selvamanickam, 2014).

Finally, the cost of superconducting tapes is steadily and predictably falling, making the technology attractive for engineering applications.

2.4.4. Flux Density Measurements

Besides the YBCO bulk, some experiments were conducted in order to determine the trapped field in 2G HTS tapes (or stack of tapes), in UNEX, Badajoz, Spain (Murta-Pina, *et al.*, 2014).

Two experiments were considered: the first measurement with a single tape (cf. Figure 2.24) and the second using two stacked tapes (cf. Figure 2.25).

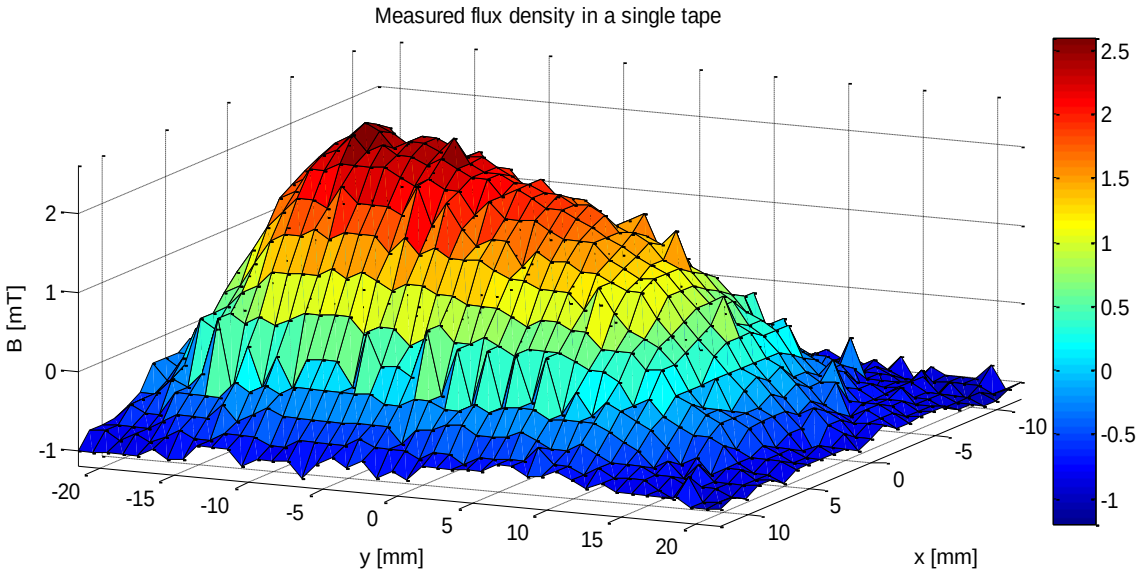

Figure 2.24 – Measured flux density in a single tape. The measurements were executed at the distance of 1 mm from the sample.

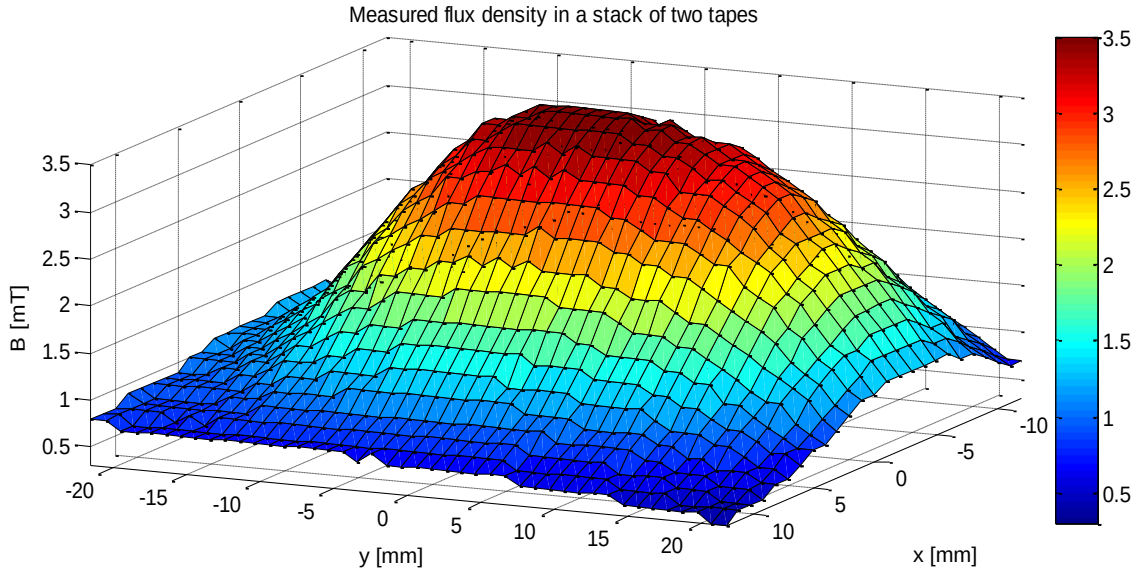

Figure 2.25 – Measured flux density in a stack of two tapes. The measurements were executed at the distance of 1 mm from the sample.

The data related to these graphic representations is detailed in Appendix 1: script_measurements_bulk_tapes.m.

In conclusion, when the stack of two tapes is used, rather than a single tape, the flux density is higher and more uniform, and so is the magnetic field.

In these stacked tapes there is only a "hill" where the field is maximum, because the current flows in a single ring, unlike the bulks, where various domains and subdomains are likely to exist, due to the mechanical cracks.

In comparison with the bulk, these two stacked tapes are only able to obtain a maximum field of 3.5 mT, while in the bulk, despite the cracks, it was possible to achieve 0.2 T. A way to increase the field is placing more tapes in the stack, as proven in this experiment.

3

3. COMSOL Simulation

3.1. Introduction

During the progress of the present dissertation, simulations were performed in COMSOL software in order to virtually determine the behavior of a HTS bulk. The HTS bulk sample (cf. Figure 3.1) was designed in 2D plane, instead of 3D to simplify and save simulation time.

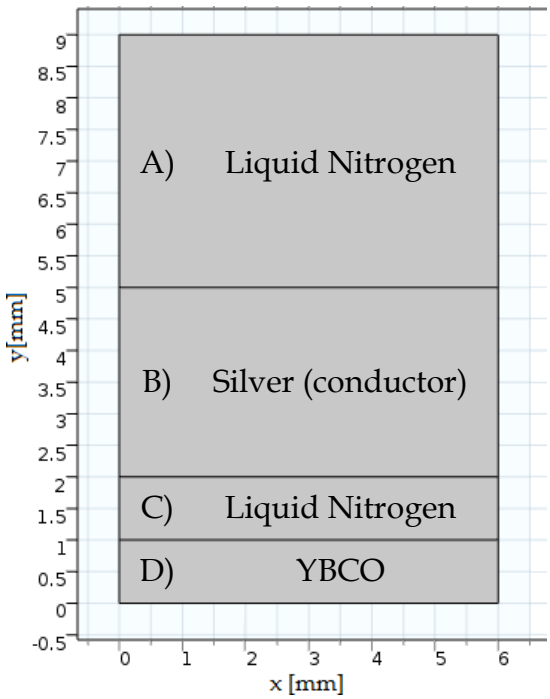

Figure 3.1 – 2D sample designed in COMSOL.

This sample includes four layers: two of liquid nitrogen (used for isolation purposes), one of silver (as electric conductor) and one of YBCO (the actual su-

perconductor) with the dimensions of length (l) along x-axis and width (w) along y-axis indicated in Table 3.1. Liquid nitrogen was used not only to provide the temperature condition for the YBCO layer to be in the superconducting state (around 77 K), but also because it is a better dielectric than air.

Table 3.1 – 2D sample dimensions.

	Liquid Nitrogen		**Silver**	**YBCO**
w [mm]	4 (layer A)	1 (layer C)	3	1
l [mm]	6			

In the silver conductor (layer B) the current $\boldsymbol{J_{ap}}$ is applied depending on the time and space in z-axis direction, perpendicular with the xy-plane, being

$$\boldsymbol{J_{ap}} = J_{ap_z}(x,t)\boldsymbol{e_z} = J_{max}\cos\left(\frac{\pi x}{2L}\right)\sin(2\pi f t)\,\boldsymbol{e_z} \tag{3.1}$$

where the maximum current density applied is $J_{max} = 500\ \mathrm{MA/m^2}$, and the considered frequency is $f = 1$ kHz.

The induced current density $\boldsymbol{J}$ within the entire sample can be obtained from Ampère's Law, in its differential form, remembering $\boldsymbol{J}$ only has component in z-axis. Thus,

$$\boldsymbol{J} = J_z\boldsymbol{e_z} = \nabla \times \boldsymbol{H} = \left(\frac{\partial H_y}{\partial x} - \frac{\partial H_x}{\partial y}\right)\boldsymbol{e_z} \tag{3.2}$$

Inside the silver conductor, the electrical field $\boldsymbol{E}$ is a result of both applied and induced current densities

$$\boldsymbol{E_{silver}} = E_{silver_z}\boldsymbol{e_z} = \rho_{silver}\left(\boldsymbol{J} + \boldsymbol{J_{ap}}\right) \tag{3.3}$$

where ρ_{silver} represents the silver conductor electrical resistivity.

On the other hand, the electrical field in the YBCO bulk in the superconducting state (around 77 K) is described by

$$\boldsymbol{E_{YBCO}} = E_{YBCO}\boldsymbol{e_z} = E_c \cdot \left(\frac{J}{J_c}\right)^n \tag{3.4}$$

where the critical electrical field is defined as $E_c = 1\ \mu\mathrm{V/cm}$. This $E_{YBCO}(J)$ dependence in the superconducting state was tested in laboratory, using a HTS

tape – detailed in Section 4.2. In practice, this means the YBCO bulk does not have significant losses by Joule effect until a critical current density J_c (considerably very high), enabling the YBCO bulk to handle high currents.

3.2. Simulation and Results

3.2.1. Magnetization Curve

After simulating, it was intended to observe the magnetization curve that should be similar to the theoretical curve observed in Section 2.2, Figure 2.7.

From COMSOL, it was possible to retrieve average values of the output current density $\boldsymbol{J}$ (only with component J_z) and output magnetic field $\boldsymbol{H}$ (with components H_x and H_y) on the surface of the superconductor layer (layer D in Figure 3.1). Considering the vectors' lengths absolute values and the magnetic permeability in the superconductor to be μ_0, the dependence $B(J)$ can be determined by

$$B(J) = \mu_0 H(J) \tag{3.5}$$

This dependence is represented in Figure 3.2.

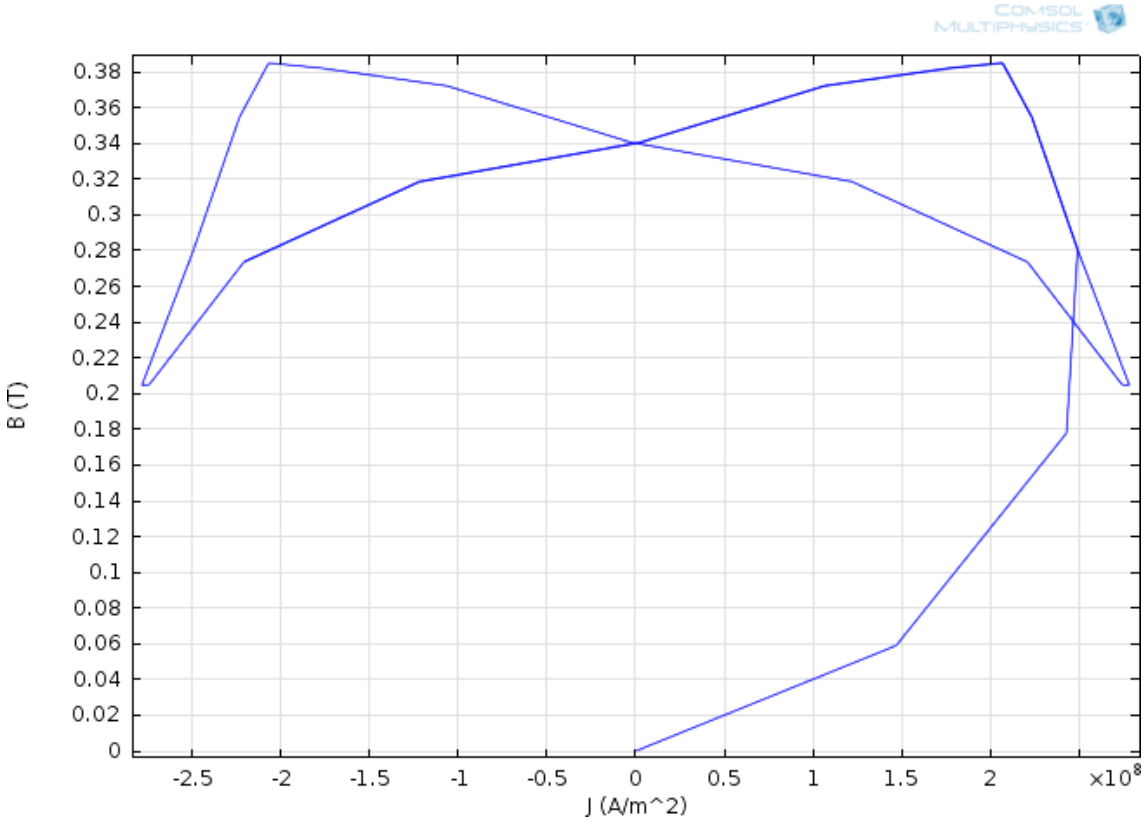

Figure 3.2 – Magnetization curve: relation between J (x-axis) and B (y-axis).

The results have shown an absolute maximum value of current density of 280 MA/m² and a maximum flux density no greater than 400 mT.

This outcome is different from expected, as the variables are not exactly the same as in Equation (2.7) and they are being compared from different axes: J from z-axis and H from xy-plane, in absolute values. The superconductor follows a curious hysteresis loop. This question may be analyzed as future work.

3.2.2. Flux and Current densities

The observation of flux and current densities in the simulation sample is equally significant to understand how the superconductor reacts to an applied current in the silver conductor. From Equation (3.1), choosing an instant t_{max} where the current density applied is at its maximum (using $f = 1$ kHz),

$$\sin(2\pi f t_{max}) = 1 \Leftrightarrow t_{max} = \frac{\arcsin(1)}{2\pi f} = \frac{1}{4f} = 250\ \mu s \tag{3.6}$$

the flux and current densities profiles are displayed in Figure 3.3, where the arrows represent flux density and the gradient colored area shows current density.

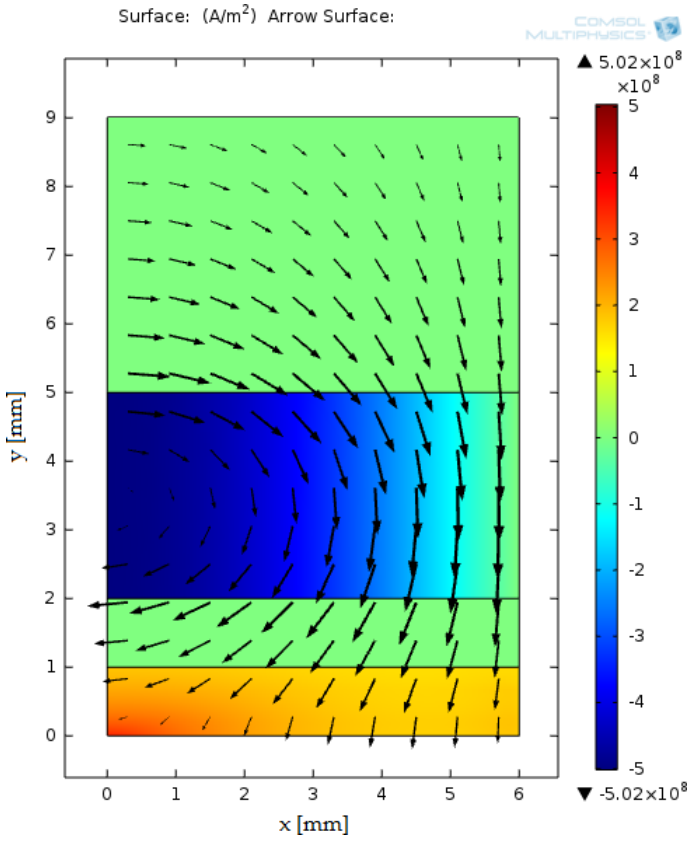

Figure 3.3 – Flux (arrows) and current (colored area) densities simulated in the 2D sample.

Inside the YBCO layer, the flux density gradually decreases as going down the y-axis. If it was a type-I superconductor there would be no flux at all. The induced current density in the superconductor has the opposite direction as the current applied in the conductor, thus showing its diamagnetic nature.

In an effort to observe the current and flux profiles depending on the position, the sample was extended up to four times along x and mirrored along y, with the superconductor in the middle, resulting as portrayed in Figure 3.4.

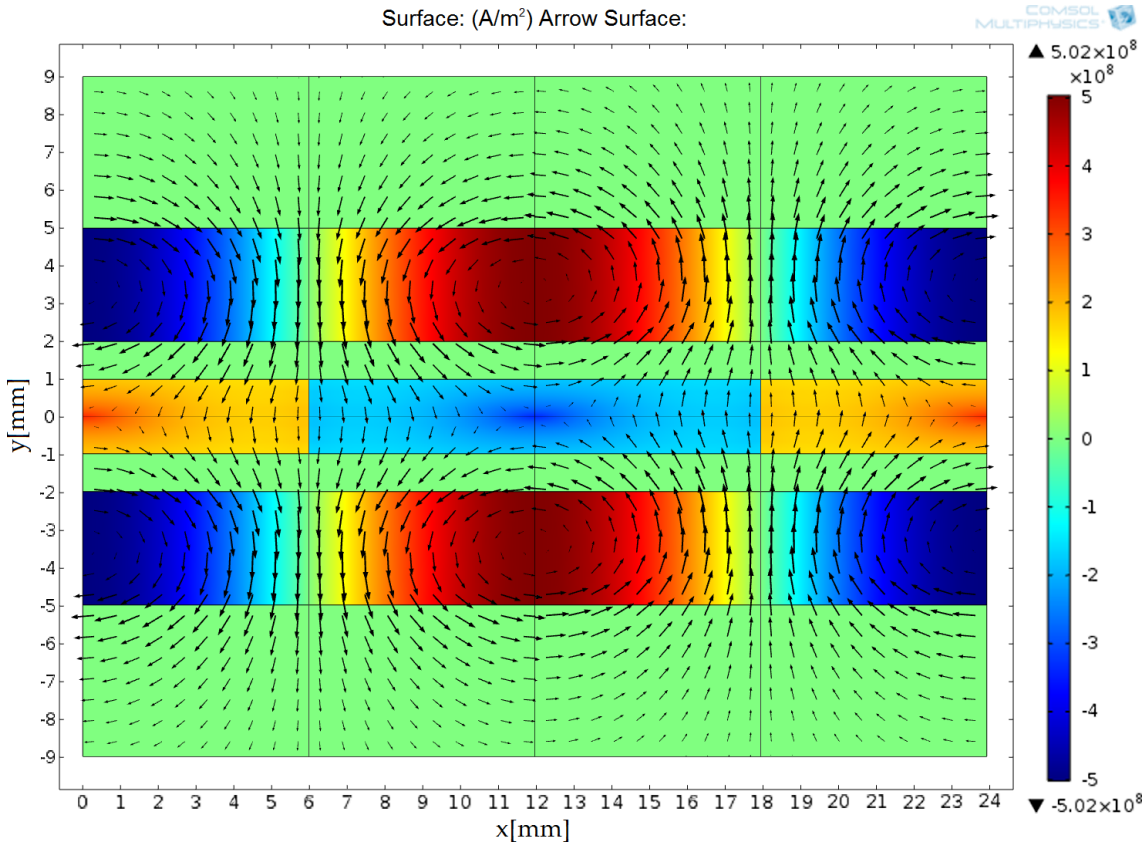

Figure 3.4 – Flux (arrows) and current (colored area) densities simulated in the 2D extended sample.

Looking at this wider picture, flux densities are weaker inside the bulk. There are two flux "corridors" in $x = 6$ mm and $x = 18$ mm, where the flux density is constant, so there is no current density, being the latter related to the variation of the former.

Inside the superconductor, the surface average current density is 210 MA/m², corresponding to a critical current of 5.04 kA flowing in one of the directions, for instance, between 6 and 8 mm in x-axis, on the YBCO layer.

4

4. HTS Tape Resistivity

Using a 2G HTS tape, it is intended to measure and observe the respective resistivity behavior at two different conditions: normal state (at room temperature, i.e., around 293 K) and superconducting state (around 77 K).

In order to accomplish so, the four-terminal sensing method was applied. This method consists on selecting a fragment of the tape and place a voltmeter between the terminals of this sample. The tape is connected to a voltage input source, which displays the established current along the tape, as a result of the respective "load", as described in Figure 4.1.

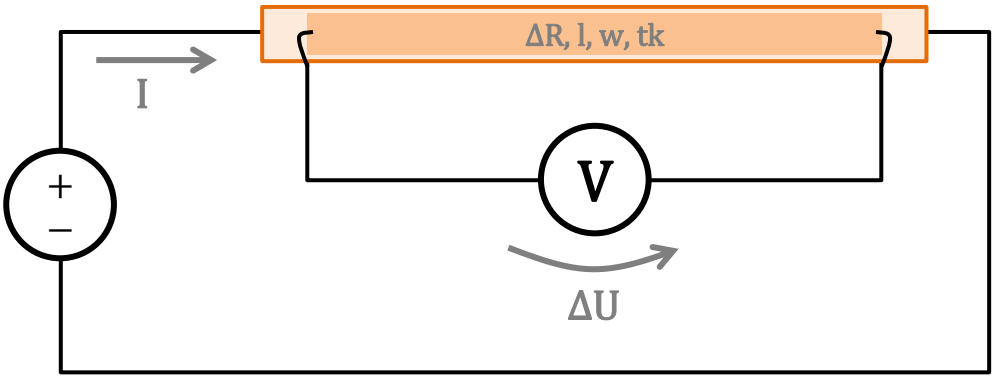

Figure 4.1 – Equivalent circuit used to measure the resistivity of the tape.

Moreover, the tape fragment dimensions are measured and shown in Table 4.1 – length (l) and cross section (S), calculated based on both width (w) and thickness (tk) of the tape. Additionally, Figure 4.2 shows the 2G HTS tape used for the experiment.

Table 4.1 – Tape fragment characteristics.

l [mm]	w [mm]	tk [µm]	S [µm^2]
81.7	4.05	90	364500

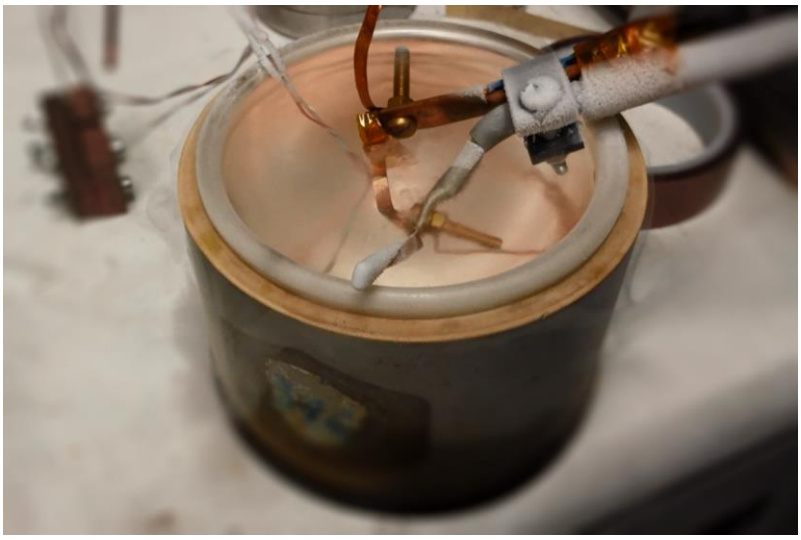

Figure 4.2 – 2G HTS tape submerged in liquid nitrogen. Photo taken during the experiment.

Basically, there were made two experiments. The first one consisted on imposing currents through the superconducting tape in the normal state (i.e. at room temperature) and the second was conducted using the tape at lower temperatures (77 K) creating favorable conditions to achieve the superconducting state, cooled with liquid nitrogen. The outputs of both experiments were the voltage between the two terminals of the fragment and the flowing current.

As it is intended to study the resistivity behavior, it was needed to convert the collected voltage data ΔU into the electrical field E and similarly to convert the input current I into current density values J. This can be achieved by:

$$E = \frac{\Delta U}{l} \tag{4.1}$$

$$J = \frac{I}{S} = \frac{I}{w \cdot tk} \tag{4.2}$$

4.1. Normal State

At the normal state, the tape is expected to conduct as a regular conductor. To make sure the tape does not get burned or damaged, the applied currents were not so high, ranging from 0 A until 4 A. Using Equations (4.1) and (4.2) it

is possible to obtain the relation between the electrical field inside the tape and the flowing current density. The results are represented in Figure 4.3.

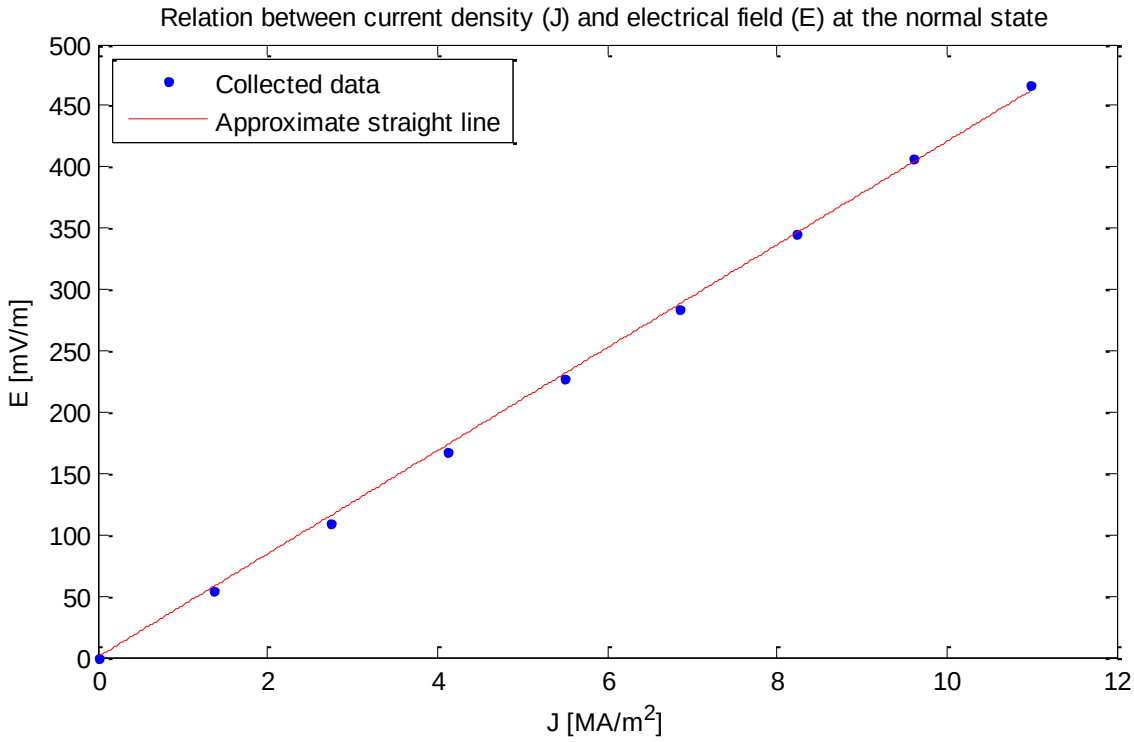

Figure 4.3 – Relation between current density (J) and the electrical field (E) along the tape at the normal state (non-superconducting).

As expected, the experiment has revealed a linear relation between the electrical field and the current density. In a linear, homogeneous, isotropic environment there is a linear ratio between these two physical variables, which is the electrical conductivity σ and it is given by the Ohm's Law:

$$J = \sigma E \Leftrightarrow E = \frac{1}{\sigma} J \tag{4.3}$$

And in this specific experiment it was possible to find the straight line which best approximates the points using the curve fitting tool (`cftool`) from MATLAB:

$$E = 4.2047 \times 10^{-8} \cdot J \Longrightarrow \sigma = \frac{1}{4.2047 \times 10^{-8}\ \Omega \cdot \mathrm{m}} = 2.3783 \times 10^{7}\ \mathrm{S/m} \tag{4.4}$$

4.2. Superconducting State

At the superconducting state, the temperature conditions are different causing the superconducting tape to conduct with no losses by Joule effect

(meaning $\Delta U \approx 0$ V). This is true until a certain limit of critical current density, called J_c, from which the voltage dramatically soars, with small increases of input current. The type of function that better approximates the data recollected is exponential:

$$E = E_c \cdot \left(\frac{J}{J_c}\right)^n \tag{4.5}$$

This dependence is expressed in Figure 4.4. Using the curve fitting tool in MATLAB once again it is possible to obtain the respective parameters n and J_c. The exponent was estimated to be

$$n = 10.99 \tag{4.6}$$

and the critical current density value J_c is found when the electrical field in the tape is the critical $E_c = 1$ μV/cm, resulting

$$J_c = 140.3 \text{ MA/m}^2 \tag{4.7}$$

The critical current value I_c in the tape results:

$$I_c = J_c S = 51.15 \text{ A} \tag{4.8}$$

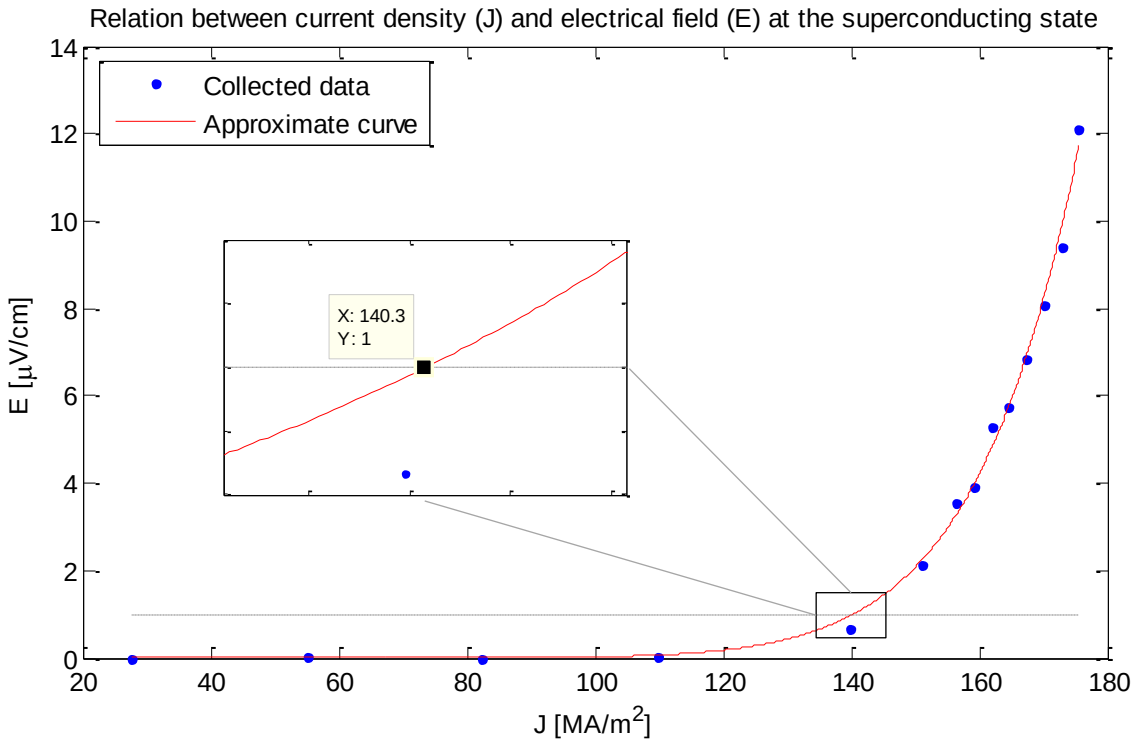

Figure 4.4 – Relation between current density (J) and the electrical field (E) along the tape at the superconducting state (cooled with liquid nitrogen).

5

5. HTS Motor

5.1. Structure

During the execution of the present work, a HTS motor (Figure 5.1) was developed in ICMAB. This motor works similarly as a normal electrical motor with the difference of using a stack of 2G HTS tapes in the rotor surface instead of the classic version using coils (further detailed in Section 5.4). This HTS motor is essentially a synchronous motor, where it is proposed to measure the output torque.

One of the main obstacles consisted on the unfeasibility to connect the motor directly to the 50 Hz grid as there is no enough initial torque to let it rotate at the equivalent speed of 3000 RPM. The solution found resides in a creation of a programming code that creates a sinusoidal wave and it is able to control the frequency, from the computer and using an Arduino board and a three-phase inverter as means to modulate the wave, using PWM (Pulse Width Modulation).

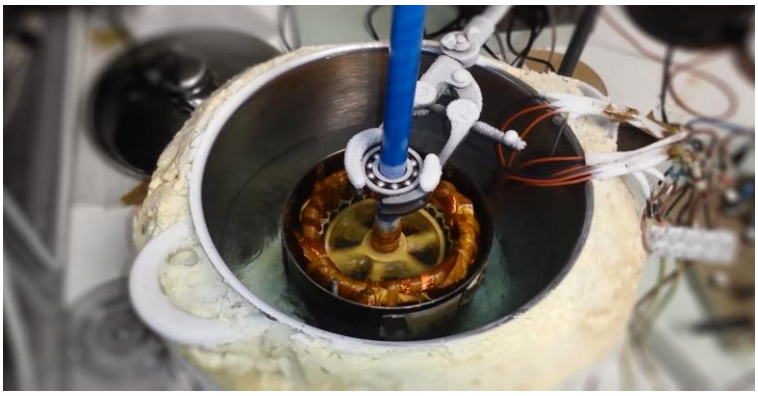

Figure 5.1 – HTS Motor developed in ICMAB.

The complete circuit is shown in Figure 5.2. It is composed by: the laptop where the wave shape and input frequency are defined; the Arduino board (blue delimited block) which runs the program sent by the laptop and creates six signals, where each two correspond to one of the three phases; the rectifier and inverter (orange delimited block) which merges each two signals per phase into one and amplifies the wave so the three phases can generate a magnetic rotating field inside the motor; and lastly the motor itself, comprised by the coils in the stator, and the rotor, which surface is covered with HTS stacks of tapes.

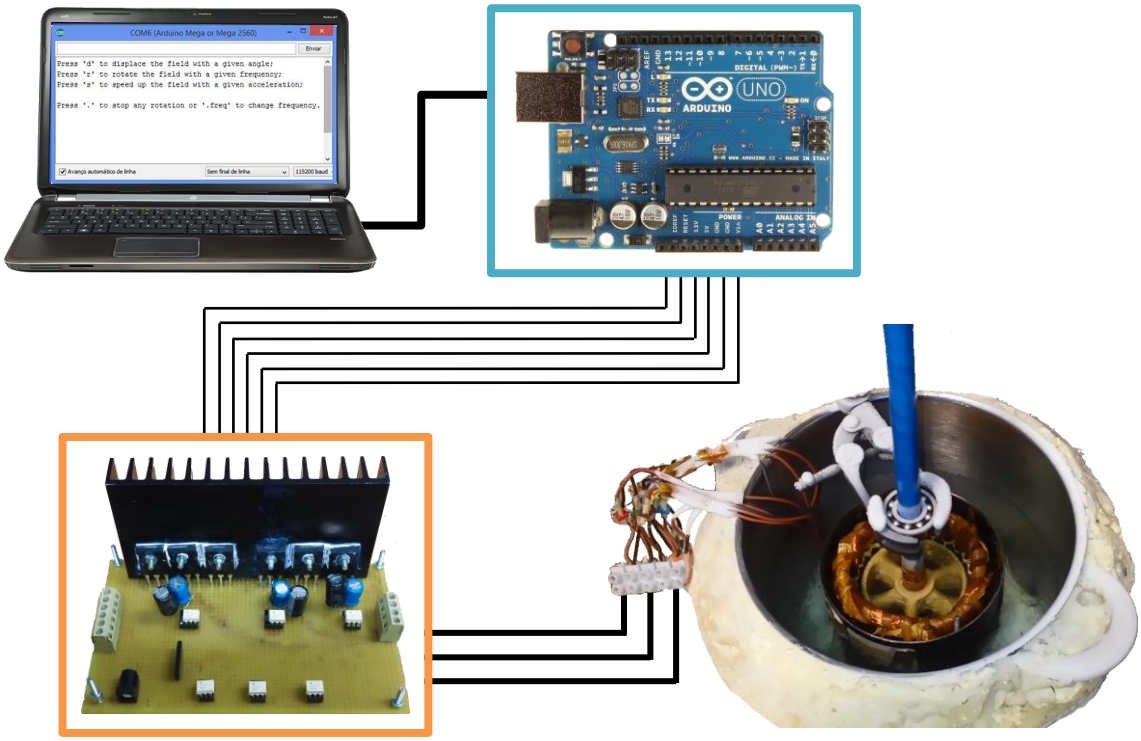

Figure 5.2 – Complete circuit of the HTS motor.

5.2. Arduino Board

The Arduino board has the function of running the programming code (script) created using Arduino software and receiving the input from the laptop keyboard. It is also able to write values into the intended variables, creating signals. Thus, a script was developed with the purpose to create the wave and define the intended frequency, among other features to control the motor and to perform the proposed experiments.

5.2.1. Wave Characteristics

The script was conceived considering six signals. Each phase contains two signals (one high and low) and they are 180° shifted. All of the signals point to a rectified sinusoidal wave, as Figure 5.3 depicts, where signals x_1 (high) and x_2 (low) correspond to symmetric signals of each phase A, B and C. The wave has an amplitude of 255 (1 byte) and is built of 720 points (script in Appendix 3: script_wave.m) making it a resolution angle step, δ_{step}, of

$$\delta_{step} = \frac{360°}{720} = 0.5° \tag{5.1}$$

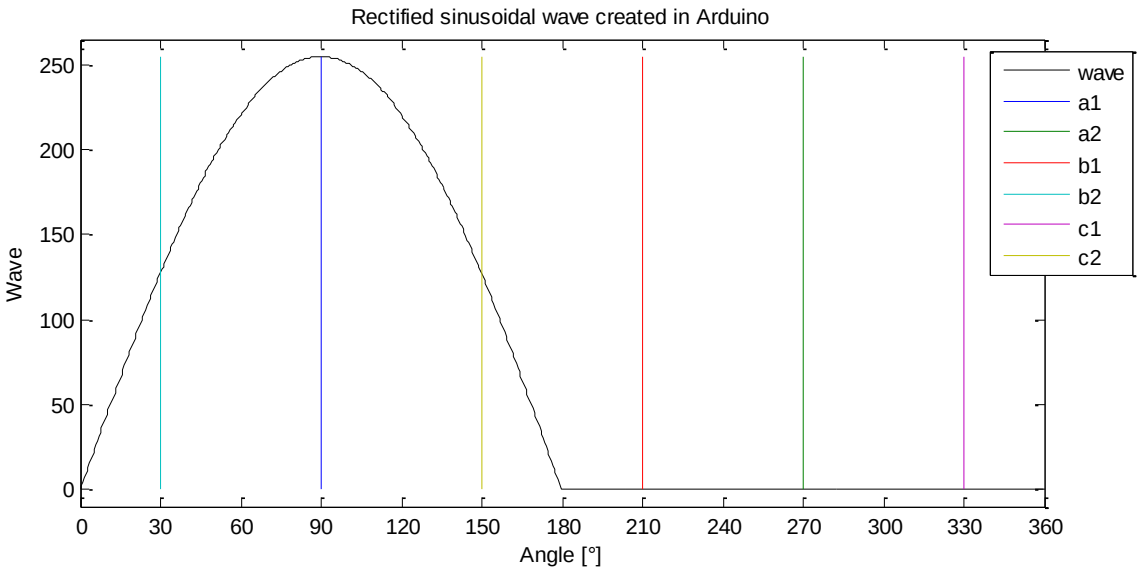

Figure 5.3 – Rectified sinusoidal wave created in Arduino.

The high signals (x_1) are defining the positive half of the final three-phase waves while the low (x_2) are defining the negative part. It must be guaranteed in every case that when a high signal is on, i.e. pointing to the wave crest, the corresponding low signal has to be off, equaling to zero (further detail in Section 5.2.1).

The objective is to have these variables shifting between 0° and 359.5° at a sample speed, f_s, which is related with the desired frequency, f. This sample speed has a direct relation with the sample time, T_s, which is the time the Arduino takes between writing two values in the same signal, given by

$$T_s = \frac{1}{f_s} = \frac{1}{f}\frac{\delta_{step}}{360°} \tag{5.2}$$

5.2.1. Programming Script

The script was created taking in account the demands of the experiments to be concretized. The program had to be able to make the field rotate to a given position, with a given displacement angle, to set a rotating frequency (and this could be achieved by accelerating the field from standing still until the desired frequency, because the rotor is considered to be is stopped when the experiment begins) and even to change from one frequency to another, continuously, without the need to stop. Along these lines, through the Arduino input interface from the software, the following menu was set:

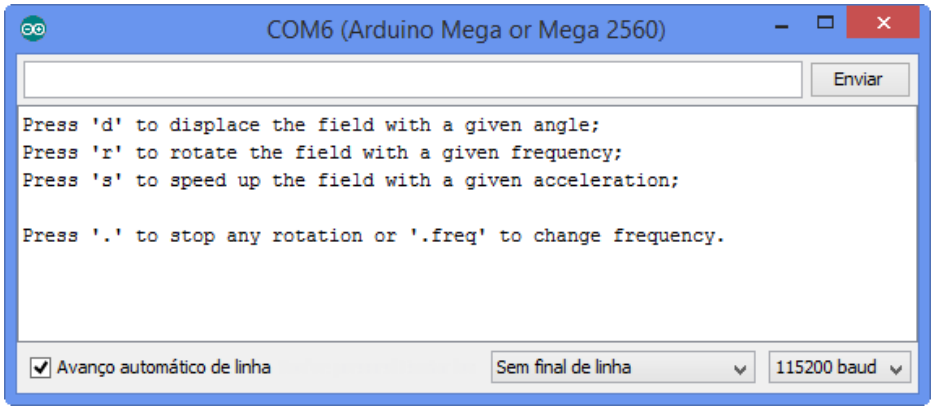

Figure 5.4 – Menu of the created programing script.

This script can be seen entirely in Appendix 4: script_motor.ino.

5.2.2. Test with LEDs

Before connecting the Arduino board to the inverter which in turn is connected to the motor, tests were conducted to make sure the output of the program was running as expected. In this way an equivalent circuit was assembled using six LEDs to match the six signals. The LEDs had two colors, green and red, representing positive and negative part of the wave, respectively.

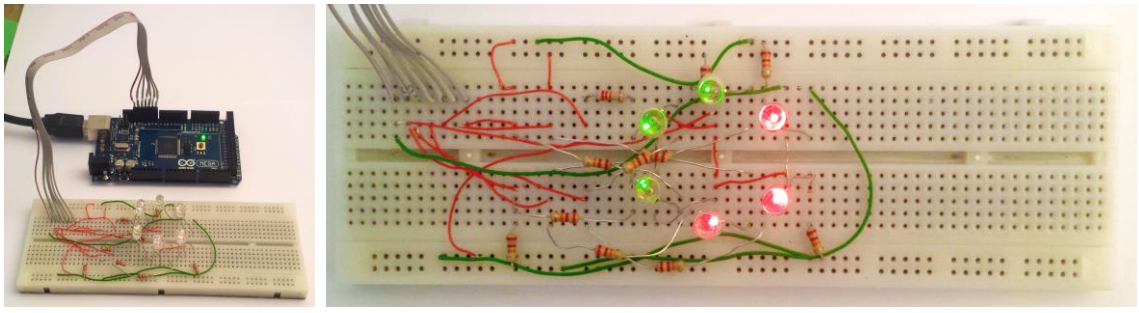

Figure 5.5 – Circuit with LEDs used to test the script.

Each phase is described by two LEDs, placed in opposite sides of the "circle". The test consisted on observing the rotation of the lights according to a predetermined frequency. The first tests led to some subsequent programming code adjustments, but overall the tests have been carried out successfully.

5.3. Inverter

Alongside the Arduino board, a three-phase inverter is needed in order to amplify the PWM-modulated signal to a proper voltage range. With the available components it was constructed the following circuit per phase:

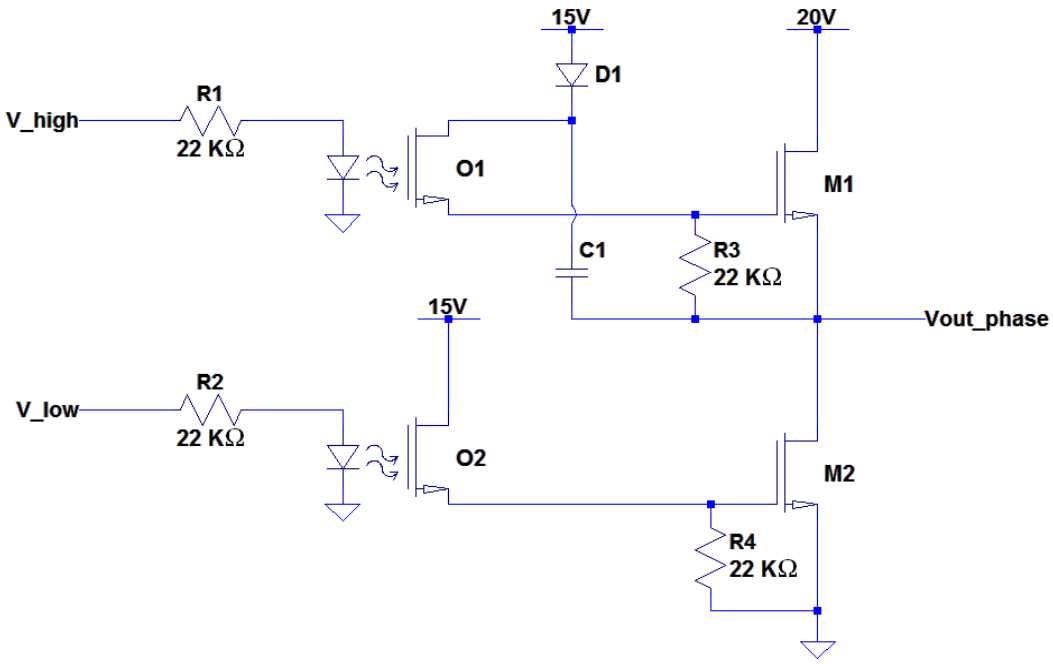

Figure 5.6 – Inverter circuit for one phase.

In each phase, the high/low outputs from the Arduino board are connected to the device O1/O2 which is an optocoupler. It is composed by a LED followed by a phototransistor. This device transfers electrical signals between two isolated circuits by using light, preventing high voltages from affecting the system receiving the signal. In this specific case it used to change the voltage range of the signal coming from the Arduino board.

In the second stage there are two CMOS transistors used to amplify and form the complete wave. The high signal is amplified in a Common Drain topology, so the signal stays positive-signed at the output forming the positive half of the wave. There is need to use the capacitor C1 because the high signal is not referred to the ground, but to the floating output voltage, which is variable.

C1 is charged when current is positive, coming from the 15V-source. When the current is negative, the diode D1 forces the capacitor to feed the optocoupler O1 and the high signal stays referred to the output node.

Analogously, the low signal is amplified in a Common Source topology, inverting the wave sign, which was positive until reaching M2, making the negative part. As abovementioned, it is imperative the high and low signals are 180° apart when pointing to the rectified wave, so both M1 and M2 transistors are never working at the same time. The inverter used can be seen in Figure 5.7.

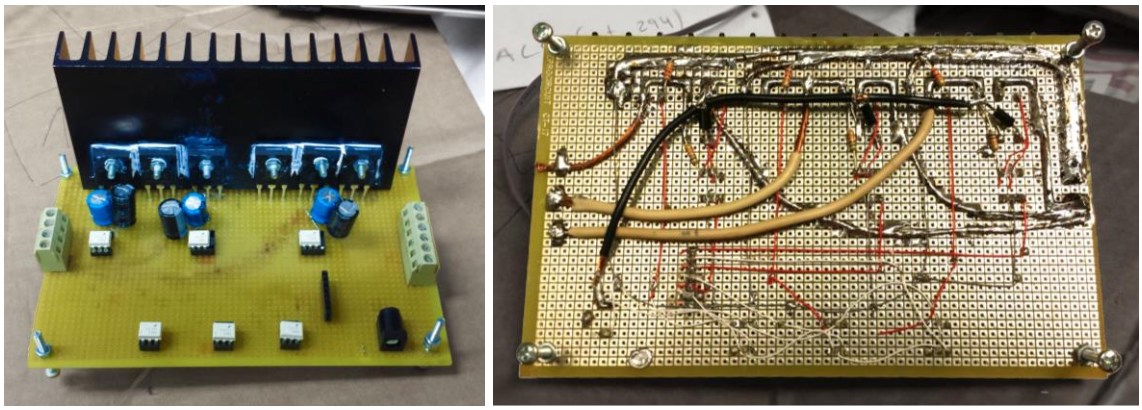

a) **b)**

Figure 5.7 – Inverter used in the experiment: a) view from above with the optocouplers, the capacitors and CMOS transistors; b) view from below with the circuit connections.

Hence, as the each phase output voltage from the inverter is connected to a coil in the motor stator, the current becomes approximately a sinusoidal wave.

5.4. Motor

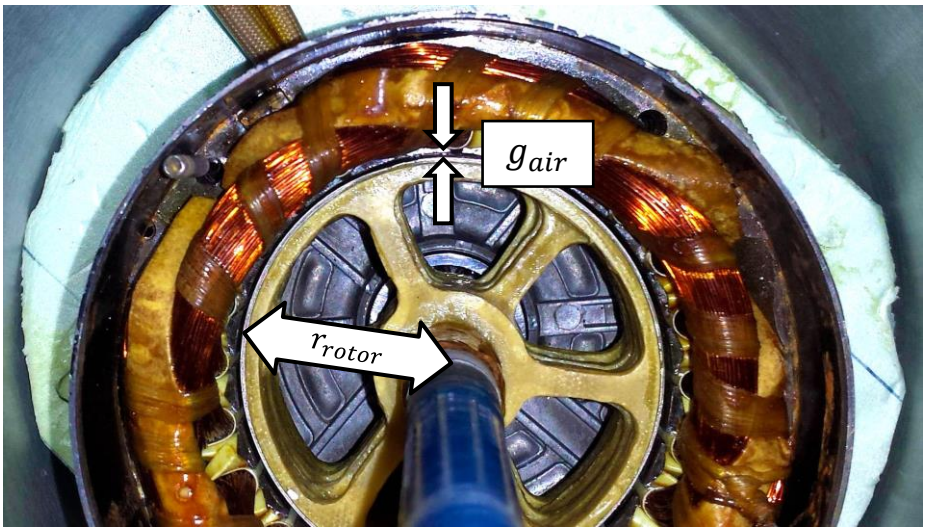

Figure 5.8 – Motor interior.

Table 5.1 – Motor dimensions: rotor radius and air gap.

r_{rotor} [mm]	g_{air} [µm]
38.24	770.4

From Figure 5.8, it is possible to observe the real rotor and airgap dimensions of the motor, stated in Table 5.1. In the stator, each phase contains two coils in series, placed in opposite sides of the stator, just as an induction motor and similarly as the LEDs were disposed in the test circuit. The three phases are connected in Y configuration.

Figure 5.9 depicts how the stacks of 2G HTS tapes are disposed, in the cylindrical surface area of the rotor. Without the stacks, the rotor would be similar to the one in Figure 5.9a. Figure 5.9b shows the used rotor with two stacks.

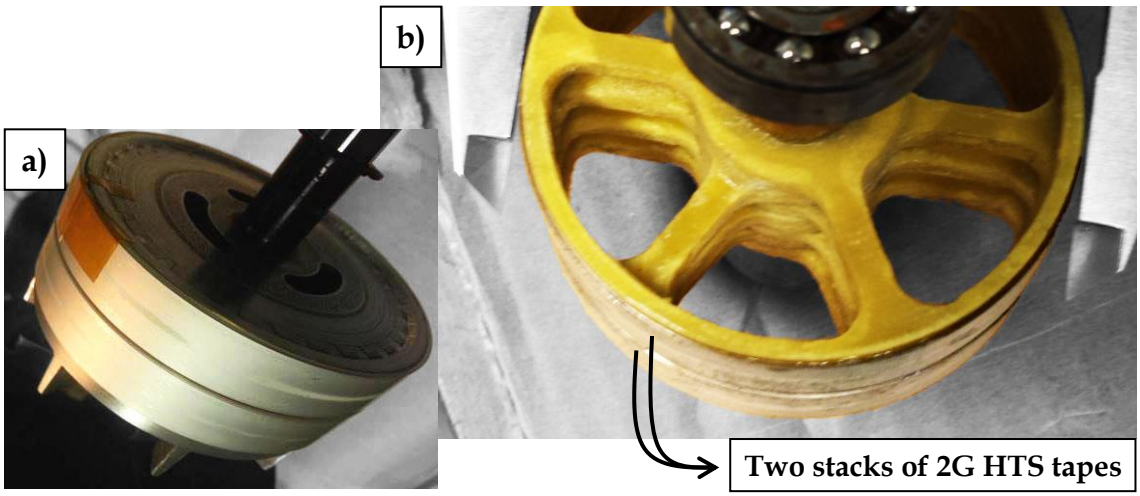

Figure 5.9 – Motor rotor: before (a) and after (b) applying the stacks of 2G HTS tapes.

5.5. Experiment and Results

5.5.1. Voltage and Current

Setting in the laptop a rotating reference frequency of

$$f_{ref} = 0.5 \text{ Hz} \tag{5.3}$$

the motor starts rotating, and the voltage and current from one of the phases are observed in the oscilloscope (Figure 5.10). The current is measured using a voltmeter at the terminals of a 1Ω-resistor. This voltmeter has a factor of 1/10, that is, the real value current amplitude is obtained multiplying by 10.

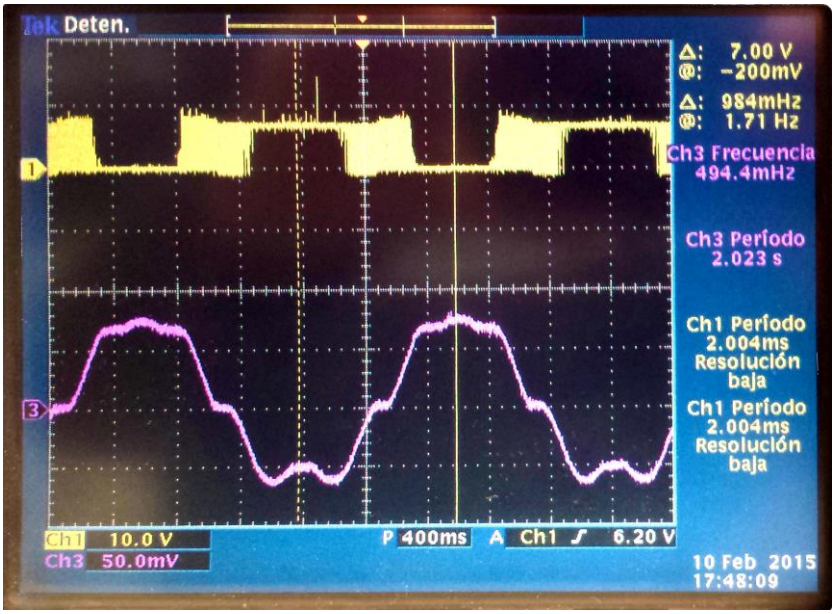

Figure 5.10 – Voltage and current waves measured from one of the phases.

The voltage signal is no more than the PWM-modulated wave, varying in a range of around 10V, while the current, whose waveform is quite similar to a sinusoid. The respective amplitude and frequency can be approximately calculated by observing the oscilloscope. So it goes

$$I_{phase} = 1.5\ \text{div} \times 50\ \text{mA/div} \times 10 = 750\ \text{mA} \tag{5.4}$$

$$f = \frac{1}{T_{cycle}} = \frac{1}{2.023\ \text{s}} = 0.4943\ \text{Hz} \approx f_{ref} \tag{5.5}$$

The final frequency is quite close to the reference, confirming the successful functioning of the script, Arduino board and inverter. For the sinusoidal current,

$$i_{phase}(t) = I_{phase} \sin(2\pi f t) \tag{5.6}$$

5.5.2. Torque

With the purpose to analyze the performance of the motor, the relation between the output torque and the displacement angle of the rotor must be obtained. To achieve this, the motor is set as described in Figure 5.11, using a wheel attached to the motor shaft to measure the angle (Figure 5.11a and b) and a metallic tape, stuck in the wheel and connected to a dynamometer, by means of a yellow pulley (cf. Figure 5.11b and c).

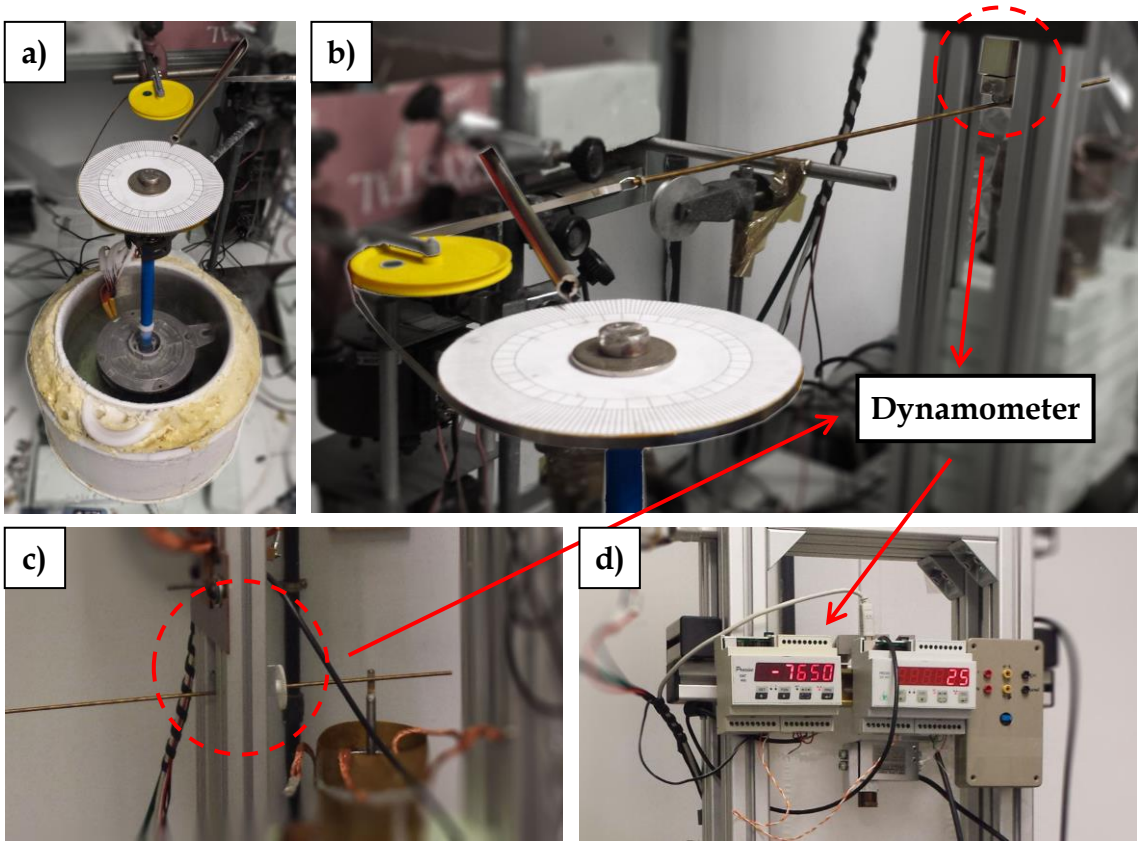

Figure 5.11 – Setting to the torque measurement: a) motor with the shaft connected to the measurement wheel; b) connection between the measurement wheel and the dynamometer; c) connection in the dynamometer; d) dynamometer display.

Basically, the idea is to turn on the magnetic field in a specific position, then cool down the motor adding liquid nitrogen – Field Cooling – and slowly pull the metal tape, using the small white wheel (cf. Figure 5.11c) and forcing the wheel and the shaft to rotate.

Thus, the force imposed by the shaft, F_{motor}, is measured every 2° of rotation, by the dynamometer, in gram-force [gf] (1 kgf = 9.8 N) and shown in the display (cf. Figure 5.11d). Given the diameter, the radius of the measurement wheel attached to the motor shaft is $r_{wheel} = 62.5$ mm and the torque, T_{motor}, is determined by

$$T_{motor}[\mathrm{N \cdot m}] = F_{motor}[\mathrm{gf}] \times r_{wheel}[\mathrm{m}] \times 9.8 \times 10^{-3}\ \mathrm{N/gf} \tag{5.7}$$

The respective graphic representation is exhibited in Figure 5.12.

Figure 5.12 – Output torque as a function of the rotor displacement angle.

Regardless the position of the rotor, the torque reveals to perform constantly around 1 N·m. The visible fluctuations correspond to the alignment with the slots in the stator, which differs depending on the position.

This behavior is typical from the hysteresis motors where the torque depends basically on the volumetric density of magnetic energy w_h stored in the motor, which corresponds to the area of the hysteresis cycle $B(H)$.

6

6. Conclusions and Future Work

The present dissertation was developed during a six month stay in Institut de Ciència de Materials de Barcelona (ICMAB), where distinct materials and machines are available to carry out the most diverse experiences. Especially during this internship, the work was divided into several phases.

Firstly, simulations in the finite element COMSOL software were conducted, which virtually resembles how certain materials react when are involved. There was simulated a YBCO sample, and it has shown maximum flux and current densities in the order of 400 mT and 280 MA/m^2, respectively. Furthermore it was observed that the flux lines do not fully penetrate in the bulk, as it was expected from the definition of HTS.

Secondly, the innovative 2G HTS tape was tested in the laboratory. Regarding the tape resistivity, two experiments were completed: at room temperature, where the resistivity was found to be linear, just like a regular conductor, with the electrical conductivity of 2.3783×10^7 S/m; and in the superconducting state, the resistivity has shown to be practically zero until the current density reaches its critical value of 140.3 MA/m^2 – corresponding to critical current of 51.15 A – from which it exponentially grows.

Finally, and with the supervision of Dr. Xavier Granados, a superconducting motor was built up, where the 2G HTS tapes were applied in the rotor. After a few misfortunes regarding the implementation, it is concluded the motor

has a constant torque of 1 N·m, independent of rotor position angle, making this a hysteresis motor.

Ultimately, a comparison table between the materials used in the work – bulk and tape – is below exposed.

Table 6.1 – Bulks and tapes comparison.

	Bulk	**Tape**
Type II HTS	Yes	Yes
Trapped flux density	Medium	High, if stacked
Protection coat	No	Yes
Mechanical flexibility	Poor, massive block	Good, flexible
Thermal stability	Poor	Good

As future work, it is left to analyze and understand the interesting question of the resulting hysteresis loop from the simulation in COMSOL, present in Figure 3.2 from Chapter 3.

Bibliography

(Bean, 1962) Bean, C. P. (1962). Magnetization of Hard Superconductors. *Physical Review Letters, 8*.

(Bean, 1964) Bean, C. P. (1964). Magnetization of High-Field Superconductors. *Reviews of Modern Physics, 36*.

(Ceballos Martínez, 2011) Ceballos Martínez, J. M. (2011). *Analysis Of AC Losses In Superconducting Electrical Components For Application In The Design Of Electrical Systems.* Universidad de Extremadura - Servicio de Publicaciones.

(Ford *et al.*, 2005) Ford, P. J., & Saunders, G. A. (2005). *The Rise of the Superconductors.* United States of America: CRC PRESS.

(Forrest, 1983) Forrest, A. (1983). Meissner and Ochsenfeld revisited. *4*.

(Krabbes *et al.*, 2006) Krabbes, G., Fuchs, G., Canders, W.-R., May, H., & Palka, R. (2006). *High Temperature Superconductor Bulk Materials.* WILEY-VCH.

(Meissner *et al.*, 1933) Meissner, W., & Ochsenfeld, R. (1933). Ein neuer Effekt bei Eintritt der Supraleitfähigkeitin. *21*.

(Murta-Pina, 2010) Murta-Pina, J. (2010). *Desenho e Modelização de Sistemas de Energia.* Universidade Nova de Lisboa.

(Murta-Pina, *et* Murta-Pina, J., Pereira, P., Ceballos, J., Alvarez, A., Amaro, N., Pronto, A., . . . Arsenio, P. (29 de October de

al., 2014) 2014). *Validation and Application of Sand Pile Modeling of Multiseeded HTS Bulk Superconductors.* Obtido de IEEE Transactions on Applied Superconductivity: http://ieeexplore.ieee.org/xpl/articleDetails.jsp?tp=&arnumber=6939640

(Poole *et al.*, 2007) Poole, C. P., Farach, H. A., Creswick, R. J., & Prozorov, R. (2007). *Superconductivity, 2nd Edition.* Academic Press.

(Rodríguez, 2013) Rodríguez, G. V. (2013). *Modelling the response of thin superconductors to applied magnetic fields and currents.* Universitat Autònoma de Barcelona.

(Selvamanickam, 2014) Selvamanickam, V. (2014, October 8). *Recent Advances in High Temperature Superconductors and Potential Applications.* Retrieved March 11, 2015, from http://vmsstreamer1.fnal.gov/Lectures/Colloquium/presentations/141008Selvamanickam.pdf

(Tinkham, 1996) Tinkham, M. (1996). *Introduction to Superconductivity.* McGraw-Hill.

(Tomita *et al.*, 2003) Tomita, M., & Murakami, M. (2003, January 30). *High-temperature superconductor bulk magnets that can trap magnetic fields of over 17 tesla at 29[thinsp]K : Article : Nature:.* Retrieved November 2014, 17, from Nature: http://www.nature.com/nature/journal/v421/n6922/full/nature01350.html

(Xiong *et al.*, 2007) Xiong, X., Lenseth, K., Reeves, J., Rar, A., Qiao, Y., Schmidt, R., . . . Selvamanickam, V. (2007). *High throughput processing of long-length IBAD MgO and Epi-Buffer templates at SuperPower.* IEEE Transactions on Applied Superconductivity.

Appendixes

1. script_measurements_bulk_tapes.m

```
clc;
clear all;
close all;

x = [0 0.75 1.5 2.25 3 3.75 4.5 5.25 6 6.75 7.5 8.25 9 9.75 10.5 11.25
12 12.75 13.5 14.25 15 15.75 16.5 17.25 18 18.75 19.5 20.25 21 21.75
22.5 23.25 24 24.75 25.5 26.25 27 27.75 28.5 29.25 30 30.75 31.5 32.25
33 33.75 34.5 35.25];
y = [0 0.75 1.5 2.25 3 3.75 4.5 5.25 6 6.75 7.5 8.25 9 9.75 10.5 11.25
12 12.75 13.5 14.25 15 15.75 16.5 17.25 18 18.75 19.5 20.25 21 21.75
22.5 23.25 24 24.75 25.5 26.25 27 27.75 28.5 29.25 30 30.75 31.5 32.25
33 33.75 34.5 35.25 36 36.75 37.5 38.25 39 39.75 40.5 41.25 42 42.75
43.5];

B_bulk_ideal = [-0.01408 -0.01442 -0.01469 -0.0149 -0.01505 -0.0152 -
0.01536 -0.01555 -0.01579 -0.01607 -0.0164 -0.01675 -0.01713 -0.01751
-0.01789 -0.01827 -0.01862 -0.01895 -0.01925 -0.01951 -0.01973 -0.0199
-0.02003 -0.02011 -0.02013 -0.02011 -0.02003 -0.0199 -0.01973 -0.01951
-0.01925 -0.01895 -0.01862 -0.01827 -0.01789 -0.01751 -0.01713 -
0.01675 -0.0164 -0.01607 -0.01579 -0.01555 -0.01536 -0.0152 -0.01505 -
0.0149 -0.01469 -0.01442
    -0.01446 -0.01469 -0.0148 -0.01477 -0.01465 -0.0145 -0.0144 -
0.01438 -0.01445 -0.01461 -0.01484 -0.01513 -0.01546 -0.01582 -0.01619
-0.01656 -0.01692 -0.01726 -0.01757 -0.01784 -0.01807 -0.01825 -
0.01838 -0.01846 -0.01849 -0.01846 -0.01838 -0.01825 -0.01807 -0.01784
-0.01757 -0.01726 -0.01692 -0.01656 -0.01619 -0.01582 -0.01546 -
0.01513 -0.01484 -0.01461 -0.01445 -0.01438 -0.0144 -0.0145 -0.01465 -
0.01477 -0.0148 -0.01469
    -0.01477 -0.01484 -0.01467 -0.01424 -0.01362 -0.01296 -0.0124 -
0.01201 -0.01179 -0.01174 -0.01182 -0.012 -0.01226 -0.01257 -0.01291 -
0.01327 -0.01362 -0.01396 -0.01427 -0.01455 -0.01479 -0.01498 -0.01512
-0.0152 -0.01523 -0.0152 -0.01512 -0.01498 -0.01479 -0.01455 -0.01427
-0.01396 -0.01362 -0.01327 -0.01291 -0.01257 -0.01226 -0.012 -0.01182
-0.01174 -0.01179 -0.01201 -0.0124 -0.01296 -0.01362 -0.01424 -0.01467
-0.01484
```

-0.01503 -0.01486 -0.01429 -0.01322 -0.01178 -0.01026 -0.00895 -
0.00797 -0.0073 -0.00692 -0.00676 -0.00677 -0.00691 -0.00714 -0.00743
-0.00775 -0.00809 -0.00842 -0.00873 -0.00901 -0.00925 -0.00944 -
0.00959 -0.00967 -0.0097 -0.00967 -0.00959 -0.00944 -0.00925 -0.00901
-0.00873 -0.00842 -0.00809 -0.00775 -0.00743 -0.00714 -0.00691 -
0.00677 -0.00676 -0.00692 -0.0073 -0.00797 -0.00895 -0.01026 -0.01178
-0.01322 -0.01429 -0.01486
-0.01524 -0.0148 -0.01372 -0.01184 -0.00927 -0.00651 -0.00407 -
0.00218 -0.00083 4.73E-05 0.000566 0.00081 0.000851 0.000749 0.000547
0.000283 -1.39E-05 -0.00032 -0.00062 -0.0009 -0.00114 -0.00133 -
0.00148 -0.00156 -0.00159 -0.00156 -0.00148 -0.00133 -0.00114 -0.0009
-0.00062 -0.00032 -1.39E-05 0.000283 0.000547 0.000749 0.000851
0.00081 0.000566 4.73E-05 -0.00083 -0.00218 -0.00407 -0.00651 -0.00927
-0.01184 -0.01372 -0.0148
-0.01545 -0.01472 -0.01313 -0.01039 -0.00658 -0.00234 0.001577
0.004739 0.007073 0.008685 0.009731 0.010353 0.010663 0.01075 0.010681
0.010508 0.010272 0.010005 0.009731 0.009471 0.009239 0.009048
0.008905 0.008817 0.008787 0.008817 0.008905 0.009048 0.009239
0.009471 0.009731 0.010005 0.010272 0.010508 0.010681 0.01075 0.010663
0.010353 0.009731 0.008685 0.007073 0.004739 0.001577 -0.00234 -
0.00658 -0.01039 -0.01313 -0.01472
-0.01567 -0.01469 -0.01264 -0.00915 -0.00421 0.001503 0.007074
0.011821 0.015489 0.01813 0.019932 0.021098 0.021796 0.022158 0.022285
0.022249 0.022108 0.021906 0.021676 0.021444 0.02123 0.021049 0.020912
0.020827 0.020799 0.020827 0.020912 0.021049 0.02123 0.021444 0.021676
0.021906 0.022108 0.022249 0.022285 0.022158 0.021796 0.021098
0.019932 0.01813 0.015489 0.011821 0.007074 0.001503 -0.00421 -0.00915
-0.01264 -0.01469
-0.01594 -0.01474 -0.01233 -0.00824 -0.0024 0.004582 0.011737
0.018215 0.023518 0.027526 0.030378 0.032314 0.033566 0.034324
0.034731 0.034895 0.034895 0.034791 0.034629 0.034443 0.03426 0.034099
0.033974 0.033896 0.033869 0.033896 0.033974 0.034099 0.03426 0.034443
0.034629 0.034791 0.034895 0.034895 0.034731 0.034324 0.033566
0.032314 0.030378 0.027526 0.023518 0.018215 0.011737 0.004582 -0.0024
-0.00824 -0.01233 -0.01474
-0.01627 -0.0149 -0.0122 -0.00767 -0.00115 0.006821 0.015309
0.023422 0.030491 0.036159 0.040395 0.043393 0.045424 0.046742
0.047549 0.047998 0.0482 0.04824 0.04818 0.048065 0.04793 0.047801
0.047697 0.04763 0.047607 0.04763 0.047697 0.047801 0.04793 0.048065
0.04818 0.04824 0.0482 0.047998 0.047549 0.046742 0.045424 0.043393
0.040395 0.036159 0.030491 0.023422 0.015309 0.006821 -0.00115 -
0.00767 -0.0122 -0.0149
-0.01664 -0.01515 -0.01225 -0.00739 -0.00037 0.008327 0.017842
0.027321 0.036049 0.043501 0.049411 0.053802 0.056902 0.059004
0.060376 0.061229 0.06172 0.061966 0.062052 0.06204 0.061977 0.061897
0.061825 0.061775 0.061757 0.061775 0.061825 0.061897 0.061977 0.06204
0.062052 0.061966 0.06172 0.061229 0.060376 0.059004 0.056902 0.053802
0.049411 0.043501 0.036049 0.027321 0.017842 0.008327 -0.00037 -
0.00739 -0.01225 -0.01515
-0.01706 -0.01548 -0.01244 -0.00734 3.38E-05 0.009256 0.019524
0.03005 0.040161 0.049286 0.056989 0.063061 0.06756 0.070736 0.072897
0.074318 0.075216 0.075754 0.076047 0.076184 0.076225 0.076216
0.076189 0.076164 0.076155 0.076164 0.076189 0.076216 0.076225
0.076184 0.076047 0.075754 0.075216 0.074318 0.072897 0.070736 0.06756
0.063061 0.056989 0.049286 0.040161 0.03005 0.019524 0.009256 3.38E-05
-0.00734 -0.01244 -0.01548
-0.01753 -0.01589 -0.01274 -0.00747 0.000151 0.009746 0.020555
0.031848 0.043018 0.053534 0.062918 0.07079 0.076975 0.081555 0.084793
0.087006 0.088476 0.089422 0.090009 0.090353 0.090541 0.090634

0.090672 0.090684 0.090687 0.090684 0.090672 0.090634 0.090541
0.090353 0.090009 0.089422 0.088476 0.087006 0.084793 0.081555
0.076975 0.07079 0.062918 0.053534 0.043018 0.031848 0.020555 0.009746
0.000151 -0.00747 -0.01274 -0.01589
    -0.01802 -0.01634 -0.01312 -0.00775 5.32E-05 0.009912 0.021104
0.032947 0.044892 0.056475 0.067256 0.076813 0.084803 0.091072
0.095718 0.099011 0.101274 0.102793 0.10379 0.104426 0.10482 0.105054
0.105184 0.105248 0.105268 0.105248 0.105184 0.105054 0.10482 0.104426
0.10379 0.102793 0.101274 0.099011 0.095718 0.091072 0.084803 0.076813
0.067256 0.056475 0.044892 0.032947 0.021104 0.009912 5.32E-05 -
0.00775 -0.01312 -0.01634
    -0.01853 -0.01684 -0.01357 -0.00812 -0.0002 0.009839 0.021302
0.033535 0.046036 0.058399 0.070251 0.081209 0.090888 0.098965
0.105303 0.110006 0.113352 0.115666 0.117234 0.118278 0.118959
0.119389 0.119648 0.119784 0.119826 0.119784 0.119648 0.119389
0.118959 0.118278 0.117234 0.115666 0.113352 0.110006 0.105303
0.098965 0.090888 0.081209 0.070251 0.058399 0.046036 0.033535
0.021302 0.009839 -0.0002 -0.00812 -0.01357 -0.01684
    -0.01905 -0.01735 -0.01407 -0.00857 -0.00057 0.009596 0.021247
0.033755 0.04665 0.059573 0.072209 0.084242 0.095326 0.105095 0.113243
0.119641 0.124397 0.127793 0.130154 0.131765 0.132845 0.133549
0.133985 0.134221 0.134296 0.134221 0.133985 0.133549 0.132845
0.131765 0.130154 0.127793 0.124397 0.119641 0.113243 0.105095
0.095326 0.084242 0.072209 0.059573 0.04665 0.033755 0.021247 0.009596
-0.00057 -0.00857 -0.01407 -0.01735
    -0.01957 -0.01788 -0.01459 -0.00907 -0.00102 0.009234 0.021014
0.033713 0.046887 0.060207 0.073407 0.086227 0.098389 0.109566
0.119408 0.127617 0.134068 0.138873 0.142312 0.144708 0.146343
0.147428 0.148109 0.148483 0.148602 0.148483 0.148109 0.147428
0.146343 0.144708 0.142312 0.138873 0.134068 0.127617 0.119408
0.109566 0.098389 0.086227 0.073407 0.060207 0.046887 0.033713
0.021014 0.009234 -0.00102 -0.00907 -0.01459 -0.01788
    -0.02008 -0.0184 -0.01512 -0.00959 -0.00151 0.008792 0.020658
0.03349 0.046858 0.06046 0.07406 0.087447 0.100399 0.112655 0.123907
0.133811 0.142073 0.148569 0.153411 0.156874 0.159277 0.16089 0.161914
0.162479 0.16266 0.162479 0.161914 0.16089 0.159277 0.156874 0.153411
0.148569 0.142073 0.133811 0.123907 0.112655 0.100399 0.087447 0.07406
0.06046 0.046858 0.03349 0.020658 0.008792 -0.00151 -0.00959 -0.01512
-0.0184
    -0.02058 -0.01892 -0.01565 -0.01012 -0.00203 0.008303 0.020223
0.033144 0.046647 0.060447 0.074332 0.088122 0.101642 0.114691
0.127024 0.138337 0.148292 0.156594 0.163118 0.167969 0.171414
0.173759 0.175259 0.176092 0.176359 0.176092 0.175259 0.173759
0.171414 0.167969 0.163118 0.156594 0.148292 0.138337 0.127024
0.114691 0.101642 0.088122 0.074332 0.060447 0.046647 0.033144
0.020223 0.008303 -0.00203 -0.01012 -0.01565 -0.01892
    -0.02106 -0.01942 -0.01616 -0.01065 -0.00255 0.007791 0.019744
0.032722 0.046316 0.060254 0.074339 0.088417 0.102343 0.115963
0.129088 0.141481 0.152842 0.16283 0.171147 0.17766 0.18246 0.1858
0.18796 0.189166 0.189553 0.189166 0.18796 0.1858 0.18246 0.17766
0.171147 0.16283 0.152842 0.141481 0.129088 0.115963 0.102343 0.088417
0.074339 0.060254 0.046316 0.032722 0.019744 0.007791 -0.00255 -
0.01065 -0.01616 -0.01942
    -0.02151 -0.0199 -0.01666 -0.01115 -0.00307 0.007276 0.019245
0.032258 0.045913 0.059945 0.074171 0.088452 0.102667 0.116694
0.130391 0.143575 0.156011 0.167395 0.177382 0.185661 0.192081
0.196712 0.19977 0.201495 0.202051 0.201495 0.19977 0.196712 0.192081
0.185661 0.177382 0.167395 0.156011 0.143575 0.130391 0.116694

```
0.102667 0.088452 0.074171 0.059945 0.045913 0.032258 0.019245
0.007276 -0.00307 -0.01115 -0.01666 -0.0199
    -0.02193 -0.02034 -0.01712 -0.01164 -0.00357 0.006775 0.018749
0.031781 0.045473 0.059568 0.073891 0.088315 0.102736 0.117054
0.131157 0.14491 0.158131 0.170579 0.181941 0.191856 0.19999 0.206156
0.210377 0.212805 0.213594 0.212805 0.210377 0.206156 0.19999 0.191856
0.181941 0.170579 0.158131 0.14491 0.131157 0.117054 0.102736 0.088315
0.073891 0.059568 0.045473 0.031781 0.018749 0.006775 -0.00357 -
0.01164 -0.01712 -0.02034
    -0.02232 -0.02075 -0.01755 -0.01209 -0.00403 0.0063 0.018271
0.031311 0.045025 0.059161 0.07355 0.088074 0.10264 0.117164 0.131557
0.145713 0.159495 0.172714 0.185116 0.196366 0.206069 0.213843 0.21943
0.222756 0.223855 0.222756 0.21943 0.213843 0.206069 0.196366 0.185116
0.172714 0.159495 0.145713 0.131557 0.117164 0.10264 0.088074 0.07355
0.059161 0.045025 0.031311 0.018271 0.0063 -0.00403 -0.01209 -0.01755
-0.02075
    -0.02267 -0.02112 -0.01794 -0.0125 -0.00446 0.005862 0.017826
0.030865 0.044591 0.058751 0.073184 0.087776 0.102443 0.117113
0.131712 0.146154 0.16033 0.174094 0.187239 0.199482 0.210444 0.219659
0.226639 0.230984 0.232457 0.230984 0.226639 0.219659 0.210444
0.199482 0.187239 0.174094 0.16033 0.146154 0.131712 0.117113 0.102443
0.087776 0.073184 0.058751 0.044591 0.030865 0.017826 0.005862 -
0.00446 -0.0125 -0.01794 -0.02112
    -0.02297 -0.02144 -0.01829 -0.01286 -0.00484 0.005468 0.017422
0.030457 0.044186 0.058361 0.072821 0.087459 0.102197 0.116969
0.131712 0.146355 0.160807 0.174949 0.188609 0.201545 0.213415
0.223741 0.23191 0.237223 0.239078 0.237223 0.23191 0.223741 0.213415
0.201545 0.188609 0.174949 0.160807 0.146355 0.131712 0.116969
0.102197 0.087459 0.072821 0.058361 0.044186 0.030457 0.017422
0.005468 -0.00484 -0.01286 -0.01829 -0.02144
    -0.02323 -0.02172 -0.01858 -0.01317 -0.00517 0.005125 0.017068
0.030097 0.043825 0.058007 0.072484 0.087152 0.101938 0.11678 0.131624
0.146406 0.161049 0.175449 0.189457 0.202857 0.215333 0.226416
0.235431 0.241481 0.243641 0.241481 0.235431 0.226416 0.215333
0.202857 0.189457 0.175449 0.161049 0.146406 0.131624 0.11678 0.101938
0.087152 0.072484 0.058007 0.043825 0.030097 0.017068 0.005125 -
0.00517 -0.01317 -0.01858 -0.02172
    -0.02345 -0.02195 -0.01883 -0.01343 -0.00544 0.004838 0.016771
0.029793 0.043518 0.057702 0.072188 0.086876 0.101693 0.116583
0.131495 0.146373 0.161146 0.175719 0.189956 0.203656 0.216514
0.228065 0.237598 0.244099 0.246448 0.244099 0.237598 0.228065
0.216514 0.203656 0.189956 0.175719 0.161146 0.146373 0.131495
0.116583 0.101693 0.086876 0.072188 0.057702 0.043518 0.029793
0.016771 0.004838 -0.00544 -0.01343 -0.01883 -0.02195
    -0.02362 -0.02214 -0.01902 -0.01364 -0.00566 0.004612 0.016536
0.029551 0.043272 0.057455 0.071947 0.086646 0.101484 0.116405
0.131363 0.146303 0.161161 0.175848 0.190232 0.204119 0.217207
0.229028 0.238845 0.245582 0.248027 0.245582 0.238845 0.229028
0.217207 0.204119 0.190232 0.175848 0.161161 0.146303 0.131363
0.116405 0.101484 0.086646 0.071947 0.057455 0.043272 0.029551
0.016536 0.004612 -0.00566 -0.01364 -0.01902 -0.02214
    -0.02374 -0.02227 -0.01916 -0.01379 -0.00581 0.004448 0.016365
0.029375 0.043092 0.057275 0.071769 0.086475 0.101324 0.116265
0.131251 0.146231 0.161143 0.175899 0.190372 0.204369 0.217589
0.229557 0.239519 0.246371 0.248859 0.246371 0.239519 0.229557
0.217589 0.204369 0.190372 0.175899 0.161143 0.146231 0.131251
0.116265 0.101324 0.086475 0.071769 0.057275 0.043092 0.029375
0.016365 0.004448 -0.00581 -0.01379 -0.01916 -0.02227
```

-0.02382 -0.02235 -0.01925 -0.01388 -0.00591 0.004349 0.016262
0.029268 0.042983 0.057164 0.071659 0.086369 0.101225 0.116176
0.131178 0.146179 0.16112 0.175914 0.190435 0.204489 0.217776 0.229815
0.239845 0.246748 0.249255 0.246748 0.239845 0.229815 0.217776
0.204489 0.190435 0.175914 0.16112 0.146179 0.131178 0.116176 0.101225
0.086369 0.071659 0.057164 0.042983 0.029268 0.016262 0.004349 -
0.00591 -0.01388 -0.01925 -0.02235
-0.02384 -0.02237 -0.01928 -0.01391 -0.00594 0.004316 0.016227
0.029232 0.042946 0.057127 0.071622 0.086333 0.101191 0.116146
0.131152 0.146161 0.16111 0.175916 0.190452 0.204524 0.217831 0.229892
0.239942 0.246859 0.249371 0.246859 0.239942 0.229892 0.217831
0.204524 0.190452 0.175916 0.16111 0.146161 0.131152 0.116146 0.101191
0.086333 0.071622 0.057127 0.042946 0.029232 0.016227 0.004316 -
0.00594 -0.01391 -0.01928 -0.02237
-0.02382 -0.02235 -0.01925 -0.01388 -0.00591 0.004349 0.016262
0.029268 0.042983 0.057164 0.071659 0.086369 0.101225 0.116176
0.131178 0.146179 0.16112 0.175914 0.190435 0.204489 0.217776 0.229815
0.239845 0.246748 0.249255 0.246748 0.239845 0.229815 0.217776
0.204489 0.190435 0.175914 0.16112 0.146179 0.131178 0.116176 0.101225
0.086369 0.071659 0.057164 0.042983 0.029268 0.016262 0.004349 -
0.00591 -0.01388 -0.01925 -0.02235
-0.02374 -0.02227 -0.01916 -0.01379 -0.00581 0.004448 0.016365
0.029375 0.043092 0.057275 0.071769 0.086475 0.101324 0.116265
0.131251 0.146231 0.161143 0.175899 0.190372 0.204369 0.217589
0.229557 0.239519 0.246371 0.248859 0.246371 0.239519 0.229557
0.217589 0.204369 0.190372 0.175899 0.161143 0.146231 0.131251
0.116265 0.101324 0.086475 0.071769 0.057275 0.043092 0.029375
0.016365 0.004448 -0.00581 -0.01379 -0.01916 -0.02227
-0.02362 -0.02214 -0.01902 -0.01364 -0.00566 0.004612 0.016536
0.029551 0.043272 0.057455 0.071947 0.086646 0.101484 0.116405
0.131363 0.146303 0.161161 0.175848 0.190232 0.204119 0.217207
0.229028 0.238845 0.245582 0.248027 0.245582 0.238845 0.229028
0.217207 0.204119 0.190232 0.175848 0.161161 0.146303 0.131363
0.116405 0.101484 0.086646 0.071947 0.057455 0.043272 0.029551
0.016536 0.004612 -0.00566 -0.01364 -0.01902 -0.02214
-0.02345 -0.02195 -0.01883 -0.01343 -0.00544 0.004838 0.016771
0.029793 0.043518 0.057702 0.072188 0.086876 0.101693 0.116583
0.131495 0.146373 0.161146 0.175719 0.189956 0.203656 0.216514
0.228065 0.237598 0.244099 0.246448 0.244099 0.237598 0.228065
0.216514 0.203656 0.189956 0.175719 0.161146 0.146373 0.131495
0.116583 0.101693 0.086876 0.072188 0.057702 0.043518 0.029793
0.016771 0.004838 -0.00544 -0.01343 -0.01883 -0.02195
-0.02323 -0.02172 -0.01858 -0.01317 -0.00517 0.005125 0.017068
0.030097 0.043825 0.058007 0.072484 0.087152 0.101938 0.11678 0.131624
0.146406 0.161049 0.175449 0.189457 0.202857 0.215333 0.226416
0.235431 0.241481 0.243641 0.241481 0.235431 0.226416 0.215333
0.202857 0.189457 0.175449 0.161049 0.146406 0.131624 0.11678 0.101938
0.087152 0.072484 0.058007 0.043825 0.030097 0.017068 0.005125 -
0.00517 -0.01317 -0.01858 -0.02172
-0.02297 -0.02144 -0.01829 -0.01286 -0.00484 0.005468 0.017422
0.030457 0.044186 0.058361 0.072821 0.087459 0.102197 0.116969
0.131712 0.146355 0.160807 0.174949 0.188609 0.201545 0.213415
0.223741 0.23191 0.237223 0.239078 0.237223 0.23191 0.223741 0.213415
0.201545 0.188609 0.174949 0.160807 0.146355 0.131712 0.116969
0.102197 0.087459 0.072821 0.058361 0.044186 0.030457 0.017422
0.005468 -0.00484 -0.01286 -0.01829 -0.02144
-0.02267 -0.02112 -0.01794 -0.0125 -0.00446 0.005862 0.017826
0.030865 0.044591 0.058751 0.073184 0.087776 0.102443 0.117113
0.131712 0.146154 0.16033 0.174094 0.187239 0.199482 0.210444 0.219659

```
0.226639 0.230984 0.232457 0.230984 0.226639 0.219659 0.210444
0.199482 0.187239 0.174094 0.16033 0.146154 0.131712 0.117113 0.102443
0.087776 0.073184 0.058751 0.044591 0.030865 0.017826 0.005862 -
0.00446 -0.0125 -0.01794 -0.02112
    -0.02232 -0.02075 -0.01755 -0.01209 -0.00403 0.0063 0.018271
0.031311 0.045025 0.059161 0.07355 0.088074 0.10264 0.117164 0.131557
0.145713 0.159495 0.172714 0.185116 0.196366 0.206069 0.213843 0.21943
0.222756 0.223855 0.222756 0.21943 0.213843 0.206069 0.196366 0.185116
0.172714 0.159495 0.145713 0.131557 0.117164 0.10264 0.088074 0.07355
0.059161 0.045025 0.031311 0.018271 0.0063 -0.00403 -0.01209 -0.01755
-0.02075
    -0.02193 -0.02034 -0.01712 -0.01164 -0.00357 0.006775 0.018749
0.031781 0.045473 0.059568 0.073891 0.088315 0.102736 0.117054
0.131157 0.14491 0.158131 0.170579 0.181941 0.191856 0.19999 0.206156
0.210377 0.212805 0.213594 0.212805 0.210377 0.206156 0.19999 0.191856
0.181941 0.170579 0.158131 0.14491 0.131157 0.117054 0.102736 0.088315
0.073891 0.059568 0.045473 0.031781 0.018749 0.006775 -0.00357 -
0.01164 -0.01712 -0.02034
    -0.02151 -0.0199 -0.01666 -0.01115 -0.00307 0.007276 0.019245
0.032258 0.045913 0.059945 0.074171 0.088452 0.102667 0.116694
0.130391 0.143575 0.156011 0.167395 0.177382 0.185661 0.192081
0.196712 0.19977 0.201495 0.202051 0.201495 0.19977 0.196712 0.192081
0.185661 0.177382 0.167395 0.156011 0.143575 0.130391 0.116694
0.102667 0.088452 0.074171 0.059945 0.045913 0.032258 0.019245
0.007276 -0.00307 -0.01115 -0.01666 -0.0199
    -0.02106 -0.01942 -0.01616 -0.01065 -0.00255 0.007791 0.019744
0.032722 0.046316 0.060254 0.074339 0.088417 0.102343 0.115963
0.129088 0.141481 0.152842 0.16283 0.171147 0.17766 0.18246 0.1858
0.18796 0.189166 0.189553 0.189166 0.18796 0.1858 0.18246 0.17766
0.171147 0.16283 0.152842 0.141481 0.129088 0.115963 0.102343 0.088417
0.074339 0.060254 0.046316 0.032722 0.019744 0.007791 -0.00255 -
0.01065 -0.01616 -0.01942
    -0.02058 -0.01892 -0.01565 -0.01012 -0.00203 0.008303 0.020223
0.033144 0.046647 0.060447 0.074332 0.088122 0.101642 0.114691
0.127024 0.138337 0.148292 0.156594 0.163118 0.167969 0.171414
0.173759 0.175259 0.176092 0.176359 0.176092 0.175259 0.173759
0.171414 0.167969 0.163118 0.156594 0.148292 0.138337 0.127024
0.114691 0.101642 0.088122 0.074332 0.060447 0.046647 0.033144
0.020223 0.008303 -0.00203 -0.01012 -0.01565 -0.01892
    -0.02008 -0.0184 -0.01512 -0.00959 -0.00151 0.008792 0.020658
0.03349 0.046858 0.06046 0.07406 0.087447 0.100399 0.112655 0.123907
0.133811 0.142073 0.148569 0.153411 0.156874 0.159277 0.16089 0.161914
0.162479 0.16266 0.162479 0.161914 0.16089 0.159277 0.156874 0.153411
0.148569 0.142073 0.133811 0.123907 0.112655 0.100399 0.087447 0.07406
0.06046 0.046858 0.03349 0.020658 0.008792 -0.00151 -0.00959 -0.01512
-0.0184
    -0.01957 -0.01788 -0.01459 -0.00907 -0.00102 0.009234 0.021014
0.033713 0.046887 0.060207 0.073407 0.086227 0.098389 0.109566
0.119408 0.127617 0.134068 0.138873 0.142312 0.144708 0.146343
0.147428 0.148109 0.148483 0.148602 0.148483 0.148109 0.147428
0.146343 0.144708 0.142312 0.138873 0.134068 0.127617 0.119408
0.109566 0.098389 0.086227 0.073407 0.060207 0.046887 0.033713
0.021014 0.009234 -0.00102 -0.00907 -0.01459 -0.01788
    -0.01905 -0.01735 -0.01407 -0.00857 -0.00057 0.009596 0.021247
0.033755 0.04665 0.059573 0.072209 0.084242 0.095326 0.105095 0.113243
0.119641 0.124397 0.127793 0.130154 0.131765 0.132845 0.133549
0.133985 0.134221 0.134296 0.134221 0.133985 0.133549 0.132845
0.131765 0.130154 0.127793 0.124397 0.119641 0.113243 0.105095
```

```
0.095326 0.084242 0.072209 0.059573 0.04665 0.033755 0.021247 0.009596
-0.00057 -0.00857 -0.01407 -0.01735
    -0.01853 -0.01684 -0.01357 -0.00812 -0.0002 0.009839 0.021302
0.033535 0.046036 0.058399 0.070251 0.081209 0.090888 0.098965
0.105303 0.110006 0.113352 0.115666 0.117234 0.118278 0.118959
0.119389 0.119648 0.119784 0.119826 0.119784 0.119648 0.119389
0.118959 0.118278 0.117234 0.115666 0.113352 0.110006 0.105303
0.098965 0.090888 0.081209 0.070251 0.058399 0.046036 0.033535
0.021302 0.009839 -0.0002 -0.00812 -0.01357 -0.01684
    -0.01802 -0.01634 -0.01312 -0.00775 5.32E-05 0.009912 0.021104
0.032947 0.044892 0.056475 0.067256 0.076813 0.084803 0.091072
0.095718 0.099011 0.101274 0.102793 0.10379 0.104426 0.10482 0.105054
0.105184 0.105248 0.105268 0.105248 0.105184 0.105054 0.10482 0.104426
0.10379 0.102793 0.101274 0.099011 0.095718 0.091072 0.084803 0.076813
0.067256 0.056475 0.044892 0.032947 0.021104 0.009912 5.32E-05 -
0.00775 -0.01312 -0.01634
    -0.01753 -0.01589 -0.01274 -0.00747 0.000151 0.009746 0.020555
0.031848 0.043018 0.053534 0.062918 0.07079 0.076975 0.081555 0.084793
0.087006 0.088476 0.089422 0.090009 0.090353 0.090541 0.090634
0.090672 0.090684 0.090687 0.090684 0.090672 0.090634 0.090541
0.090353 0.090009 0.089422 0.088476 0.087006 0.084793 0.081555
0.076975 0.07079 0.062918 0.053534 0.043018 0.031848 0.020555 0.009746
0.000151 -0.00747 -0.01274 -0.01589
    -0.01706 -0.01548 -0.01244 -0.00734 3.38E-05 0.009256 0.019524
0.03005 0.040161 0.049286 0.056989 0.063061 0.06756 0.070736 0.072897
0.074318 0.075216 0.075754 0.076047 0.076184 0.076225 0.076216
0.076189 0.076164 0.076155 0.076164 0.076189 0.076216 0.076225
0.076184 0.076047 0.075754 0.075216 0.074318 0.072897 0.070736 0.06756
0.063061 0.056989 0.049286 0.040161 0.03005 0.019524 0.009256 3.38E-05
-0.00734 -0.01244 -0.01548
    -0.01664 -0.01515 -0.01225 -0.00739 -0.00037 0.008327 0.017842
0.027321 0.036049 0.043501 0.049411 0.053802 0.056902 0.059004
0.060376 0.061229 0.06172 0.061966 0.062052 0.06204 0.061977 0.061897
0.061825 0.061775 0.061757 0.061775 0.061825 0.061897 0.061977 0.06204
0.062052 0.061966 0.06172 0.061229 0.060376 0.059004 0.056902 0.053802
0.049411 0.043501 0.036049 0.027321 0.017842 0.008327 -0.00037 -
0.00739 -0.01225 -0.01515
    -0.01627 -0.0149 -0.0122 -0.00767 -0.00115 0.006821 0.015309
0.023422 0.030491 0.036159 0.040395 0.043393 0.045424 0.046742
0.047549 0.047998 0.0482 0.04824 0.04818 0.048065 0.04793 0.047801
0.047697 0.04763 0.047607 0.04763 0.047697 0.047801 0.04793 0.048065
0.04818 0.04824 0.0482 0.047998 0.047549 0.046742 0.045424 0.043393
0.040395 0.036159 0.030491 0.023422 0.015309 0.006821 -0.00115 -
0.00767 -0.0122 -0.0149
    -0.01594 -0.01474 -0.01233 -0.00824 -0.0024 0.004582 0.011737
0.018215 0.023518 0.027526 0.030378 0.032314 0.033566 0.034324
0.034731 0.034895 0.034895 0.034791 0.034629 0.034443 0.03426 0.034099
0.033974 0.033896 0.033869 0.033896 0.033974 0.034099 0.03426 0.034443
0.034629 0.034791 0.034895 0.034895 0.034731 0.034324 0.033566
0.032314 0.030378 0.027526 0.023518 0.018215 0.011737 0.004582 -0.0024
-0.00824 -0.01233 -0.01474
    -0.01567 -0.01469 -0.01264 -0.00915 -0.00421 0.001503 0.007074
0.011821 0.015489 0.01813 0.019932 0.021098 0.021796 0.022158 0.022285
0.022249 0.022108 0.021906 0.021676 0.021444 0.02123 0.021049 0.020912
0.020827 0.020799 0.020827 0.020912 0.021049 0.02123 0.021444 0.021676
0.021906 0.022108 0.022249 0.022285 0.022158 0.021796 0.021098
0.019932 0.01813 0.015489 0.011821 0.007074 0.001503 -0.00421 -0.00915
-0.01264 -0.01469
```

```
    -0.01545 -0.01472 -0.01313 -0.01039 -0.00658 -0.00234 0.001577
0.004739 0.007073 0.008685 0.009731 0.010353 0.010663 0.01075 0.010681
0.010508 0.010272 0.010005 0.009731 0.009471 0.009239 0.009048
0.008905 0.008817 0.008787 0.008817 0.008905 0.009048 0.009239
0.009471 0.009731 0.010005 0.010272 0.010508 0.010681 0.01075 0.010663
0.010353 0.009731 0.008685 0.007073 0.004739 0.001577 -0.00234 -
0.00658 -0.01039 -0.01313 -0.01472
    -0.01524 -0.0148 -0.01372 -0.01184 -0.00927 -0.00651 -0.00407 -
0.00218 -0.00083 4.73E-05 0.000566 0.00081 0.000851 0.000749 0.000547
0.000283 -1.39E-05 -0.00032 -0.00062 -0.0009 -0.00114 -0.00133 -
0.00148 -0.00156 -0.00159 -0.00156 -0.00148 -0.00133 -0.00114 -0.0009
-0.00062 -0.00032 -1.39E-05 0.000283 0.000547 0.000749 0.000851
0.00081 0.000566 4.73E-05 -0.00083 -0.00218 -0.00407 -0.00651 -0.00927
-0.01184 -0.01372 -0.0148
    -0.01503 -0.01486 -0.01429 -0.01322 -0.01178 -0.01026 -0.00895 -
0.00797 -0.0073 -0.00692 -0.00676 -0.00677 -0.00691 -0.00714 -0.00743
-0.00775 -0.00809 -0.00842 -0.00873 -0.00901 -0.00925 -0.00944 -
0.00959 -0.00967 -0.0097 -0.00967 -0.00959 -0.00944 -0.00925 -0.00901
-0.00873 -0.00842 -0.00809 -0.00775 -0.00743 -0.00714 -0.00691 -
0.00677 -0.00676 -0.00692 -0.0073 -0.00797 -0.00895 -0.01026 -0.01178
-0.01322 -0.01429 -0.01486
    -0.01477 -0.01484 -0.01467 -0.01424 -0.01362 -0.01296 -0.0124 -
0.01201 -0.01179 -0.01174 -0.01182 -0.012 -0.01226 -0.01257 -0.01291 -
0.01327 -0.01362 -0.01396 -0.01427 -0.01455 -0.01479 -0.01498 -0.01512
-0.0152 -0.01523 -0.0152 -0.01512 -0.01498 -0.01479 -0.01455 -0.01427
-0.01396 -0.01362 -0.01327 -0.01291 -0.01257 -0.01226 -0.012 -0.01182
-0.01174 -0.01179 -0.01201 -0.0124 -0.01296 -0.01362 -0.01424 -0.01467
-0.01484
    -0.01446 -0.01469 -0.0148 -0.01477 -0.01465 -0.0145 -0.0144 -
0.01438 -0.01445 -0.01461 -0.01484 -0.01513 -0.01546 -0.01582 -0.01619
-0.01656 -0.01692 -0.01726 -0.01757 -0.01784 -0.01807 -0.01825 -
0.01838 -0.01846 -0.01849 -0.01846 -0.01838 -0.01825 -0.01807 -0.01784
-0.01757 -0.01726 -0.01692 -0.01656 -0.01619 -0.01582 -0.01546 -
0.01513 -0.01484 -0.01461 -0.01445 -0.01438 -0.0144 -0.0145 -0.01465 -
0.01477 -0.0148 -0.01469
    -0.01408 -0.01442 -0.01469 -0.0149 -0.01505 -0.0152 -0.01536 -
0.01555 -0.01579 -0.01607 -0.0164 -0.01675 -0.01713 -0.01751 -0.01789
-0.01827 -0.01862 -0.01895 -0.01925 -0.01951 -0.01973 -0.0199 -0.02003
-0.02011 -0.02013 -0.02011 -0.02003 -0.0199 -0.01973 -0.01951 -0.01925
-0.01895 -0.01862 -0.01827 -0.01789 -0.01751 -0.01713 -0.01675 -0.0164
-0.01607 -0.01579 -0.01555 -0.01536 -0.0152 -0.01505 -0.0149 -0.01469
-0.01442];

B_bulk_real = [-0.01511 -0.01297 -0.01114 -0.0087 -0.00595 -0.00244 -
0.00153 0.002441 0.002747 0.007172 0.007629 0.010223 0.009766 0.007019
0.013733 0.010834 0.013733 0.013733 0.010834 0.011139 0.012512
0.011597 0.010986 0.01236 0.012207 0.013428 0.011902 0.012817 0.012665
0.01297 0.012665 0.018616 0.019073 0.016937 0.014954 0.017548 0.018768
0.018005 0.019989 0.021057 0.016327 0.015564 0.016327 0.00946 0.011292
0.004578 0.005493 -0.00168
    -0.01175 -0.00809 -0.00946 -0.00275 -0.00244 0.000305 0.008698
0.007782 0.010071 0.010376 0.014038 0.016937 0.018158 0.019531
0.019379 0.022888 0.020447 0.020599 0.020142 0.01709 0.020294 0.016785
0.021362 0.022583 0.022278 0.022736 0.022278 0.022278 0.020599
0.024414 0.025482 0.031738 0.028534 0.027618 0.030518 0.027466
0.024414 0.031891 0.031738 0.028687 0.027008 0.024414 0.020752
0.020447 0.013275 0.013428 0.005646 0.00473
    -0.0119 -0.00839 -0.00427 -0.00214 -0.00183 0.00473 0.005951
0.01236 0.018158 0.020599 0.021362 0.021515 0.027313 0.031891 0.030365
```

0.032196 0.033264 0.034637 0.030823 0.032806 0.034332 0.03418 0.032349
0.03479 0.03479 0.036621 0.036469 0.035858 0.036011 0.037689 0.039673
0.041656 0.039673 0.039215 0.044098 0.039673 0.037079 0.043335
0.041351 0.040283 0.037842 0.035248 0.03006 0.025482 0.022125 0.014954
0.013123 0.002136
    -0.00916 -0.00794 -0.0029 0.001526 0.004578 0.009155 0.012665
0.019684 0.026398 0.028229 0.032349 0.034332 0.035858 0.040131
0.040588 0.044403 0.045319 0.045013 0.046387 0.049896 0.044708
0.051117 0.050049 0.049744 0.049744 0.049133 0.048676 0.050049
0.054169 0.05188 0.050049 0.055847 0.054626 0.054932 0.057831 0.052948
0.05127 0.057678 0.057678 0.054016 0.050354 0.046692 0.041809 0.034943
0.030212 0.021973 0.014496 0.009613
    -0.00443 -0.0061 -0.00168 0.007477 0.009766 0.015106 0.020294
0.029297 0.031586 0.037994 0.041046 0.046387 0.04776 0.05188 0.052795
0.057678 0.058594 0.064087 0.061493 0.063782 0.062103 0.060425
0.067139 0.065765 0.066528 0.065613 0.064392 0.066833 0.06485 0.070648
0.068054 0.070648 0.070038 0.06958 0.067749 0.069885 0.069122 0.072479
0.06958 0.070648 0.063629 0.058594 0.05188 0.044556 0.039215 0.029755
0.020294 0.012665
    -0.00717 -0.00229 0.00412 0.007324 0.014038 0.020142 0.028381
0.033722 0.03952 0.046997 0.050049 0.056152 0.060883 0.063782 0.069885
0.071259 0.073547 0.075226 0.076141 0.081329 0.079803 0.081482
0.082092 0.082092 0.084839 0.084991 0.083618 0.08255 0.084076 0.085602
0.087738 0.088348 0.08667 0.088043 0.087891 0.087738 0.092621 0.086212
0.086823 0.081177 0.074158 0.069427 0.062408 0.052338 0.042114
0.034943 0.023651 0.014954
    -0.00534 -0.00458 0.004425 0.009155 0.01709 0.025177 0.030518
0.040283 0.047607 0.056915 0.060272 0.066833 0.071411 0.079193
0.081482 0.084839 0.088043 0.091248 0.093231 0.09903 0.09552 0.092468
0.098877 0.10025 0.103455 0.10498 0.101166 0.100555 0.102539 0.101624
0.102081 0.106049 0.105286 0.104065 0.103607 0.099945 0.100861
0.102234 0.098572 0.095215 0.087128 0.080109 0.071106 0.06012 0.05127
0.03952 0.027161 0.021973
    -0.00336 -0.00198 0.006561 0.013275 0.023499 0.030823 0.041656
0.049744 0.056 0.063324 0.072021 0.081635 0.085144 0.089874 0.094757
0.100708 0.103912 0.108948 0.108948 0.113525 0.111847 0.117798
0.116425 0.116882 0.120087 0.117798 0.120087 0.118256 0.11734 0.118713
0.119171 0.121765 0.120392 0.11795 0.121002 0.117493 0.115204 0.115356
0.109406 0.106354 0.097504 0.088806 0.078278 0.066833 0.054626
0.042267 0.033875 0.022583
    -0.00229 0.000153 0.009003 0.016174 0.024719 0.03952 0.04303
0.053101 0.068054 0.074921 0.08194 0.090332 0.098724 0.103607 0.111694
0.111542 0.120239 0.121918 0.131378 0.127563 0.131531 0.134277
0.133209 0.134888 0.136566 0.136871 0.13504 0.135803 0.133972 0.133972
0.136871 0.136414 0.136871 0.136566 0.13092 0.133667 0.126953 0.126801
0.122833 0.117493 0.107422 0.097351 0.086517 0.073242 0.059509
0.048676 0.032196 0.025482
    -0.00046 0.002899 0.00946 0.022125 0.030518 0.040588 0.05127
0.061646 0.073242 0.083771 0.092316 0.104675 0.109863 0.117035 0.12146
0.127411 0.134277 0.137024 0.138245 0.143738 0.147095 0.148315
0.150909 0.149384 0.15274 0.15274 0.15213 0.150452 0.149994 0.148315
0.15213 0.154114 0.149078 0.145721 0.145111 0.142365 0.13855 0.134888
0.132751 0.12207 0.113983 0.104828 0.093994 0.077667 0.063019 0.049591
0.038147 0.026855
    -0.00015 0.005341 0.014191 0.022888 0.034485 0.042419 0.056458
0.070953 0.081177 0.09201 0.102692 0.112762 0.122223 0.131226 0.135498
0.142212 0.148468 0.15213 0.157166 0.162048 0.164185 0.164032 0.164795
0.165863 0.168304 0.16449 0.166016 0.162964 0.162048 0.162048 0.165863
0.161438 0.157166 0.157471 0.157013 0.151367 0.146942 0.144196

0.139618 0.130005 0.119629 0.10788 0.095062 0.080414 0.06485 0.05127
0.039062 0.028381
    0.001526 0.000916 0.014954 0.026855 0.036621 0.047302 0.060883
0.07782 0.089264 0.098114 0.110168 0.122833 0.132294 0.13916 0.1474
0.153809 0.16037 0.165405 0.172272 0.170135 0.171967 0.17746 0.179443
0.178528 0.17868 0.177002 0.179901 0.177002 0.175629 0.175934 0.175018
0.172882 0.171814 0.171051 0.16571 0.160065 0.157928 0.151672 0.14389
0.136261 0.125732 0.113373 0.097198 0.082245 0.067596 0.052795
0.037537 0.025482
    0.001984 0.006866 0.0177 0.028229 0.039062 0.05127 0.06546
0.080109 0.095367 0.106354 0.118408 0.131531 0.140076 0.15274 0.15686
0.163879 0.167542 0.176239 0.180969 0.183716 0.187225 0.186157
0.188904 0.191345 0.189056 0.187073 0.189667 0.18692 0.188904 0.183563
0.180206 0.181885 0.18158 0.175323 0.172119 0.167542 0.163116 0.15564
0.148926 0.140839 0.128479 0.114288 0.101013 0.08194 0.069275 0.052795
0.042114 0.03006
    0.003662 0.010834 0.019073 0.030823 0.041656 0.055237 0.068207
0.082703 0.097351 0.11322 0.128632 0.137939 0.148773 0.155945 0.165863
0.172577 0.180359 0.18219 0.190125 0.192108 0.196381 0.196991 0.196991
0.197754 0.203247 0.198517 0.198517 0.191803 0.19455 0.191498 0.189209
0.189362 0.186157 0.181274 0.17807 0.171967 0.167694 0.158691 0.149536
0.140839 0.127563 0.117035 0.103455 0.080872 0.07019 0.05249 0.040131
0.032196
    -0.00031 0.010529 0.019989 0.032806 0.042419 0.055237 0.072479
0.084076 0.10437 0.115814 0.130615 0.143433 0.154877 0.163727 0.169983
0.178528 0.186768 0.189819 0.197296 0.198517 0.200348 0.203705
0.203552 0.204468 0.20401 0.20401 0.203247 0.198517 0.201263 0.197601
0.194702 0.193634 0.190582 0.185394 0.180817 0.175476 0.170898 0.16037
0.151062 0.14328 0.13031 0.118408 0.103912 0.084991 0.070343 0.055237
0.041656 0.029907
    0.002899 0.011597 0.020599 0.031433 0.045319 0.059204 0.074615
0.090179 0.106659 0.116882 0.130005 0.146332 0.158081 0.1651 0.173798
0.181885 0.187225 0.192108 0.196228 0.199738 0.202332 0.20401 0.207062
0.205536 0.203857 0.209351 0.206451 0.2034 0.204468 0.19928 0.199585
0.193939 0.192871 0.187378 0.182495 0.176849 0.169067 0.161591
0.155792 0.144348 0.1297 0.118103 0.102539 0.082855 0.070801 0.055389
0.041656 0.029907
    0.004883 0.011749 0.022125 0.032196 0.050201 0.058594 0.072479
0.094299 0.107727 0.122528 0.135193 0.148163 0.160522 0.166321 0.17334
0.182648 0.187073 0.187531 0.194092 0.201569 0.203094 0.202026
0.206146 0.205231 0.207672 0.205688 0.205383 0.205536 0.203552
0.201721 0.202332 0.195007 0.19165 0.188293 0.182343 0.175171 0.171204
0.162964 0.158539 0.142212 0.131531 0.118408 0.102234 0.083313
0.070496 0.054169 0.042114 0.03067
    0.002594 0.012207 0.020142 0.032043 0.046234 0.062561 0.076599
0.091248 0.108185 0.119476 0.136719 0.149384 0.15976 0.167084 0.177612
0.182953 0.187073 0.194397 0.197449 0.199127 0.203094 0.200653
0.203857 0.206757 0.206146 0.203552 0.202789 0.203247 0.202026
0.200195 0.197754 0.194855 0.193024 0.185394 0.181885 0.175171
0.168762 0.162506 0.15152 0.144348 0.130005 0.117035 0.102234 0.086365
0.070496 0.056 0.041199 0.031586
    0.006714 0.011444 0.020599 0.033264 0.046234 0.057831 0.076447
0.090179 0.106812 0.122375 0.13031 0.146179 0.157623 0.162964 0.170441
0.178833 0.184174 0.185852 0.194397 0.195312 0.195923 0.195618
0.199585 0.202332 0.198517 0.200806 0.197754 0.200348 0.197906
0.197144 0.194855 0.19165 0.188751 0.182648 0.177307 0.172882 0.166473
0.160522 0.152283 0.14267 0.130463 0.118408 0.101166 0.084534 0.070343
0.054169 0.040588 0.032043

0.003357 0.009613 0.022583 0.032654 0.046234 0.059052 0.072632
0.089264 0.105286 0.118256 0.134277 0.143433 0.153046 0.162201
0.170898 0.173645 0.180969 0.185852 0.186157 0.188751 0.191956
0.194855 0.192566 0.193939 0.194855 0.193787 0.192413 0.19455 0.19165
0.188904 0.189514 0.184784 0.184784 0.180511 0.174103 0.169983
0.167236 0.158234 0.149536 0.136566 0.128937 0.115662 0.097198
0.083618 0.06546 0.052032 0.038147 0.032349

0.003052 0.00824 0.022278 0.029602 0.044861 0.055847 0.072479
0.088348 0.101624 0.117645 0.129547 0.140533 0.149841 0.155792
0.162354 0.167694 0.169525 0.17334 0.179291 0.182037 0.183258 0.181427
0.184937 0.180206 0.183868 0.185089 0.183716 0.187988 0.184174
0.185394 0.182648 0.178528 0.177765 0.171356 0.172272 0.168457
0.160217 0.159912 0.147858 0.137482 0.126953 0.113068 0.098114
0.081787 0.066986 0.052643 0.038757 0.029449

0.004425 0.012512 0.021057 0.03067 0.044098 0.054779 0.072327
0.083923 0.09964 0.114136 0.123138 0.134735 0.143433 0.149536 0.157166
0.161438 0.168152 0.171509 0.171204 0.172577 0.173035 0.174561
0.175476 0.176849 0.177765 0.175018 0.175781 0.173798 0.174713
0.175781 0.175171 0.172424 0.169983 0.171051 0.167847 0.166779
0.160217 0.152283 0.143738 0.137177 0.122681 0.116272 0.096436
0.079498 0.06546 0.054321 0.03891 0.028076

0.000763 0.011444 0.019073 0.027924 0.042267 0.056305 0.071716
0.081329 0.096283 0.107117 0.118866 0.130768 0.138397 0.143585 0.14801
0.153961 0.153809 0.16037 0.162659 0.162964 0.166779 0.164795 0.166626
0.167389 0.162811 0.165253 0.163879 0.164642 0.16571 0.166473 0.166473
0.161591 0.167542 0.163116 0.157776 0.158997 0.151978 0.147552
0.141144 0.130005 0.119781 0.110321 0.095978 0.079041 0.062561
0.053558 0.038147 0.029144

0.00412 0.010376 0.021362 0.028229 0.044098 0.052032 0.066071
0.079803 0.092163 0.10498 0.11322 0.124359 0.130005 0.137634 0.141907
0.146027 0.144043 0.151672 0.152588 0.153961 0.15564 0.153961 0.157928
0.154266 0.15625 0.156403 0.157166 0.154877 0.158539 0.158539 0.159912
0.157776 0.15976 0.15625 0.154266 0.15213 0.149994 0.142365 0.135498
0.130463 0.11734 0.106049 0.088501 0.076904 0.065613 0.049744 0.036316
0.028839

0.002747 0.011444 0.015564 0.03067 0.040741 0.052338 0.066223
0.078278 0.091553 0.10376 0.10849 0.120544 0.128937 0.133057 0.138245
0.140686 0.142975 0.1474 0.149536 0.149384 0.149078 0.149536 0.147705
0.150604 0.145416 0.148926 0.150299 0.150452 0.151215 0.153046
0.149994 0.152588 0.154572 0.150146 0.151062 0.149231 0.142822
0.137329 0.131683 0.130768 0.111847 0.100861 0.090027 0.076447
0.061035 0.050201 0.034027 0.029297

0.003052 0.010681 0.019226 0.032043 0.040588 0.054474 0.063171
0.078583 0.0914 0.098114 0.108643 0.12085 0.12619 0.13092 0.132294
0.138702 0.139923 0.142517 0.142517 0.144348 0.140686 0.141754
0.141602 0.144196 0.144043 0.141754 0.14389 0.14267 0.144043 0.143738
0.145874 0.147858 0.149078 0.148315 0.145721 0.145111 0.140076
0.135956 0.128784 0.121613 0.110931 0.09903 0.088043 0.072784 0.057831
0.047913 0.035858 0.026855

0.002747 0.009613 0.017395 0.03006 0.042419 0.054169 0.068512
0.07843 0.089264 0.099182 0.112 0.118713 0.124969 0.131836 0.132904
0.136566 0.13855 0.135498 0.141907 0.140533 0.141907 0.139618 0.137482
0.140991 0.13855 0.136719 0.13916 0.140381 0.139008 0.142365 0.141907
0.144958 0.147858 0.146484 0.14267 0.143433 0.142517 0.133209 0.128021
0.119781 0.110779 0.102234 0.090179 0.072937 0.062408 0.049133 0.0354
0.027008

0.00351 0.011749 0.020142 0.031128 0.04425 0.055542 0.06897
0.078583 0.093842 0.106201 0.11261 0.121918 0.127411 0.131531 0.135803
0.13855 0.140381 0.141602 0.142059 0.139618 0.136414 0.140839 0.139618

0.136566 0.137634 0.135193 0.136108 0.137024 0.140228 0.140991
0.145264 0.145569 0.147247 0.144501 0.145874 0.142517 0.140686
0.133057 0.128174 0.119934 0.109406 0.097046 0.08728 0.071259 0.061035
0.045013 0.035858 0.025482
    0.006256 0.013123 0.025635 0.036926 0.046692 0.057678 0.070343
0.08316 0.097351 0.107422 0.119629 0.12619 0.132904 0.136719 0.141296
0.13916 0.142212 0.144653 0.145264 0.142822 0.141449 0.141602 0.138092
0.133667 0.13504 0.13443 0.139008 0.136261 0.140228 0.142517 0.146027
0.147858 0.148773 0.151062 0.145416 0.145721 0.14389 0.138702 0.131073
0.122223 0.112915 0.101013 0.091248 0.075989 0.06073 0.048523 0.035706
0.027161
    0.008087 0.018158 0.023193 0.036316 0.048523 0.062408 0.07431
0.088196 0.101318 0.109711 0.118103 0.128937 0.137329 0.141754
0.147247 0.146637 0.149231 0.150299 0.15152 0.145874 0.144501 0.142822
0.143127 0.137939 0.139618 0.136261 0.138092 0.138855 0.140076
0.144043 0.149536 0.15152 0.15274 0.154114 0.151825 0.150146 0.1474
0.142365 0.134888 0.126038 0.116425 0.102844 0.090637 0.075378
0.059357 0.048218 0.03479 0.027008
    0.008545 0.017853 0.025024 0.037537 0.049133 0.062866 0.079803
0.090485 0.102234 0.114288 0.124359 0.13382 0.144196 0.14679 0.150452
0.151672 0.154419 0.152435 0.15152 0.149841 0.154419 0.146179 0.143585
0.141296 0.137482 0.137939 0.140991 0.140228 0.142212 0.146637
0.155487 0.153656 0.15564 0.158081 0.156097 0.157318 0.153961 0.145264
0.137939 0.129242 0.119019 0.106354 0.094452 0.077362 0.063324
0.049286 0.037994 0.028992
    0.008545 0.015259 0.024261 0.037689 0.049438 0.065918 0.078735
0.090942 0.107117 0.119476 0.129242 0.138092 0.145569 0.150604
0.156097 0.152893 0.159454 0.159454 0.158997 0.154724 0.155792
0.143585 0.146332 0.139008 0.137634 0.139923 0.136719 0.139923
0.145416 0.149231 0.153198 0.157776 0.160217 0.162506 0.163116
0.159302 0.159149 0.14801 0.142059 0.131226 0.120544 0.108337 0.09491
0.079803 0.060577 0.052032 0.037231 0.028229
    0.00824 0.017853 0.029755 0.03891 0.051727 0.066071 0.077209
0.093231 0.108948 0.119934 0.1297 0.140991 0.148315 0.153809 0.158997
0.160675 0.163422 0.162811 0.159149 0.160065 0.154724 0.149536 0.1474
0.142212 0.139008 0.13855 0.14267 0.140686 0.146027 0.150757 0.15564
0.164032 0.163879 0.164795 0.167999 0.164948 0.159302 0.155487 0.14328
0.138092 0.123138 0.111084 0.097809 0.079041 0.064545 0.051117
0.040436 0.030212
    0.00946 0.019836 0.025482 0.040741 0.052185 0.066071 0.082245
0.094757 0.108795 0.121613 0.131226 0.144196 0.15274 0.158539 0.162354
0.166779 0.164185 0.167389 0.161591 0.160828 0.158234 0.15152 0.147705
0.143127 0.139313 0.135193 0.133972 0.142365 0.146179 0.151062
0.154266 0.163422 0.166321 0.171814 0.168152 0.167389 0.163422
0.153961 0.147858 0.138397 0.128174 0.112305 0.098724 0.083008
0.068665 0.053558 0.039978 0.030365
    0.010376 0.019226 0.027466 0.040741 0.052643 0.067596 0.082245
0.095367 0.109558 0.123138 0.132141 0.143127 0.149841 0.157013 0.16037
0.166016 0.16922 0.168762 0.167694 0.161133 0.159454 0.154419 0.147552
0.142822 0.140228 0.136566 0.137024 0.139771 0.144501 0.151825
0.159302 0.160522 0.167847 0.171204 0.171967 0.169373 0.168762
0.158691 0.147552 0.140839 0.127411 0.114899 0.100708 0.082245
0.070496 0.054474 0.040741 0.026855
    0.009613 0.016785 0.027924 0.042877 0.054169 0.067291 0.081482
0.097656 0.112152 0.122375 0.133514 0.144196 0.150146 0.160217
0.165863 0.167236 0.170135 0.171356 0.172272 0.165253 0.159149 0.15564
0.145416 0.140686 0.13916 0.131989 0.132141 0.137482 0.14328 0.149078
0.154114 0.164795 0.168304 0.171661 0.171814 0.172577 0.165253

0.160522 0.15152 0.138092 0.131378 0.115967 0.104523 0.08316 0.067749
0.054932 0.037842 0.032501
    0.011139 0.017395 0.028992 0.039062 0.055389 0.066833 0.084534
0.094299 0.110626 0.123749 0.134125 0.144958 0.153198 0.162354
0.166016 0.167999 0.172577 0.16922 0.167236 0.164337 0.158081 0.15213
0.144043 0.136414 0.135956 0.1297 0.133514 0.132751 0.140839 0.147705
0.156403 0.160065 0.166473 0.170746 0.173035 0.169067 0.167694 0.16037
0.153503 0.141296 0.131226 0.116119 0.105438 0.086212 0.069885
0.053864 0.041656 0.030365
    0.012207 0.021057 0.027313 0.046539 0.054474 0.06897 0.08316
0.099487 0.111237 0.124207 0.136414 0.146179 0.15564 0.163422 0.161285
0.170593 0.172424 0.171661 0.169983 0.163727 0.157928 0.151367
0.144043 0.135193 0.131989 0.126495 0.130157 0.135651 0.139008 0.14328
0.151367 0.157623 0.167236 0.171661 0.172424 0.17334 0.168762 0.161133
0.151367 0.142975 0.130463 0.115967 0.099182 0.084229 0.067444
0.054474 0.042267 0.029144
    0.011597 0.025024 0.028076 0.041351 0.053101 0.069122 0.085754
0.098572 0.11261 0.122986 0.139313 0.147858 0.158386 0.161133 0.169373
0.170746 0.173492 0.172272 0.168762 0.163116 0.157623 0.150757
0.141144 0.136261 0.129852 0.126038 0.125122 0.127563 0.136871
0.139008 0.151672 0.156403 0.162048 0.16861 0.170898 0.171814 0.167389
0.158997 0.151825 0.145416 0.132294 0.115662 0.101013 0.08316 0.069275
0.056 0.041199 0.028229
    0.01236 0.017853 0.032043 0.041962 0.054626 0.070648 0.085907
0.10025 0.114288 0.126801 0.138245 0.148621 0.157928 0.163116 0.167999
0.171509 0.171204 0.170746 0.167999 0.165405 0.155945 0.148621
0.140228 0.131836 0.12558 0.120697 0.123901 0.124969 0.126495 0.137787
0.140228 0.151215 0.158691 0.1651 0.168457 0.168915 0.164337 0.161285
0.150909 0.140686 0.128479 0.113678 0.104218 0.085449 0.068207
0.054932 0.041656 0.034027
    0.010376 0.019989 0.034332 0.042725 0.054321 0.070953 0.086365
0.09964 0.114441 0.124512 0.138245 0.14801 0.157623 0.163727 0.166779
0.170135 0.167847 0.16922 0.167694 0.160675 0.155029 0.145569 0.13855
0.128479 0.121613 0.119781 0.120239 0.118866 0.125427 0.132751
0.140991 0.149078 0.154724 0.162964 0.166626 0.164185 0.162811
0.160217 0.150299 0.140991 0.128326 0.11673 0.102539 0.082855 0.068054
0.055084 0.043182 0.03418
    0.01236 0.02121 0.02655 0.043335 0.055084 0.071564 0.085602
0.10437 0.112305 0.128326 0.137329 0.146332 0.15564 0.161438 0.164948
0.16861 0.171051 0.166626 0.163116 0.157776 0.15213 0.144043 0.132751
0.127563 0.123444 0.118713 0.113525 0.116272 0.12085 0.128021 0.134583
0.146332 0.153503 0.155792 0.158997 0.162811 0.158691 0.15564 0.145721
0.138397 0.125732 0.114288 0.101166 0.086212 0.069427 0.05661 0.042572
0.028992
    0.013275 0.021515 0.028839 0.042114 0.057373 0.072021 0.084381
0.098724 0.11261 0.125122 0.136108 0.146637 0.151825 0.160828 0.163116
0.163116 0.166016 0.164642 0.162354 0.154877 0.148926 0.139771
0.131378 0.123901 0.115814 0.110474 0.109558 0.112305 0.11673 0.124054
0.128479 0.14267 0.147552 0.154877 0.15686 0.157928 0.156708 0.157471
0.146027 0.135803 0.125122 0.111237 0.099792 0.081329 0.067139
0.052948 0.042572 0.029755
    0.00946 0.020447 0.02594 0.039062 0.055542 0.067444 0.082703
0.09613 0.110321 0.121918 0.134277 0.142517 0.147552 0.157471 0.161591
0.161743 0.161896 0.159607 0.157471 0.151825 0.142517 0.140991
0.130005 0.120087 0.111237 0.113525 0.105591 0.107727 0.111389
0.118103 0.125427 0.132599 0.144806 0.149078 0.151978 0.153198
0.153656 0.151825 0.140228 0.131683 0.122375 0.109253 0.094147
0.077209 0.066986 0.05722 0.038757 0.028839

0.009155 0.018768 0.026398 0.037079 0.053101 0.064392 0.079956
0.093384 0.1091 0.11795 0.127258 0.137787 0.143738 0.147858 0.150604
0.154419 0.154572 0.156403 0.150909 0.149384 0.141144 0.132904
0.123901 0.115662 0.10849 0.099182 0.104218 0.10437 0.106354 0.108948
0.120087 0.124664 0.131683 0.141449 0.148468 0.147705 0.1474 0.145264
0.139618 0.126495 0.119934 0.108337 0.095215 0.080261 0.065918 0.05249
0.041809 0.027313
0.008545 0.0177 0.025635 0.039215 0.048828 0.062561 0.07431
0.089111 0.10025 0.115509 0.122223 0.129852 0.13504 0.146332 0.145874
0.148163 0.147247 0.146027 0.144806 0.141144 0.133667 0.124969
0.117798 0.110321 0.102539 0.097351 0.095215 0.098267 0.099487
0.106201 0.114288 0.120697 0.12558 0.135498 0.135651 0.141907 0.13916
0.137024 0.131378 0.123138 0.114136 0.104065 0.092773 0.076599 0.06485
0.050201 0.039673 0.027466
0.006409 0.016022 0.024261 0.033569 0.041809 0.057373 0.071869
0.082245 0.093384 0.105438 0.114899 0.121613 0.127411 0.133667
0.135803 0.138245 0.137024 0.136108 0.135498 0.130005 0.123749
0.117645 0.110779 0.10376 0.097809 0.095978 0.090485 0.092621 0.095215
0.098724 0.106659 0.111389 0.118561 0.12558 0.130157 0.132141 0.132141
0.126953 0.128479 0.118561 0.10849 0.100403 0.086517 0.072784 0.061188
0.048981 0.038757 0.032043
0.009308 0.013733 0.021057 0.031128 0.041962 0.052643 0.063629
0.075378 0.088654 0.099487 0.105133 0.115967 0.119171 0.121918
0.125732 0.128632 0.127716 0.126801 0.12146 0.120544 0.116425 0.113831
0.102234 0.098267 0.088806 0.082092 0.084381 0.082855 0.087891
0.093536 0.097046 0.102844 0.110626 0.116272 0.122528 0.121155
0.121155 0.120392 0.12085 0.110474 0.102692 0.094604 0.079803 0.068512
0.056763 0.043488 0.035553 0.025482
0.006256 0.01297 0.0177 0.026855 0.037537 0.052032 0.057678
0.067291 0.082092 0.086975 0.098724 0.10437 0.106964 0.111389 0.113678
0.116119 0.115509 0.115356 0.113831 0.109558 0.108337 0.103149
0.093994 0.090332 0.080109 0.073547 0.074921 0.0737 0.079193 0.085297
0.084839 0.093231 0.099792 0.104675 0.108643 0.110168 0.10849 0.110168
0.106659 0.10025 0.094147 0.085602 0.078888 0.066223 0.054169 0.043335
0.033264 0.029144
0.002136 0.010529 0.016327 0.023804 0.032349 0.041962 0.051117
0.06073 0.06546 0.078125 0.086975 0.09079 0.093689 0.099487 0.101776
0.102234 0.104065 0.101624 0.099335 0.101318 0.095367 0.091095
0.084686 0.078125 0.073547 0.068054 0.069427 0.06897 0.070648 0.077362
0.079346 0.084686 0.091705 0.09552 0.097198 0.098572 0.09964 0.102386
0.097046 0.091858 0.08606 0.078278 0.066223 0.057983 0.050201 0.039215
0.030365 0.02243
0.002594 0.006561 0.012817 0.020447 0.027771 0.036011 0.045624
0.054626 0.066376 0.067444 0.0737 0.079346 0.080872 0.084381 0.08728
0.088501 0.088043 0.087128 0.083618 0.080872 0.085602 0.07843 0.074615
0.066223 0.062714 0.058594 0.058594 0.059967 0.063171 0.061951
0.067291 0.072174 0.077362 0.081329 0.084991 0.088806 0.088348
0.088196 0.081482 0.079956 0.07309 0.070496 0.058746 0.049133 0.045166
0.035858 0.025482 0.020752
0.000916 0.005188 0.00824 0.016479 0.021515 0.028076 0.0354
0.041809 0.05249 0.058289 0.06134 0.063782 0.068054 0.07019 0.072174
0.072174 0.070648 0.076904 0.069275 0.070953 0.068512 0.064087
0.060883 0.056458 0.052032 0.049133 0.045776 0.050354 0.051117
0.054932 0.05722 0.063629 0.061188 0.068207 0.068512 0.077057 0.069427
0.070496 0.069733 0.068817 0.063782 0.058594 0.052032 0.044556
0.037079 0.030212 0.023193 0.016632
-0.00183 0.001984 0.005798 0.009766 0.017853 0.020752 0.03067
0.037842 0.038757 0.046997 0.050659 0.053253 0.052185 0.055695
0.058746 0.059204 0.058899 0.05661 0.060577 0.05722 0.055084 0.055542

```
0.048828 0.045319 0.041504 0.039978 0.042419 0.040588 0.042419 0.04303
0.043488 0.050049 0.054169 0.057678 0.061035 0.059967 0.060425
0.057678 0.059052 0.058136 0.05188 0.048065 0.044861 0.035553 0.030212
0.024414 0.018158 0.01297
    -0.00488 0.000916 0.002441 0.009155 0.011139 0.018158 0.021973
0.023193 0.026855 0.033722 0.040436 0.041504 0.041809 0.04364 0.045776
0.044403 0.046234 0.045166 0.043945 0.040588 0.044556 0.036774
0.037231 0.032654 0.031738 0.030823 0.029449 0.032349 0.033264
0.032501 0.037842 0.035858 0.045166 0.042419 0.04715 0.047913 0.049133
0.045166 0.047607 0.047607 0.043945 0.038757 0.034637 0.027924
0.024109 0.020599 0.014648 0.010071
    -0.00626 -0.00397 0.003052 0.003357 0.006409 0.006256 0.014801
0.019836 0.02182 0.023651 0.020905 0.03006 0.028229 0.032196 0.031891
0.032043 0.034485 0.033417 0.037537 0.029144 0.032654 0.032806
0.026093 0.023193 0.022736 0.021057 0.022583 0.02182 0.022583 0.02594
0.025787 0.026703 0.03006 0.030365 0.036621 0.037384 0.037384 0.035095
0.033722 0.035858 0.03067 0.027466 0.025177 0.02243 0.018616 0.013123
0.014191 0.006561
    -0.00717 -0.00443 -0.00229 0.001678 0.002747 0.003967 0.006714
0.010681 0.014191 0.018311 0.019684 0.019684 0.022583 0.022888
0.025177 0.023651 0.025177 0.022125 0.022583 0.022736 0.025635
0.018921 0.019379 0.016632 0.015259 0.01358 0.014648 0.014648 0.016327
0.016937 0.018921 0.01358 0.023041 0.023499 0.024719 0.024567 0.028381
0.024872 0.024719 0.023346 0.024872 0.0177 0.017395 0.014496 0.012207
0.011749 0.010834 0.00885
    -0.00473 -0.00244 -0.00351 -0.00275 -0.0032 -0.00092 0.00473
0.005951 0.00885 0.009155 0.006866 0.011749 0.00946 0.013275 0.012817
0.014496 0.014648 0.016937 0.013733 0.017548 0.010986 0.009613
0.010529 0.00946 0.008087 0.008087 0.010223 0.007935 0.010223 0.010681
0.009918 0.006409 0.015411 0.014343 0.015106 0.017548 0.016327
0.013123 0.014496 0.01358 0.012054 0.012817 0.013275 0.007782 0.008698
0.00885 0.006409 0.011902
    -0.00275 -0.00244 -0.00061 -0.00427 -0.00275 -0.00305 -0.00015
0.001526 0.000916 0.005646 0.003967 0.006866 0.007019 0.005341
0.006714 0.008392 0.009766 0.006866 0.005798 0.003815 0.00885 0.00412
0.006256 0.003967 0.002136 0.002747 0.003357 0.00412 0.003815 0.003662
0.003662 0.005798 0.005341 0.007935 0.010529 0.010223 0.008392
0.010834 0.00885 0.008698 0.008545 0.010529 0.006561 0.007782 0.008545
0.011292 0.015411 0.017548
    0.000916 0.000916 -0.00061 -0.00076 -0.00443 -0.00076 -0.00687 -
0.0032 -0.00168 -0.00168 -0.00061 0.001068 0.003357 0.002899 0 0
0.002594 0.003967 0.000458 0 -0.00046 -0.00244 -0.00046 -0.00015 -
0.00214 -0.00214 -0.00168 -0.00214 -0.00122 0.001221 -0.00061 -0.00015
0.001526 0.000458 0.005188 0.003967 0.00351 0.004425 0.007477 0.005035
0.002747 0.003052 0.005646 0.007782 0.009766 0.009155 0.018158
0.0177];

[x,y] = meshgrid(x,y);

figure;
surf(x,y,B_bulk_ideal); colorbar; axis tight; view(130,25);
xlabel('x [mm]'); ylabel('y [mm]'); zlabel('B [T]');
title('Ideal flux density in a bulk');

figure;
surf(x,y,B_bulk_real); colorbar; axis tight; view(130,25);
xlabel('x [mm]'); ylabel('y [mm]'); zlabel('B [T]');
title('Measured flux density in a bulk');
```

```
x = [-12 -11 -10 -9 -8 -7 -6 -5 -4 -3 -2 -1 0 1 2 3 4 5 6 7 8 9 10 11
12];
y = [-21.5 -20.5 -19.5 -18.5 -17.5 -16.5 -15.5 -14.5 -13.5 -12.5 -11.5
-10.5 -9.5 -8.5 -7.5 -6.5 -5.5 -4.5 -3.5 -2.5 -1.5 -0.5 0.5 1.5 2.5
3.5 4.5 5.5 6.5 7.5 8.5 9.5 10.5 11.5 12.5 13.5 14.5 15.5 16.5 17.5
18.5 19.5 20.5 21.5];

B_1tape = [-0.8 -1.0 -0.8 -0.9 -0.8 -0.8 -0.8 -0.8 -0.8 -0.7 -0.8 -0.9
-1.0 -0.9 -0.8 -1.0 -0.9 -0.7 -0.9 -0.9 -1.0 -0.9 -0.9 -1.0 -0.9 -0.8
-0.8 -0.9 -0.9 -0.9 -0.8 -0.9 -0.9 -1.0 -1.0 -0.8 -1.1 -0.9 -1.0 -1.0
-1.0 -0.8 -1.1 -1.0
    -0.7 -0.8 -0.8 -0.8 -0.8 -0.9 -0.8 -0.8 -0.7 -0.7 -0.7 -0.8 -0.7 -
0.8 -1.0 -0.8 -0.9 -0.8 -0.8 -1.0 -0.6 -0.7 -0.8 -0.8 -1.1 -0.8 -0.9 -
0.9 -1.1 -0.8 -0.8 -0.9 -0.8 -0.9 -0.8 -0.9 -1.0 -1.0 -1.0 -1.0 -1.0 -
1.0 -1.1 -1.0
    -0.8 -0.8 -0.7 -0.7 -0.7 -0.7 -0.7 -0.6 -0.7 -0.6 -0.9 -0.6 -0.7 -
0.7 -0.7 -0.7 -0.7 -0.7 -0.7 -0.7 -0.7 -0.7 -0.6 -0.7 -0.7 -0.7 -0.7 -
0.6 -0.8 -0.7 -0.8 -0.7 -0.9 -0.8 -0.9 -0.8 -0.9 -1.0 -0.8 -1.1 -0.9 -
1.1 -1.0 -1.1
    -0.5 -0.8 -0.7 -0.7 -0.7 -0.6 -0.6 -0.5 -0.6 -0.4 -0.5 -0.4 -0.8 -
0.5 -0.4 -0.5 -0.5 -0.5 -0.5 -0.4 -0.6 -0.5 -0.6 -0.6 -0.7 -0.6 -0.5 -
0.6 -0.6 -0.7 -0.7 -0.7 -0.7 -0.7 -0.7 -0.8 -0.8 -1.2 -0.9 -0.8 -1.0 -
1.0 -1.0 -1.1
    -0.7 -0.7 -0.7 -0.5 -0.4 -0.3 -0.4 -0.4 -0.3 -0.3 -0.4 -0.3 -0.3 -
0.3 -0.4 -0.3 -0.4 -0.3 -0.4 -0.3 -0.3 -0.3 -0.3 -0.3 -0.3 -0.3 -0.5 -
0.4 -0.5 -0.5 -0.6 -0.5 -0.6 -0.6 -0.7 -0.3 -0.8 -0.8 -0.8 -0.8 -0.9 -
0.9 -1.0 -1.0
    -0.6 -0.6 -0.3 -0.4 -0.4 0.3 -0.2 -0.1 -0.3 0.3 -0.4 -0.1 -0.1 0.0
-0.4 0.3 -0.1 -0.1 -0.4 -0.1 -0.3 0.2 -0.3 -0.1 -0.2 -0.2 -0.3 0.2 -
0.3 -0.3 -0.3 -0.4 -0.4 -0.5 -0.5 -0.6 -0.6 -1.0 -0.8 -0.8 -0.9 -0.9 -
1.0 -1.0
    -0.6 -0.4 -0.3 -0.3 -0.1 0.3 0.2 0.2 0.2 0.3 0.3 0.3 0.3 0.3 0.3
0.3 0.1 0.3 0.2 0.1 0.2 0.2 0.1 0.2 0.1 0.1 -0.1 0.2 -0.1 -0.4 -0.1 -
0.2 -0.3 -0.3 -0.4 -0.4 -0.5 -0.7 -0.7 -0.8 -0.7 -0.9 -0.9 -0.9
    -0.4 -0.3 -0.2 0.3 0.1 0.3 0.4 0.5 0.6 0.7 0.6 0.7 0.7 0.7 0.7 0.6
0.5 0.6 0.6 0.3 0.5 0.4 0.4 0.4 0.4 0.4 0.4 0.2 0.2 0.1 0.2 0.4 -0.1
0.1 -0.3 -0.6 -0.5 -0.5 -0.7 -0.8 -0.8 -0.8 -0.9 -0.9
    -0.3 -0.6 -0.1 0.3 0.1 0.6 0.8 0.9 1.0 1.0 1.1 1.1 1.0 1.1 1.0 1.1
1.0 1.1 1.0 0.9 0.9 0.8 0.8 0.8 0.8 0.7 0.6 0.5 0.5 0.4 0.3 0.4 0.1
0.1 -0.3 -0.2 -0.3 -0.4 -0.6 -0.8 -0.8 -0.8 -0.9 -0.9
    -0.2 -0.5 -0.1 0.3 0.5 0.9 1.1 1.3 1.3 1.5 1.2 1.6 1.5 1.5 1.5 1.7
1.4 1.4 1.3 1.0 1.2 1.2 1.1 1.1 0.9 1.1 0.9 0.9 0.8 0.7 0.6 0.5 0.5
0.1 -0.3 0.2 -0.2 -0.4 -0.2 -0.7 -0.7 -0.7 -0.8 -0.9
    -0.2 -0.1 0.2 0.5 0.8 1.1 1.3 1.6 1.7 1.9 1.9 1.9 1.8 1.9 1.8 1.8
1.7 1.8 1.7 1.6 1.5 1.4 1.5 1.3 1.3 1.3 1.2 1.1 1.0 1.0 0.7 0.8 0.6
0.4 0.3 0.2 -0.1 -0.3 -0.4 -0.4 -0.8 -0.7 -0.8 -0.9
    -0.2 -0.1 0.3 0.6 1.1 1.3 1.6 1.8 2.0 2.1 2.4 2.2 2.2 2.3 2.1 2.1
2.2 2.0 2.0 1.8 1.8 1.7 1.7 1.7 1.6 1.4 1.5 1.6 1.2 1.1 1.0 0.9 0.7
0.6 0.3 0.2 0.0 -0.3 -0.4 -0.6 -0.7 -0.8 -0.8 -0.8
    -0.2 0.0 0.3 0.7 1.1 1.4 1.7 2.0 2.2 2.2 2.5 2.4 2.3 2.4 2.4 2.3
2.2 2.2 2.1 2.0 1.9 2.0 1.8 1.8 1.6 1.6 1.5 1.4 1.4 1.3 1.5 1.0 0.8
0.6 0.4 0.3 0.0 -0.1 -0.3 -0.5 -0.6 -0.7 -0.9 -0.9
    -0.1 0.0 0.3 0.7 1.1 1.5 1.9 2.1 2.3 2.4 2.6 2.5 2.3 2.4 2.4 2.3
2.5 2.2 2.1 2.1 2.0 2.0 1.9 1.9 1.8 1.8 1.7 1.5 1.5 1.4 1.2 1.1 0.9
0.7 0.8 0.3 0.0 -0.2 -0.4 -0.6 -0.5 -0.7 -0.8 -1.0
```

```
    -0.2 -0.1 0.2 0.6 1.1 1.4 1.8 1.9 2.2 2.3 2.5 2.3 2.4 2.3 2.3 2.2
2.3 2.2 2.1 2.1 1.9 2.0 1.9 1.8 1.8 1.7 1.6 1.5 1.4 1.3 1.2 1.1 0.9
0.7 0.5 0.3 0.0 -0.1 -0.3 -0.5 -0.7 -1.0 -0.9 -0.9
    -0.2 -0.1 0.2 0.6 0.9 1.1 1.7 1.8 2.1 2.1 2.2 2.2 2.2 2.2 2.1 2.0
2.1 2.0 2.0 1.7 1.9 1.7 1.7 1.7 1.6 1.5 1.5 1.5 1.3 1.2 1.1 1.1 0.9
0.6 0.4 0.2 0.0 -0.2 -0.4 -0.5 -0.7 -0.9 -0.8 -0.9
    -0.3 -0.3 0.1 0.4 0.8 1.1 1.4 1.6 1.8 1.8 1.7 2.0 1.8 1.8 1.8 1.7
2.1 1.6 1.9 1.6 1.4 1.5 1.5 1.2 1.4 1.3 1.3 1.2 1.2 1.1 1.0 1.0 0.7
0.5 0.3 -0.1 0.0 -0.4 -0.4 -0.5 -0.8 -0.8 -0.9 -0.9
    -0.3 -0.4 0.1 0.2 0.6 0.7 1.0 1.3 1.4 1.4 1.5 1.4 1.5 1.5 1.5 1.3
1.5 1.3 1.4 1.3 1.3 1.3 1.2 1.1 1.1 1.0 1.0 1.0 0.8 1.1 0.8 0.6 0.5
0.4 0.2 -0.1 -0.3 -0.3 -0.4 -0.5 -0.7 -0.8 -0.9 -0.9
    -0.3 -0.5 -0.2 -0.2 0.4 0.5 0.7 0.8 1.0 1.0 1.0 1.0 1.1 1.0 1.1
1.0 0.9 1.0 1.0 0.9 0.9 0.8 0.8 0.8 0.7 0.6 0.7 0.7 0.6 0.6 0.4 0.4
0.4 0.2 0.2 -0.1 -0.2 -0.3 -0.4 -0.7 -0.8 -0.8 -0.8 -0.9
    -0.6 -0.6 -0.4 -0.2 0.4 0.3 0.5 0.4 0.5 0.4 0.5 0.6 0.6 0.6 0.6
0.4 0.5 0.5 0.3 0.4 0.6 0.4 0.4 0.5 0.4 0.3 0.4 0.4 0.4 0.3 0.2 0.2
0.1 -0.2 -0.1 -0.3 -0.4 -0.5 -0.5 -0.6 -0.8 -0.9 -0.9 -1.0
    -0.7 -0.6 -0.5 -0.3 -0.4 -0.2 0.5 -0.4 0.2 -0.3 0.1 -0.3 0.1 0.1
0.1 -0.2 0.5 0.1 0.1 0.0 0.6 -0.2 0.4 -0.3 0.4 -0.3 0.4 -0.2 0.4 -0.3
0.0 -0.3 -0.1 -0.2 -0.3 -0.4 -0.6 -0.8 -0.7 -0.9 -0.8 -0.8 -0.9 -0.9
    -0.8 -0.6 -0.7 -0.7 -0.4 -0.4 -0.4 -0.4 -0.2 -0.3 -0.2 -0.3 -0.2 -
0.2 -0.2 -0.2 -0.2 -0.2 -0.3 -0.3 -0.2 -0.2 -0.3 -0.3 -0.2 -0.3 -0.2 -
0.2 -0.2 -0.3 -0.3 -0.3 -0.3 -0.4 -0.5 -0.6 -0.8 -0.7 -0.9 -0.7 -0.9 -
0.9 -0.9 -0.9
    -0.8 -0.8 -0.8 -0.8 -0.7 -0.6 -0.6 -0.6 -0.4 -0.6 -0.5 -0.4 -0.5 -
0.5 -0.5 -0.5 -0.5 -0.5 -0.5 -0.5 -0.7 -0.5 -0.5 -0.4 -0.4 -0.5 -0.5 -
0.5 -0.4 -0.5 -0.6 -0.6 -0.5 -0.6 -0.7 -0.7 -0.7 -0.8 -0.8 -0.9 -0.9 -
0.9 -1.0 -1.0
    -0.8 -0.8 -0.9 -0.8 -0.9 -0.8 -0.7 -0.8 -0.8 -0.7 -0.7 -0.7 -0.8 -
0.8 -0.7 -0.7 -0.7 -0.7 -0.6 -0.7 -0.7 -0.7 -0.8 -0.7 -0.7 -0.8 -0.7 -
0.7 -0.7 -0.7 -0.5 -0.7 -0.7 -0.8 -0.7 -0.8 -0.8 -0.8 -0.9 -1.0 -0.7 -
1.0 -1.0 -0.9
    -1.0 -1.0 -1.0 -1.0 -1.0 -0.9 -1.0 -1.0 -0.8 -0.8 -0.8 -1.0 -0.9 -
0.9 -0.9 -1.1 -0.9 -0.8 -0.9 -0.8 -1.0 -0.9 -1.0 -0.8 -0.8 -0.8 -0.8 -
0.8 -0.7 -0.7 -0.8 -0.8 -0.7 -0.8 -0.9 -0.8 -0.9 -0.9 -0.9 -0.9 -0.9 -
1.0 -1.0 -1.0]';

B_2tapes = [1.0 0.9 1.0 1.0 1.1 1.1 1.2 1.2 1.3 1.4 1.5 1.5 1.6 1.6
1.7 1.7 1.8 1.8 1.8 1.8 1.8 1.8 1.8 1.7 1.7 1.7 1.7 1.7 1.6 1.6 1.6
1.5 1.5 1.4 1.4 1.3 1.2 1.2 1.1 1.0 0.9 0.8 0.7 0.7
    1.1 1.0 1.0 1.0 1.1 1.2 1.3 1.4 1.5 1.5 1.7 1.7 1.8 1.9 1.9 2.0
2.0 2.0 2.0 2.0 2.0 2.0 2.0 2.0 2.0 2.0 1.9 1.9 1.9 1.9 1.8 1.8 1.7
1.7 1.6 1.5 1.4 1.3 1.2 1.1 1.0 0.9 0.8 0.7
    1.1 1.0 1.1 1.1 1.2 1.3 1.4 1.5 1.6 1.7 1.9 1.9 2.0 2.1 2.2 2.2
2.3 2.3 2.3 2.3 2.3 2.3 2.3 2.3 2.3 2.2 2.2 2.2 2.1 2.2 2.1 2.0 2.0
1.9 1.8 1.7 1.6 1.5 1.4 1.3 1.2 1.0 0.9 0.8
    1.1 1.0 1.1 1.2 1.3 1.4 1.5 1.6 1.8 1.9 2.0 2.2 2.3 2.4 2.4 2.5
2.5 2.6 2.6 2.6 2.6 2.6 2.6 2.6 2.5 2.5 2.5 2.4 2.4 2.4 2.3 2.3 2.2
2.1 2.0 1.9 1.8 1.7 1.5 1.4 1.3 1.1 1.0 0.9
    1.1 1.1 1.1 1.2 1.3 1.4 1.6 1.7 1.9 2.1 2.2 2.4 2.5 2.6 2.7 2.8
2.8 2.8 2.8 2.9 2.9 2.9 2.8 2.8 2.8 2.8 2.7 2.7 2.6 2.7 2.6 2.5 2.4
2.3 2.2 2.1 2.0 1.9 1.7 1.6 1.4 1.3 1.1 1.0
    1.2 1.1 1.2 1.3 1.4 1.5 1.7 1.8 2.0 2.2 2.4 2.5 2.7 2.8 2.9 3.0
3.0 3.1 3.1 3.1 3.1 3.1 3.1 3.1 3.0 3.0 3.0 2.9 2.9 2.9 2.8 2.7 2.6
2.5 2.4 2.3 2.1 2.0 1.8 1.7 1.5 1.3 1.2 1.0
    1.2 1.1 1.2 1.3 1.4 1.6 1.7 1.9 2.1 2.3 2.5 2.7 2.8 3.0 3.1 3.2
3.2 3.3 3.3 3.3 3.3 3.3 3.3 3.3 3.2 3.2 3.1 3.1 3.1 3.1 3.0 2.9 2.8
2.7 2.6 2.4 2.3 2.1 2.0 1.8 1.6 1.4 1.2 1.1
```

```
    1.2 1.1 1.2 1.3 1.5 1.6 1.8 2.0 2.2 2.4 2.6 2.8 3.0 3.1 3.2 3.3
3.3 3.4 3.4 3.4 3.4 3.4 3.4 3.4 3.3 3.4 3.3 3.2 3.2 3.2 3.1 3.0 2.9
2.8 2.7 2.5 2.4 2.2 2.0 1.9 1.7 1.5 1.3 1.1
    1.2 1.1 1.2 1.3 1.5 1.6 1.8 2.0 2.2 2.4 2.6 2.8 3.0 3.1 3.3 3.3
3.4 3.5 3.5 3.5 3.5 3.5 3.5 3.5 3.4 3.4 3.4 3.3 3.3 3.2 3.1 3.1 3.0
2.9 2.8 2.6 2.4 2.3 2.1 1.9 1.7 1.5 1.3 1.1
    1.2 1.1 1.2 1.3 1.5 1.6 1.8 2.0 2.2 2.4 2.6 2.8 3.0 3.1 3.3 3.3
3.4 3.4 3.5 3.5 3.5 3.5 3.5 3.5 3.5 3.4 3.4 3.3 3.3 3.2 3.1 3.1 3.0
2.9 2.8 2.6 2.4 2.3 2.1 1.9 1.7 1.5 1.3 1.1
    1.1 1.1 1.2 1.3 1.4 1.6 1.8 2.0 2.2 2.4 2.6 2.7 2.9 3.0 3.2 3.2
3.3 3.4 3.4 3.4 3.4 3.4 3.4 3.4 3.4 3.3 3.3 3.2 3.2 3.1 3.0 3.0 2.9
2.8 2.7 2.5 2.4 2.2 2.1 1.9 1.7 1.5 1.3 1.1
    1.1 1.1 1.2 1.3 1.4 1.5 1.7 1.9 2.1 2.3 2.5 2.6 2.8 2.9 3.0 3.1
3.2 3.2 3.2 3.2 3.3 3.2 3.3 3.2 3.2 3.2 3.2 3.1 3.1 2.9 2.9 2.9 2.8
2.7 2.6 2.4 2.3 2.1 2.0 1.8 1.6 1.4 1.3 1.1
    1.1 1.1 1.1 1.2 1.3 1.5 1.6 1.8 2.0 2.2 2.3 2.5 2.6 2.7 2.9 2.9
3.0 3.0 3.1 3.0 3.1 3.0 3.1 3.0 3.0 3.0 3.0 2.9 2.9 2.8 2.7 2.7 2.6
2.5 2.4 2.3 2.2 2.0 1.9 1.7 1.5 1.4 1.2 1.0
    1.1 1.1 1.1 1.2 1.3 1.4 1.5 1.7 1.9 2.0 2.2 2.3 2.4 2.5 2.6 2.7
2.7 2.8 2.8 2.8 2.8 2.8 2.8 2.8 2.8 2.8 2.7 2.7 2.6 2.5 2.5 2.5 2.4
2.3 2.3 2.1 2.0 1.9 1.7 1.6 1.4 1.3 1.1 1.0
    1.1 1.0 1.1 1.1 1.2 1.3 1.4 1.6 1.7 1.8 2.0 2.1 2.2 2.3 2.4 2.4
2.5 2.5 2.5 2.5 2.5 2.5 2.6 2.5 2.5 2.5 2.5 2.4 2.4 2.3 2.3 2.2 2.2
2.1 2.0 1.9 1.8 1.7 1.6 1.4 1.3 1.2 1.0 0.9
    1.0 1.0 1.0 1.1 1.1 1.2 1.3 1.4 1.5 1.7 1.8 1.8 2.0 2.0 2.1 2.1
2.2 2.2 2.3 2.2 2.3 2.2 2.3 2.2 2.2 2.2 2.2 2.1 2.1 2.0 2.0 2.0 1.9
1.8 1.8 1.7 1.6 1.5 1.4 1.3 1.2 1.1 0.9 0.8
    1.0 1.0 1.0 1.0 1.1 1.1 1.2 1.3 1.4 1.5 1.6 1.7 1.7 1.8 1.9 1.9
1.9 1.9 2.0 2.0 2.0 2.0 2.0 2.0 2.0 1.9 1.9 1.9 1.9 1.8 1.7 1.7 1.7
1.6 1.6 1.5 1.4 1.3 1.2 1.1 1.1 0.9 0.8 0.7
    0.9 0.9 0.9 1.0 1.0 1.1 1.1 1.2 1.3 1.3 1.4 1.5 1.5 1.6 1.6 1.6
1.7 1.7 1.7 1.7 1.7 1.7 1.7 1.7 1.7 1.7 1.7 1.6 1.6 1.5 1.5 1.5 1.5
1.4 1.4 1.3 1.3 1.1 1.1 1.0 0.9 0.8 0.7 0.7
    0.9 0.9 0.9 0.9 0.9 1.0 1.0 1.1 1.2 1.2 1.2 1.3 1.3 1.4 1.4 1.4
1.5 1.5 1.5 1.5 1.5 1.5 1.5 1.5 1.5 1.4 1.4 1.4 1.4 1.3 1.3 1.3 1.3
1.2 1.2 1.1 1.1 1.0 0.9 0.9 0.8 0.7 0.7 0.6
    0.9 0.9 0.9 0.9 0.9 0.9 0.9 1.0 1.0 1.1 1.1 1.1 1.2 1.2 1.2 1.2
1.3 1.3 1.3 1.3 1.3 1.3 1.3 1.3 1.2 1.2 1.2 1.2 1.2 1.1 1.1 1.1 1.1
1.1 1.0 0.9 0.9 0.9 0.8 0.8 0.7 0.6 0.6 0.5
    0.9 0.8 0.8 0.8 0.8 0.8 0.9 0.9 0.9 1.0 1.0 1.0 1.0 1.0 1.1 1.1
1.1 1.1 1.1 1.1 1.1 1.1 1.1 1.1 1.1 1.1 1.0 1.0 1.0 1.0 0.9 0.9 0.9
0.9 0.9 0.8 0.8 0.7 0.7 0.6 0.6 0.6 0.5 0.5
    0.9 0.8 0.8 0.8 0.8 0.8 0.8 0.8 0.8 0.9 0.9 0.9 0.9 0.9 0.9 0.9
0.9 0.9 0.9 0.9 0.9 0.9 0.9 0.9 0.9 0.9 0.9 0.9 0.9 0.8 0.8 0.8 0.8
0.8 0.8 0.7 0.7 0.6 0.6 0.6 0.5 0.5 0.5 0.4
    0.8 0.8 0.8 0.8 0.7 0.8 0.7 0.8 0.8 0.8 0.8 0.8 0.8 0.8 0.8 0.8
0.8 0.8 0.8 0.8 0.8 0.8 0.8 0.8 0.8 0.8 0.8 0.8 0.7 0.7 0.7 0.7 0.7
0.7 0.6 0.6 0.6 0.6 0.5 0.5 0.5 0.4 0.4 0.4
    0.8 0.8 0.7 0.7 0.7 0.7 0.7 0.7 0.7 0.7 0.7 0.7 0.7 0.7 0.7 0.7
0.7 0.7 0.7 0.7 0.7 0.7 0.7 0.7 0.7 0.7 0.7 0.7 0.6 0.6 0.6 0.6 0.6
0.6 0.6 0.5 0.5 0.5 0.5 0.4 0.4 0.4 0.4 0.4
    0.8 0.8 0.7 0.7 0.7 0.7 0.7 0.7 0.7 0.7 0.7 0.7 0.7 0.7 0.7 0.7
0.7 0.7 0.6 0.7 0.6 0.6 0.6 0.6 0.6 0.6 0.6 0.6 0.6 0.5 0.5 0.5 0.5
0.5 0.5 0.5 0.4 0.4 0.4 0.4 0.4 0.4 0.3 0.3]';

[x,y] = meshgrid(x,y);

figure;
```

lxx

```
surf(x,y,B_1tape); colorbar; axis tight; view(115,25);
xlabel('x [mm]'); ylabel('y [mm]'); zlabel('B [mT]');
title('Measured flux density in a single tape');

figure;
surf(x,y,B_2tapes); colorbar; axis tight; view(115,25);
xlabel('x [mm]'); ylabel('y [mm]'); zlabel('B [mT]');
title('Measured flux density in a stack of two tapes');
```

2. script_tape_resistivity.m

```
clc;
clear all;
close all;

display('Tape Characteristics');
wdts=[4.15 4.05 4.05 4 4]*1e-3;
wdt=mean(wdts)  % [m]
tkn=90e-6       % [m]
S=wdt*tkn;      % [m^2]
leng=81.7e-3    % [m]

display('Normal state (non-superconducting)');
I=[0:0.5:4]';   % [A]
DeltaU=[0 4.391 8.905 13.739 18.632 23.17 28.17 33.27 38.2]'*1e-3; %
[V]

J=I/S;          % [A/m^2]
E=DeltaU/leng;  % [V/m]
rho=mean(E'/J') % [Ohm.m]
1/rho
n_elem=1000;
J_app=linspace(J(1),J(end),n_elem)'; % [A/m^2]
E_app=rho*J_app;                     % [V/m]

figure;
plot(J*1e-6,E*1e3,'.',J_app*1e-6,E_app*1e3,'r');
xlabel('J [MA/m^2]'); ylabel('E [mV/m]');
legend('Collected data','Approximate straight
line','Location','NorthWest');
title('Relation between current density (J) and electrical field (E)
at the normal state');

display('Superconducting state (cooled with liquid Nitrogen)');
data=[10 0
    20 0.01
    30 0
    40 0.12
    51 5.430
    55 17.420
    57 29
    58 32
    59 43
    60 47
    61 56
    62 66
    63 77
```

```
    64 99];

I=data(:,1);            % [A]
DeltaU=data(:,2)*1e-6; % [V]

E0=1e-4;     % [V/m]
U0=E0*leng; % [V]
n=10.99
I_C=51.15  % [A]
J_C=I_C/S   % [A/m^2]

J=I/S;          % [A/m^2]
E=DeltaU/leng; % [V/m]

J_app=linspace(J(1),J(end),n_elem)'; % [A/m^2]
E_app=E0*(J_app/J_C).^n;             % [V/m]

figure;
plot(J*1e-6,E*1e6/1e2,'.',J_app*1e-6,E_app*1e6/1e2,'r'); hold on;
plot([J_app(1) J_app(end)]*1e-6,[1 1],'--','Color',[.5 .5 .5]);
xlabel('J [MA/m^2]'); ylabel('E [\muV/cm]');
legend('Collected data','Approximate curve','Location','NorthWest');
title('Relation between current density (J) and electrical field (E)
at the superconducting state');
```

3. script_wave.m

```
clc;
close all;
clear all;

n=90*2;

a1=repmat(rem(n+0,720),1,2);
a2=repmat(rem(n+360,720),1,2);
b1=repmat(rem(n+240,720),1,2);
b2=repmat(rem(n+240+360,720),1,2);
c1=repmat(rem(n+480,720),1,2);
c2=repmat(rem(n+480+360,720),1,2);
z=[0 255];

wave=[0, 2, 4, 7, 9, 11, 13, 16, 18, 20, 22, 24, 27, 29, 31, 33, 36,
38, 40, 42, 44, 47, 49, 51, 53, 55, 57, 60, 62, 64, 66, 68, 70, 73,
75, 77, 79, 81, 83, 85, 87, 89, 92, 94, 96, 98, 100, 102, 104, 106,
108, 110, 112, 114, 116, 118, 120, 122, 124, 126, 128, 130, 131, 133,
135, 137, 139, 141, 143, 145, 146, 148, 150, 152, 154, 155, 157, 159,
161, 162, 164, 166, 167, 169, 171, 172, 174, 176, 177, 179, 181, 182,
184, 185, 187, 188, 190, 191, 193, 194, 196, 197, 198, 200, 201, 203,
204, 205, 206, 208, 209, 210, 212, 213, 214, 215, 216, 218, 219, 220,
221, 222, 223, 224, 225, 226, 227, 228, 229, 230, 231, 232, 233, 234,
235, 236, 237, 237, 238, 239, 240, 241, 241, 242, 243, 243, 244, 245,
245, 246, 246, 247, 248, 248, 249, 249, 250, 250, 250, 251, 251, 252,
252, 252, 253, 253, 253, 253, 254, 254, 254, 254, 254, 255, 255, 255,
255, 255, 255, 255, 255, 255, 255, 255, 255, 255, 255, 254, 254, 254,
254, 254, 254, 253, 253, 253, 252, 252, 252, 251, 251, 251, 250, 250,
249, 249, 248, 248, 247, 247, 246, 246, 245, 244, 244, 243, 242, 242,
```

```
241, 240, 239, 239, 238, 237, 236, 235, 234, 234, 233, 232, 231, 230,
229, 228, 227, 226, 225, 224, 223, 222, 220, 219, 218, 217, 216, 215,
213, 212, 211, 210, 208, 207, 206, 205, 203, 202, 200, 199, 198, 196,
195, 193, 192, 190, 189, 187, 186, 184, 183, 181, 180, 178, 177, 175,
173, 172, 170, 168, 167, 165, 163, 162, 160, 158, 156, 155, 153, 151,
149, 147, 146, 144, 142, 140, 138, 136, 134, 132, 131, 129, 127, 125,
123, 121, 119, 117, 115, 113, 111, 109, 107, 105, 103, 101, 99, 97,
95, 93, 90, 88, 86, 84, 82, 80, 78, 76, 74, 71, 69, 67, 65, 63, 61,
59, 56, 54, 52, 50, 48, 45, 43, 41, 39, 37, 34, 32, 30, 28, 26, 23,
21, 19, 17, 14, 12, 10, 8, 6, 3, 0, 0, 0, 0, 0, 0, 0, 0, 0, 0, 0, 0,
0, 0, 0, 0, 0, 0, 0, 0, 0, 0, 0, 0, 0, 0, 0, 0, 0, 0, 0, 0, 0, 0, 0,
0, 0, 0, 0, 0, 0, 0, 0, 0, 0, 0, 0, 0, 0, 0, 0, 0, 0, 0, 0, 0, 0, 0,
0, 0, 0, 0, 0, 0, 0, 0, 0, 0, 0, 0, 0, 0, 0, 0, 0, 0, 0, 0, 0, 0, 0,
0, 0, 0, 0, 0, 0, 0, 0, 0, 0, 0, 0, 0, 0, 0, 0, 0, 0, 0, 0, 0, 0, 0,
0, 0, 0, 0, 0, 0, 0, 0, 0, 0, 0, 0, 0, 0, 0, 0, 0, 0, 0, 0, 0, 0, 0,
0, 0, 0, 0, 0, 0, 0, 0, 0, 0, 0, 0, 0, 0, 0, 0, 0, 0, 0, 0, 0, 0, 0,
0, 0, 0, 0, 0, 0, 0, 0, 0, 0, 0, 0, 0, 0, 0, 0, 0, 0, 0, 0, 0, 0, 0,
0, 0, 0, 0, 0, 0, 0, 0, 0, 0, 0, 0, 0, 0, 0, 0, 0, 0, 0, 0, 0, 0, 0,
0, 0, 0, 0, 0, 0, 0, 0, 0, 0, 0, 0, 0, 0, 0, 0, 0, 0, 0, 0, 0, 0, 0,
0, 0, 0, 0, 0, 0, 0, 0, 0, 0, 0, 0, 0, 0, 0, 0, 0, 0, 0, 0, 0, 0, 0,
0, 0, 0, 0, 0, 0, 0, 0, 0, 0, 0, 0, 0, 0, 0, 0, 0, 0, 0, 0, 0, 0, 0,
0, 0, 0, 0, 0, 0, 0, 0, 0, 0, 0, 0, 0, 0, 0, 0, 0, 0, 0, 0, 0, 0, 0,
0, 0, 0, 0, 0, 0, 0, 0, 0, 0, 0, 0, 0, 0, 0, 0, 0, 0, 0, 0, 0, 0, 0,
0, 0, 0, 0, 0, 0, 0, 0, 0, 0, 0, 0, 0, 0, 0, 0, 0, 0, 0, 0, 0, 0, 0,
0, 0, 0, 0];

figure(1);
plot((0:length(wave)-1)/2,wave,'k'); axis([0 360 -10 265]); hold on;
plot(a1/2,z,a2/2,z,b1/2,z,b2/2,z,c1/2,z,c2/2,z);
legend('wave','a1','a2','b1','b2','c1','c2');
xlabel('Angle [°]'); ylabel('Wave');
title('Rectified sinusoidal wave created in Arduino');
```

4. script_motor.ino

```
int a1, Pin1H = 8;
int a2, Pin1L = 9;
int b1, Pin2H = 10;
int b2, Pin2L = 11;
int c1, Pin3H = 12;
int c2, Pin3L = 13;

char inByte;
int long pos = 0, LONG_MAX = 2147483647;
float delta = 0, delta_step = 0.5, f = 0, f_end, f_step, a_freq;
float T_freq_step = 1;

byte wave[] = {0, 2, 4, 7, 9, 11, 13, 16, 18, 20, 22, 24, 27, 29, 31,
33, 36, 38, 40, 42, 44, 47, 49, 51, 53, 55, 57, 60, 62, 64, 66, 68,
70, 73, 75, 77, 79, 81, 83, 85, 87, 89, 92, 94, 96, 98, 100, 102, 104,
106, 108, 110, 112, 114, 116, 118, 120, 122, 124, 126, 128, 130, 131,
133, 135, 137, 139, 141, 143, 145, 146, 148, 150, 152, 154, 155, 157,
159, 161, 162, 164, 166, 167, 169, 171, 172, 174, 176, 177, 179, 181,
182, 184, 185, 187, 188, 190, 191, 193, 194, 196, 197, 198, 200, 201,
203, 204, 205, 206, 208, 209, 210, 212, 213, 214, 215, 216, 218, 219,
220, 221, 222, 223, 224, 225, 226, 227, 228, 229, 230, 231, 232, 233,
234, 235, 236, 237, 237, 238, 239, 240, 241, 241, 242, 243, 243, 244,
```

```
245, 245, 246, 246, 247, 248, 248, 249, 249, 250, 250, 250, 251, 251,
252, 252, 252, 253, 253, 253, 253, 254, 254, 254, 254, 254, 255, 255,
255, 255, 255, 255, 255, 255, 255, 255, 255, 255, 255, 255, 254, 254,
254, 254, 254, 254, 253, 253, 253, 252, 252, 252, 251, 251, 251, 250,
250, 249, 249, 248, 248, 247, 247, 246, 246, 245, 244, 244, 243, 242,
242, 241, 240, 239, 239, 238, 237, 236, 235, 234, 234, 233, 232, 231,
230, 229, 228, 227, 226, 225, 224, 223, 222, 220, 219, 218, 217, 216,
215, 213, 212, 211, 210, 208, 207, 206, 205, 203, 202, 200, 199, 198,
196, 195, 193, 192, 190, 189, 187, 186, 184, 183, 181, 180, 178, 177,
175, 173, 172, 170, 168, 167, 165, 163, 162, 160, 158, 156, 155, 153,
151, 149, 147, 146, 144, 142, 140, 138, 136, 134, 132, 131, 129, 127,
125, 123, 121, 119, 117, 115, 113, 111, 109, 107, 105, 103, 101, 99,
97, 95, 93, 90, 88, 86, 84, 82, 80, 78, 76, 74, 71, 69, 67, 65, 63,
61, 59, 56, 54, 52, 50, 48, 45, 43, 41, 39, 37, 34, 32, 30, 28, 26,
23, 21, 19, 17, 14, 12, 10, 8, 6, 3, 0, 0, 0, 0, 0, 0, 0, 0, 0, 0, 0,
0, 0, 0, 0, 0, 0, 0, 0, 0, 0, 0, 0, 0, 0, 0, 0, 0, 0, 0, 0, 0, 0, 0,
0, 0, 0, 0, 0, 0, 0, 0, 0, 0, 0, 0, 0, 0, 0, 0, 0, 0, 0, 0, 0, 0, 0,
0, 0, 0, 0, 0, 0, 0, 0, 0, 0, 0, 0, 0, 0, 0, 0, 0, 0, 0, 0, 0, 0, 0,
0, 0, 0, 0, 0, 0, 0, 0, 0, 0, 0, 0, 0, 0, 0, 0, 0, 0, 0, 0, 0, 0, 0,
0, 0, 0, 0, 0, 0, 0, 0, 0, 0, 0, 0, 0, 0, 0, 0, 0, 0, 0, 0, 0, 0, 0,
0, 0, 0, 0, 0, 0, 0, 0, 0, 0, 0, 0, 0, 0, 0, 0, 0, 0, 0, 0, 0, 0, 0,
0, 0, 0, 0, 0, 0, 0, 0, 0, 0, 0, 0, 0, 0, 0, 0, 0, 0, 0, 0, 0, 0, 0,
0, 0, 0, 0, 0, 0, 0, 0, 0, 0, 0, 0, 0, 0, 0, 0, 0, 0, 0, 0, 0, 0, 0,
0, 0, 0, 0, 0, 0, 0, 0, 0, 0, 0, 0, 0, 0, 0, 0, 0, 0, 0, 0, 0, 0, 0,
0, 0, 0, 0, 0, 0, 0, 0, 0, 0, 0, 0, 0, 0, 0, 0, 0, 0, 0, 0, 0, 0, 0,
0, 0, 0, 0, 0, 0, 0, 0, 0, 0, 0, 0, 0, 0, 0, 0, 0, 0, 0, 0, 0, 0, 0,
0, 0, 0, 0, 0, 0, 0, 0, 0, 0, 0, 0, 0, 0, 0, 0, 0, 0, 0, 0, 0, 0, 0,
0, 0, 0, 0, 0, 0, 0, 0, 0, 0, 0, 0, 0, 0, 0, 0, 0, 0, 0, 0, 0, 0, 0,
0, 0, 0, 0, 0, 0, 0, 0, 0, 0, 0, 0, 0, 0, 0, 0, 0, 0, 0, 0, 0, 0, 0,
0, 0, 0, 0, 0, 0, 0, 0, 0, 0, 0, 0, 0, 0, 0, 0, 0, 0, 0, 0, 0, 0, 0,
0, 0, 0, 0, 0};

void setup()  {

  Serial.begin(115200);
  Serial.println("\nPress 'd' to displace the field with a given an-
gle;");
  Serial.println("Press 'r' to rotate the field with a given frequen-
cy;");
  Serial.println("Press 's' to speed up the field with a given accel-
eration;\n");
  Serial.println("Press '.' to stop any rotation or '.freq' to change
frequency.\n");

}

void loop()  {

label_1:
  if (Serial.available() > 0) {
    inByte = Serial.read();
    Serial.print("Read ");
    Serial.println(inByte);
  }
  else
    goto label_1;

  if (inByte == 'd') {
```

```
    setAngle(0);

label_2:
    Serial.print("\nDisplacement angle of the field ");
    Serial.print("[");
    Serial.print(char(176));
    Serial.print("]: ");

    float aux = readFloat();
    delta += aux;

    if (delta < 0) {
      Serial.println("Negative position of the field! Try again...");
      delta -= aux;
      goto label_2;
    }

    rotateField(int (2 * delta), 0.5, 1);

    Serial.print("Rotated to the position [");
    Serial.print(char(176));
    Serial.print("]: ");
    Serial.println(delta);

    goto label_2;
  }

  if (inByte == 'r') {

label_3:
    setAngle(0);
    Serial.print("\nFrequency (max ~ 64) [Hz]: ");
    f = readFloat();

    if (f > 64) {
      Serial.println("Chosen frequency is too high! Try again...");
      goto label_3;
    }

    for (delta_step = 0.5; f >= delta_step * 8 && delta_step < 8; del-
ta_step *= 2);

    Serial.print("Angle step [");
    Serial.print(char(176));
    Serial.print("]: ");
    Serial.println(delta_step);

    Serial.print("\nRotating at the frequency [Hz]: ");
    Serial.println(f);

    if (rotateField(LONG_MAX, delta_step, f) == false)
      Serial.println("Working frequency is too high! Try again...");

    if (pos == LONG_MAX)
      Serial.println("Out of memory! Try again...");

    pos = 0;
    goto label_3;
  }
```

```
  if (inByte == 's') {

label_4:
    setAngle(0);
    Serial.print("\nFinal frequency (max ~ 64) [Hz]: ");
    f_end = readFloat();

    if (f_end > 64) {
      Serial.println("Chosen final frequency is too high! Try
again...");
      goto label_4;
    }

label_5:
    a_freq = abs(f - f_end) / float(10);
    if (a_freq < 0.1)
      a_freq = 0.1;
    Serial.print("Frequency acceleration [Hz/s]: ");
    Serial.println(a_freq);

    f_step = a_freq * T_freq_step;
    Serial.print("Frequency step (considering T_freq_step = ");
    Serial.print(T_freq_step);
    Serial.print(" s) [Hz]: ");
    Serial.println(f_step);

    if (accelerateField(f_step) == false)
      Serial.println("Working frequency is too high! Try again...");

    if (pos == LONG_MAX)
      Serial.println("Out of memory! Try again...");

    if (inByte == '.') {

      if (f_end > 64) {
        Serial.println("\nChosen final frequency is too high! Try
again...");
        goto label_6;
      }

      if (f == f_end) {
        Serial.println("\nThe frequency selected is the same! Try
again...");
        goto label_6;
      }

      Serial.print("\nChanging frequency to [Hz]: ");
      Serial.println(f_end);
      goto label_5;
    }

label_6:
    pos = 0;
    f = 0;
    goto label_4;
  }
}
```

```
float readFloat() {
label_read_float:
  if (Serial.available() > 0) {
    float aux = Serial.parseFloat();
    Serial.println(aux);
    return aux;
  }
  else
    goto label_read_float;
}

void setAngle(int long fadeValue) {

  fadeValue += 90 * 2;

  a1 = (fadeValue) % 720;
  a2 = (fadeValue + 360) % 720;
  b1 = (fadeValue + 240) % 720;
  b2 = (fadeValue + 240 + 360) % 720;
  c1 = (fadeValue + 480) % 720;
  c2 = (fadeValue + 480 + 360) % 720;

  analogWrite(Pin1H, int(wave[a1]));
  analogWrite(Pin1L, int(wave[a2]));
  analogWrite(Pin2H, int(wave[b1]));
  analogWrite(Pin2L, int(wave[b2]));
  analogWrite(Pin3H, int(wave[c1]));
  analogWrite(Pin3L, int(wave[c2]));
}

boolean rotateField (int long pos_end, float delta_step, float f) {

  unsigned long t0, t1;
  int pos_step = int(2 * delta_step);

  if (f == 0) {
    setAngle(pos);
    return true;
  }

  float Ts = delta_step / (f * 360) * 1E6;

  if (pos >= pos_end) {
    pos *= -1;
    pos_end *= -1;
  }

  t0 = micros();
  for (pos += pos_step; pos < pos_end; pos += pos_step) {
    setAngle(abs(pos));

    inByte = Serial.read();
    if (inByte == '.') {
      pos = abs(pos);
      return true;
    }

    t1 = micros() - t0;
```

```
    if (Ts <= t1)
      if (pos_step < 16)
        pos_step *= 2;
      else {
        pos = abs(pos);
        return false;
      }

    delayMicroseconds(Ts - t1);
    t0 = micros();
  }

  pos = abs(pos_end);
  setAngle(pos);
  return true;
}

boolean accelerateField(float f_step) {

  if (f > f_end) {
    f *= -1;
    f_end *= -1;
  }

  Serial.println("\nRotating at the frequency [Hz]: ");
  for (f += f_step; f < f_end; f += f_step) {

    for (delta_step = 0.5; abs(f) >= delta_step * 8 && delta_step < 8;
delta_step *= 2);

    Serial.println(abs(f));
    if (rotateField(pos + abs(f) * T_freq_step * 720, delta_step,
abs(f)) == false) {
      f = abs(f);
      return false;
    }

    if (inByte == '.') {
      f = abs(f);
      f_end = Serial.parseFloat();
      return true;
    }
  }

  f = abs(f_end);
  for (delta_step = 0.5; f >= delta_step * 8 && delta_step < 8; del-
ta_step *= 2);

  Serial.print("\nRotating at the final frequency [Hz]: ");
  Serial.println(f);

  if (rotateField(LONG_MAX, delta_step, f) == false)
    return false;

  if (inByte == '.')
    f_end = Serial.parseFloat();

  return true;
}
```

5. script_torque_measurement.m

```
clc;
close all;
clear all;

mass_force=[0
    1490
    1560
    1620
    1640
    1340
    1365
    1480
    1520
    1519
    1615
    1590
    1680
    1680
    1560
    1720
    1780
    1680
    1630
    1640
    1650
    1530
    1600
    1615
    1540
    1510
    1600
    1540
    1525
    1610
    1570
    1550
    1520
    1550
    1560
    1580
    1595
    1660
    1640
    1660
    1650
    1680
    1660
    1650
    1660
    1660
    1720
    1740
    1720
    1740
    1740];
```

```
d=125e-3;
r=d/2;
angle=(0:length(mass_force)-1)*2;

torque=mass_force*r*9.8e-3;

figure;
plot(angle,torque);
xlabel('Rotor displacement angle [°]');
ylabel('Torque [N.m]');
title('Output torque as a function of the rotor displacement angle');
```